COLLEGE OF HEALTH SCIENCES

SCHOOL OF PHARMACY

DEPARTMENT OF PHARMACEUTICS & SOCIAL PHARMACY

Physicochemical Characterization of Native and Microcrystalline Cellulose from Banana Pseudostem, Peduncle, and Leaf (*Musa x paradisiaca L.*) and their Evaluation as Directly Compressible Excipients

By: Amanuel Wledesilasse (B. Pharm)

December, 2023

Addis Ababa, Ethiopia

Physicochemical Characterization of Native Cellulose and Microcrystalline Cellulose from Banana Pseudostem, Banana Peduncle, and Banana Leaf (*Musa x paradisiaca L.*) and Evaluation of Microcrystalline Cellulose as a Directly Compressible Excipient

A Thesis Submitted to the Department of Pharmaceutics and Social Pharmacy, School of Pharmacy, College of Health Sciences, Addis Ababa University as a Partial Fulfillment of the Requirements of a Degree of Master of Science in Pharmaceutics under the supervision of Dr. Anteneh Belete, Dr. Nisha Mary Joseph, and Dr. Tesfaye Gabriel.

By:

Amanuel Wledesilasse (B. Pharm)

December, 2023

Addis Ababa, Ethiopia

Addis Ababa University

School of Graduate Studies

This is to certify that the thesis prepared by Amanuel Wledesilasse, entitled: Physicochemical Characterization of Native Cellulose and Microcrystalline Cellulose from Banana Pseudostem, Banana Peduncle, and Banana Leaf (Musa x paradisiaca L.) and Evaluation of Microcrystalline Cellulose as a Directly Compressible Excipient. and submitted in partial fulfillment of the requirements for the Degree of Master of Science in Pharmaceutics complies with the regulations of the University and meets the accepted standards concerning originality and quality.

By: Amanuel Wledesilasse

Approved by:

Name	Signature	Date
Dr. Anteneh Belete (Advisor)	……	……
Dr. Nisha Mary Joseph (Advisor)	…….	…. …….
Dr. Tesfaye Gabriel (Advisor)	……	……
Mr. Yonas Brhane (Internal Examiner)	……	.....
Dr. Mohd Yasir (External Examiner)	Mohdyasir	**18-01-2024**

Dean, School of Pharmacy, AAU

Contents

Pages

ACKNOWLEDGEMENTS

First of all, I must praise the only Beloved Son of Almighty God, Lord and Saviour, Jesus Christ for the marvelous things he has done for me. I can do nothing without his great mercy and unending love.

I am especially grateful to my advisors, Dr. Anteneh Belete, Dr. Nisha Joseph, and Dr. Tesfaye Gabriel, for allowing me to work on this interesting topic and for their confidence and freedom in my preparation of this work. I deeply appreciate their assistance and advice on all matters, and I am especially grateful for their professional and scientific guidance.

I am deeply grateful to all the staff members of the Department of Pharmaceutics and Social Pharmacy, especially Mr. Fekade Tefera and Abrham Temesgen for their generous support and unreserved assistance. I would also like to thank my classmates for their helpful collaboration and friendship during my research.

I would like to express my sincere gratitude to Cadila Pharmaceutical Manufacturing Company for providing me with access to their Fourier Transform Infrared spectroscopy (FTIR) and for donating paracetamol powder; Adama Science and Technology University for allowing me to use their X-ray diffractometer (XRD), Thermogravimetric and Differential Thermal Analysis Apparatus (TGA), Scanning electron microscope (SEM); Addis Ababa Science and Technology University for providing me Differential Scanning Calorimetry (DSC) for thermal analysis; and Ethiopian Pharmaceutical Manufacturing Sh. Co. (EPHARM) for providing me with access to their tablet compression machine and laboratory for my studies. I am grateful to the R&D and QC departments for their guidance and support during my stay. I would also like to thank the Ethiopian Public Health Institute for conducting microbial tests.

I would like to express my sincere gratitude to Dilla Zuria Woreda Agriculture Office for their suggestions on the banana plant farm area land.

I am also grateful to Addis Ababa University and Dilla University for sponsoring my study.

Finally, I would like to thank my family for their love, support, and prayer

ACRONYMS/ABBREVIATIONS

AA	Acetic Acid
AP	Alkaline Pre-treatment
API	Active Pharmaceutical Ingredients
BL	Banana Leaves
BP	Banana Peduncle
BS	Banana Pseudostem
CrI	Compressibility Index
CrI	Crystallinity Index
DC	Direct Compression
DP	Degree of Polymerization
DSC	Differential Scanning Calorimetry
DTA	Differential Thermal Analysis
FA	Formic Acid
FT-IR	Fourier Transform Infrared
HR	Hausner Ratio
LCB	Ligno-Cellulosic Biomass
LRS	Lubricant Sensitivity Ratio
MgSt	Magnesium Stearate
MCC	Microcrystalline cellulose
KBr	Potassium Bromide
RH	Relative Humidity
SD	Standard Deviation
TGA	Thermo Gravimetric Analysis
USP	United States Pharmacopeia
XRD	X-Ray Diffraction

LIST OF TABLES

LIST of FIGURES

ABSTRACT

Wood is the most common source of cellulose, but over exploitation and deforestation have led to a need for alternative sources. Banana (*Musa spp*.) is produced as a multi-purpose crop in terms of food security, income generation, job opportunities, and animal feeding in Ethiopia. However, the cultivation of bananas gives rise to a large number of byproducts such as pseudostem, leaves, inflorescence, rhizomes, pith, sap, and fibers. This study therefore aimed to isolate and characterize native cellulose and microcrystalline cellulose (MCC) from banana leaf (BL), Banana pseudostem (BS), and Banana peduncle (BP) and evaluate MCC as a directly compressible pharmaceutical excipient. Cellulose fibers were obtained using a chlorine-free extraction process that began with sodium hydroxide pretreatment. The fibers were then delignified with a mixture of formic acid, acetic acid, and hydrogen peroxide, and bleached with alkaline hydrogen peroxide. MCC was prepared by hydrolyzing the native cellulose fibers with hydrochloric acid (HCl). The isolated cellulose and MCC were then characterized using different analytical techniques: Fourier-transform infrared spectroscopy (FTIR), X-ray diffraction (XRD), Scanning electron microscopy (SEM), and Thermogravimetric analysis (TGA). The formulated tablets were evaluated for uniformity of weight, hardness, friability, disintegration time, and dissolution rate. The FTIR results tracked the gradual removal of non-cellulosic components from the extracted cellulose. SEM images showed that the cellulose samples had a micro-fibrillated structure, while the MCC samples had a rod-like shape with some irregular aggregated particles. All samples of cellulose and MCC showed thermal stability. XRD analysis showed that BL-MCC, BS-MCC, BP-MCC, and Avicel PH-101 had crystallinity indices of 77%, 84%, 83%, and 85%, respectively, and degree of polymerization (DP) values of 270, 265, 255, and 240, respectively. The yields of cellulose and MCC from BL, BS, and BP were 23.1 ± 1.41%, 37.33 ± 1.4%, and 45 ± 0.8%, respectively. The yields of MCC from BL, BS, and BP were 77.5 ± 0.4%, 85 ± 0.7%, and 87.3 ± 0.47%, respectively. Both without paracetamol and paracetamol-loaded tablets made with BS-MCC and BP-MCC had acceptable crushing, tensile strength, and friability. The disintegration times and drug release profiles of all paracetamol-loaded tablets made with BS-MCC, BP-MCC, and Avicel PH-101 were similar and within the acceptable range specified in the USP. This study proposes that BL, BS, and BP are locally available

sources of cellulose and MCC with potential as direct-compressible tablet excipients in pharmaceuticals, providing an alternative to local sources.

Keywords: Banana leaves, Banana pseudostems, Banana peduncles, Cellulose, Microcrystalline cellulose, Directly compressible excipient

1. INTRODUCTION

1.1 Cellulose

Natural fibers are replacing synthetic fibers in composites because they are better for the environment. These fibers are used to make a variety of biocomposites (Lobmann & Svagan, 2017). Natural fiber-reinforced polymer composites have many advantages over synthetic composites and traditional metal-based materials (Thakur, 2014). Natural fibers present important advantages such as low density, low cost, biological degradability, renewability, good mechanical properties, and non-toxicity (Azraaie *et al*., 2014). The interest in using natural fibers has increased significantly in the last few years. Cellulose, the most abundant natural polymer on earth with an annual biomass manufacture of 50 billion tons, has a promising future for diversified applications (Bhandari *et al*., 2020).

Cellulose is a linear unbranched polysaccharide consisting of β-1,4-linked D-glucose units (Figure 1), and many parallel cellulose molecules that form crystalline microfibrils. The crystalline microfibrils are mechanically strong and highly resistant to enzymatic attack and are aligned with each other to provide structure to the cell wall (Guo *et al.*, 1998).

Many properties of cellulose depend on its chain length or the degree of polymerization, the total number of glucose units that make up one polymer molecule (Neves *et al.*, 2021). Plant-derived cellulose is generally found in a mixture with pectin, hemicelluloses, lignin, and other substances, while microbial cellulose is pure, has a much higher moisture content, and consists of long chains (Meng *et al*., 2019).

Currently, cellulose which is derived from wood and cotton has its use in industrial applications. However, wood and cotton are expensive and limited. This is because of the shortage of wood resources and the long growth cycle which is considered a limited natural resource from the environmental perspective (Rohadi *et al.*, 2020).

Biodegradable and biomass-based products can increase the value of agricultural waste and drive innovation in science and technology (Gabriel *et al*., 2020). Lignocellulosic biomass, such as corn cobs, rice straw, groundnut shell, sugarcane bagasse, and banana fiber, can be used to produce these products (Diarsa & Gupte, 2021). Banana (*genus Musa*)

is a monocotyledonous herbaceous plant of the Musaceae family (Abdullah *et al*., 2013; El-Sakhawy & Hassan, 2007).

Most bananas are produced in traditional agricultural systems for home consumption and local markets. Banana pseudostem and peduncle fibers contain high levels of cellulose, which is used to produce microcrystalline cellulose (MCC) (Jayaprabha *et al.*, 2011). Recent research has focused on converting underutilized lignocellulosic materials into value-added products at a low cost (Ismail *et al*., 2021). MCC is a low molecular weight, purified, and partially depolymerized cellulose obtained through hydrolysis. Manufacturing MCC from diverse agricultural waste and using it as a green filler is a cost-effective way to develop future green products (Bhandari *et al*., 2020). Natural fibers are a good alternative for extracting MCC from agricultural waste because commercially produced MCC is expensive (Diarsa & Gupte, 2021). There is limited research on using banana fiber waste as a natural fiber reinforcement in the pharmaceutical sector.

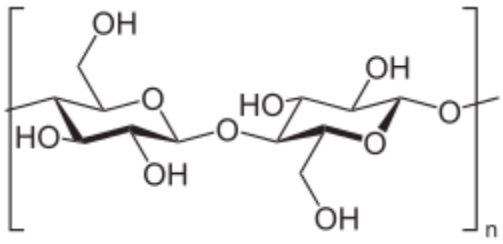

Figure 1: Cellulose structure (Orlando J., 2016).

1.2 Sources of Cellulose

The four most common cellulose polymorphs are cellulose I**,** cellulose II**,** cellulose III, and cellulose IV**.** Cellulose I is the native form of cellulose, found in plants. It is made up of a mixture of cellulose Iα (triclinic structure) and cellulose Iβ (monoclinic structure). Cellulose II is the most common form of regenerated cellulose, produced by processing cellulose with chemicals. It is the thermodynamically most stable cellulose polymorph. In nature, cellulose is found in a crystalline form called cellulose I. This can be irreversibly changed into cellulose II by mercerization (e.g., treatment with concentrated sodium hydroxide solution) or precipitation (regeneration) from the solution (Trache *et al*., 2016a).

Cellulose III is an amorphous form not found in nature. It is formed by treating cellulose I or II with certain chemicals like amines, causing the chains to lose their ordered structure and become more readily dissolvable. Cellulose IV the least common polymorph, produced by heating cellulose III at high temperatures. It has a distorted chain structure with weakened hydrogen bonds, leading to an even more amorphous state than III (Gong *et al*., 2017).

Due to its abundance and unique structural qualities, cellulose is a high-quality product. Vascular plants are the primary industrial source of cellulose (Hassan & El-Sakhawy, 2007). In terms of current society's environmental preferences, lignocellulose resources, particularly agro-industrial wastes, are important as reinforcement products for the building construction material sector (Munarin *et al*., 2013).

Currently, increasing environmental issue has motivated the development of sustainable process and product. This need to develop biodegradable materials to replace synthetic products has led researchers to search for natural and renewable resources (Tibolla *et al*., 2018). The most common source of cellulose is lignocellulosic materials in forests, with wood being the most common (Kambli *et al.*, 2018).

The overuse of such sources by competing industries such as energy and construction, as well as global deforestation, has increased the need for cellulose from herbaceous plants, crops, and/or non-woody plants (Gabriel *et al*., 2020). Agricultural waste is a valuable source of cellulose, a versatile and abundant material with a wide range of applications.

Examples of agricultural waste that can be used to produce cellulose include Sugarcane straw (Menezes *et al*., 2016), rice straw (Fan *et al*., 2017), corn husks (Reddy & Yang, 2005), cotton stalks (El-Sakhawy & Hassan, 2007), date seeds (Abu-Thabit *et al*., 2020a) bamboo fiber (Rasheed *et al*., 2020), banana plant waste (Ibrahim et al., 2013), Enset fiber, Sugarcane bagasse, coffee hull (Gabriel *et al*., 2020) and Teff straw (Getachew *et al*., 2023a).

1.3 Banana plant as source of cellulose

Banana is the second most important fruit crop in the world. It is grown in 130 countries of the world (Diarsa & Gupte, 2021). The banana is the world's cheapest and most popular fruit in tropical and subtropical regions. In the period 2017–2019, worldwide banana production averaged 116 million tons (Nascimento *et al*., 2021).

Direct use of banana biomass waste has a long history. Banana leaves are employed as a covering, matting, and barrier walls in several nations in Africa and Latin America (Muhamad *et al*., 2019). Banana pseudostem fibers are used to make a variety of fabric and rope varieties. A tiny amount of banana biomass is also used as animal feed, compost, and biogas production. At the beginning of the twenty-first century, attention was given to the thermal method for converting banana biomass waste to energy and value-added products (Kumar *et al*., 2020).

Bananas (*Musa spp*.) are important fruits in the tropics and subtropics (Meng *et al*., 2019). Banana (*genus Musa*) is a Musaceae family monocotyledonous herbaceous plant (Okareh, 2015). Bananas provide sufficient carbohydrates with high nutrition, and banana plants produce enormous pseudo-stem residues rich in lignocellulose (Liu *et al*., 2021).

Ethiopia is among the tropical countries where its vast arable land is suitable for banana cultivation. Banana ranks first among fruit crops in area coverage (67,387 ha) and production (539,443 tons). Banana is produced as a multi-purpose crop in terms of food security, income generation, job opportunities, and animal feeding in Ethiopia (Dagnew *et al*., 2021). The southern and south-western parts of Ethiopia account for about 69 % (37 thousand ha) of the country's land coverage for banana production, accounting for 77.53 % (370 thousand tons) of Ethiopia's annual fresh banana production by 22.38 % (1.5 million) of the country's banana producers (Mitiku *et al*., 2020).

Banana production generates a significant amount of lignocellulosic waste, which is high in cellulose. This residual resource has attracted interest due to the potential applications of such materials (Flores-Velázquez *et al.*, 2020; Gabhane *et al*., 2014)

Banana peduncles (BP), banana leaves (BL), and banana pseudostem (BS) generate a lot of waste (Figure 2) and these wastes can be unique lignocelluloses for pulping Zuluaga et al., 2007 Yilmaz et al., 2017). The fibrous residue of pseudostems (Pappu *et al*., 2015), leaves (Elanthikkal *et al*., 2010) and peduncles (Manimaran *et al*., 2019) left behind after banana cultivation make up the banana plant fibers. The BP, BL, and BS are left in the field to decompose and be utilized as organic fertilizer, but because there is an excess of banana biomass in the field, decomposition can pollute the environment (Mitiku *et al*., 2020; Nascimento et al., 2021). Extraction of fibers from these banana residues will aid natural degradation, hence resulting in ecological balances (Jayaprabha *et al*., 2011).

Due to its high cellulose contents, Banana fiber is a potential raw material for biofuel production (Shimizu *et al*., 2018). After the harvesting of banana, the waste including leaves (Nada *et al*., 2010), rachis (peduncle) (Zuluaga *et al*., 2009), and pseudostems (Li *et al.*, 2015) contain high levels of cellulose. These cellulose-rich wastes are removed and left to decay (Meng *et al*., 2019).

Figure 2**:** a,Banana tree,b,Banana penducle,c,Banana leaf,d,Banana pseudostem picture taken by Amanuel W/silasse.

1.4 Cellulose Extraction from Lignocellulosic Materials

Cellulose is the most abundant renewable polymer resource available today, and it is considered an almost inexhaustible source of raw material for the increasing demand for environmentally friendly and biocompatible products (Garrote *et al.*, 1999; Brinchi *et al.*, 2013). Because lignocellulosic biomass (LCB) is made up of a complex mixture of cellulose, hemicellulose, and lignin, proper separation methods are required to make the optimum use of its constituents (Batista Meneses *et al.*, 2022).

Cellulose is the major structural component of plant cell walls, while hemicellulose macromolecules are often repeated polymers of pentoses and hexoses. Lignin contains three aromatic alcohols (coniferyl alcohol, sinapyl alcohol, and p-coumaryl alcohol) produced through a biosynthetic process, and it forms a protective seal around the other two components (i.e., cellulose and hemicelluloses) (Kumar *et al*., 2009).

Plant cellulose, hemicellulose, and lignin are chemically linked in a complex manner, making separation difficult. The most reliable approach for extracting these substances necessitates the use of powerful chemicals such as acids, bases, and organic solvents in a high-temperature, high-pressure environment (Shikinaka *et al*., 2018).

Pretreatment is an important tool for cellulose conversion processes and is essential to change the structure of cellulosic biomass to make cellulose more available to the enzymes that convert the carbohydrate polymers into fermentable sugars (Amin *et al*., 2017). For the objective of obtaining acceptable yields in the components, additional pretreatment steps are generally required. During the pretreatment stage, the natural characteristics of lignocellulosic compound bonds are modified by altering the supramolecular structures (Ramos, 2003). Pretreatment of the lignocellulosic material is carried out to overcome recalcitrance through the combination of chemical and structural changes to the lignin and carbohydrates (Amin *et al*., 2017).

As shown in the schematic diagram (Figure 3), pretreatment is required to change the structure of cellulosic biomass to make cellulose more accessible to enzymes that convert carbohydrate polymers into fermentable sugars (Mosier *et al*., 2005).

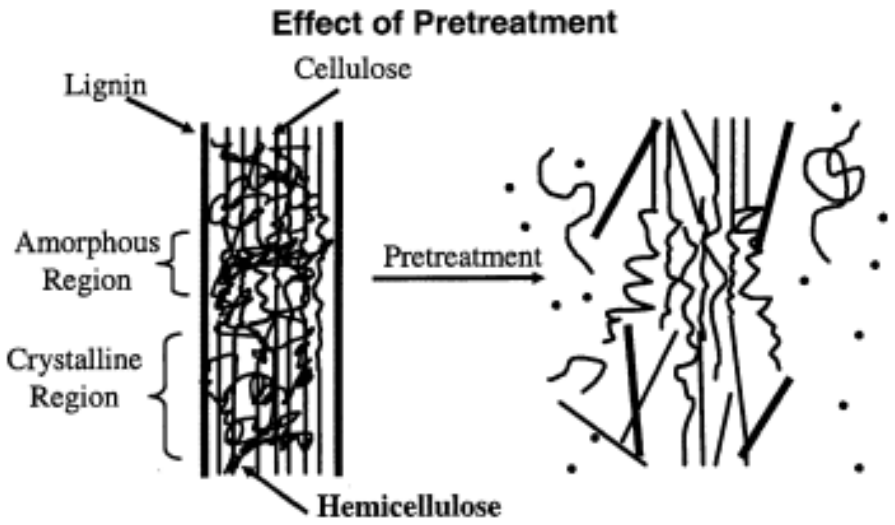

Figure 3: Schematic of goals of pretreatment on lignocellulosic material (Mosier *et al*., 2005).

1.4.1 Chemical Method

1.4.1.1 Acid pretreatment

There are various advantages to acid pretreatment of lignocellulosic biomass. There are acid solutions that can remove lignin and hemicellulose without any prior treatment and at a low cost (Amin *et al*., 2017). Various types of mineral acids can be used, with sulfuric acid (H_2SO_4), nitic acid (HNO_3), formic acid (HCO_2H), hydrochloric acid (HCl) acetic acid (CH_3COOH) being the most commonly used ones (Das *et al*., 2015; Meneses *et al*., 2022).

Because of its excellent potency for the removal of lignin and degradation of hemicellulose, acidic hydrolysis is one of the most desirable traditional pretreatment methods for lignocellulose (Das *et al*., 2015). However, studies have shown that higher acid concentrations can cause serious damage to instruments. As a result, the acidic pretreatment temperature and acid concentration must be chosen carefully (Roy *et al*., 2020).

Organic acid extraction is widely accepted as a viable delignification alternative (Ma *et al*., 2021). By degrading lignocellulosic material in aqueous acetic acid or formic acid, the three primary components, cellulose, hemicellulose, and lignin, may be successfully separated. Formic acid (FA), acetic acid (AA), and water (H_2O) can effectively depolymerize the lignocellulosic biomass (LCB) into fibers by dissolving lignin and

hemicellulose. The lignin and hemicellulose dissolved in the solvent systems can be separated easily, and the solvents themselves can be recovered by an industrial process and used again (Ma *et al*., 2021).

The proton supply is from FA, while the lignin solvent is AA. FA has potential as a chemical agent for biomass fractionation because it is a cheap and easily available organic solvent. Because the lignin β-O-4 links are cleaved during FA pulping, lignin dissolves into black liquid, while hemicellulose degrades into mono and oligosaccharides, leaving solid cellulose in the residue (Zhang *et al*., 2010).

The lignin and hemicellulose dissolved in the solvent systems can be easily separated, and the solvents can be collected and reused by an industrial process (Ligero *et al.*, 2008; Yu *et al*., 2013;Ma *et al*., 2021). Oxoacid-based processes are among the most effective, allowing both woody and non-woody materials to be delignified efficiently (Sidiras & Salapa, 2015). When H_2O_2 is added to formic/AA solution, peroxy- formic/peracetic acids are formed. Peroxyformic and peracetic acids are strong oxidants, which generate electrophilic HO^+ ions to react with lignin by ring hydroxylation, oxidative ring opening, side chain substitution, cleavage of β-aryl bonds, etc., resulting in the formation of lignin fragments. Pulping of lignocellulose by FA is effective for delignification when FA concentration is higher than 80%, but delignification is inadequate at formic acid strengths below 70% (Zhang *et al*., 2010).

1.4.1.2 Alkaline pre-treatment

Pretreatment of lignocellulosic materials with certain bases is possible, and the effect of alkaline pretreatment is dependent on the lignin content of the materials (Shimizu *et al*., 2018). Other pretreatment technologies use higher temperatures and pressures, whereas alkaline pretreatment procedures use lower temperatures and pressures (Kumar *et al*., 2009).

Pre-treatment of lignocellulosic wastes can easily be accomplished using alkalis or certain bases. Alkaline pretreatment can be done at room temperature, which is a benefit over other chemical treatments, but it is also a drawback because pre-treatment timeframes are measured in hours and days rather than minutes or seconds (Das *et al*., 2015).

Alkaline methods frequently employ reagents such as sodium hydroxide, sodium carbonate, ammonia, and calcium hydroxide (Meneses *et al*., 2022). The fundamental characteristics of alkaline pretreatment are that it eliminates lignin selectively without damaging carbohydrates and increases porosity and surface area, hence increasing enzymatic hydrolysis. Alkaline pretreatment is effective in the delignification of biomass, without significantly affecting its cellulosic structure (Kim *et al.*, 2016; Ravindran & Jaiswal, 2016).

1.4.2 Physical Pretreatment

Physical pretreatment methods, including mechanical operations, different types of irradiation, and ultrasonic pretreatment, have been utilized to enhance the accessibility to hydrolyzable polymers within lignocellulosic material (Amin *et al*., 2017). Physical comminution, such as grinding, and chopping, can diminish the crystallinity of cellulose (Das *et al*., 2015).

1.4.3 Physicochemical Pretreatments

LCB can also be pretreated physically and chemically in combination. For example, milling, a physical pretreatment, can be performed alongside alkali pretreatment to enhance pretreatment efficiency (Cheah *et al*., 2020). Examples of combined pretreatments are steam explosion, ammonia fiber explosion (AFEX), carbon dioxide explosive, and liquid hot water (Cheah *et al*., 2020).

The most common and effective pretreatment method is a steam explosion, which is often a mix of mechanical forces and chemical effects applied to LCBs. The biomass is exposed to extremely saturated steam (0.69–4.83 MPa) at a temperature of 160–260 °C in this process, allowing water molecules to penetrate the substrate structure (Baruah *et al*., 2018). It is the most widely used pretreatment method for depolymerization of lignocellulosic materials, as it aids in the loosening of cellulose, hemicellulose, and lignin bonds (Das *et al*., 2015 ; Amin *et al*., 2017).

1.5 Modification of cellulose

Due to its suitable physical and mechanical properties, cellulose and its derivatives have attracted a lot of interest as biocompatible polymers for biomedical applications

(Abdelmouleh *et al*., 2004). As cellulose contains three hydroxyl groups per repeating anhydroglucose unit, it is easily modified chemically (Neves *et al*., 2021).

Cellulosic materials may be easily modified to produce useful products due to their chemical functionality. Physical modification (e.g., microcrystalline cellulose (MCC), chemical modification (e.g., ethyl cellulose, hydroxyethyl cellulose, hydroxypropyl cellulose, and carboxymethyl cellulose), enzymatic, or mechanical treatments can all be used to achieve these results. Pharmaceuticals, food, and paper are some of the applications for modified cellulose (Arca *et al.*, 2018; Seddiqi *et al*., 2021).

1.6 Microcrystalline Cellulose (MCC)

MCC was discovered by Battista and Smith in 1955 and first marketed as a pharmaceutical tableting excipient in 1963 under the brand name Avicel (Dinand *et al*., 1996). The crystalline structure sections of cellulose microfibrils can be extracted when they are treated with an appropriate mix of mechanical, chemical, and/or enzymatic treatments, resulting in the formation of MCC (Seddiqi *et al*., 2021). MCC occurs as white, odorless, and tasteless crystalline powder and is extracted from various lignocellulosic materials (Neves *et al.*, 2021). MCC is interesting as reinforcement in composites since it is stable, chemically inactive, light, stiff, and strong (Seddiqi *et al*., 2021; Trache *et al*., 2016a). The chemical composition (proportions of cellulose, hemicelluloses, and lignin) and structural organization (regions that are more crystalline or amorphous) of these woods differ significantly (Thorens *et al*., 2014a).

Woody plants and cotton are the major industrial sources of MCC but cost has made it imperative that other materials be investigated (Trache *et al*., 2016a). In literature, there is evidence that diverse sources are already being used to produce MCC. For example, it can be extracted from groundnut shells, cereal straw bagasse, corn cob, bamboo, sugar beet pulp, corn husks (Vora & Shah, 2015), wheat straw (Reddy & Yang, 2007) rice straw (Ibrahim et al., 2013), oil palm biomass, fodder grass, wastepaper, filter paper and cotton waste (Arca *et al*., 2018, Seddiqi *et al*., 2021). Different sources of biomass with evolving isolation techniques are under continuous research to meet the increasing demand for such cellulose derivatives due to their promising potential for renewability, non-toxicity, large surface area, and economic importance (Haldar & Purkait, 2020).

MCC is a widely used pharmaceutical excipient with excellent compression properties, making it suitable for direct compression, wet granulation, and pelletization (Badawy *et al*., 2006). MCC is a common excipient used in direct compression tablet formulations that contain poorly compressible API. Pharmaceutical manufacturers now have access to a wide variety of MCC grades from different brands, which has led to variability in the properties of MCC (Setu *et al*., 2014).

1.6.1 Physicochemical Properties of MCC

MCC represents a novel form of commercial cellulose and exists as a fine, white, odorless, crystalline powder (Das *et al*., 2010).

Long chains of β-(1 4)-linked d-anhydroglucopyranose moieties repeating units make up cellulose, a linear carbohydrate polymer (Figure 4). It is called a polysaccharide since cellulose is made up of sugar monomers (Trache *et al*., 2016a). Three hydroxyl groups are attached to the carbons in each monomeric unit of the cellulose chain: at the primary C-6 atom (–CH2OH) and at two secondary carbons (C-2 and C-3) in the anhydroglucose unit (Westermarck *et al.,* 1999). The capacity of these OH groups to establish hydrogen bonds is critical for controlling the physicochemical properties of cellulose as well as directing its ultra-structure. Micro-fibrils are formed by bundling together cellulosic chains (20–300), which are then grouped to create cellulose fibers. Each asymmetric polymeric chain has two different end-units: a reducing and a non-reducing end (El-Sakhawy & Hassan, 2007; Trache *et al*., 2016a).

Among the four different crystalline polymorphs, cellulose I, II, III, and IV, cellulose I is thermodynamically less stable while cellulose II is the most stable structure. Liquid ammonia treatment of cellulose I and cellulose II gives crystalline cellulose III, and the heating of cellulose III generates cellulose IV crystalline form (Lavanya *et al*., 2015).

MCC is prepared by treating wood pulp or linters with dilute mineral acid and is described as purified, partially depolymerized cellulose with a degree of polymerization (DP) below 350 (Cheah *et al*., 2020).

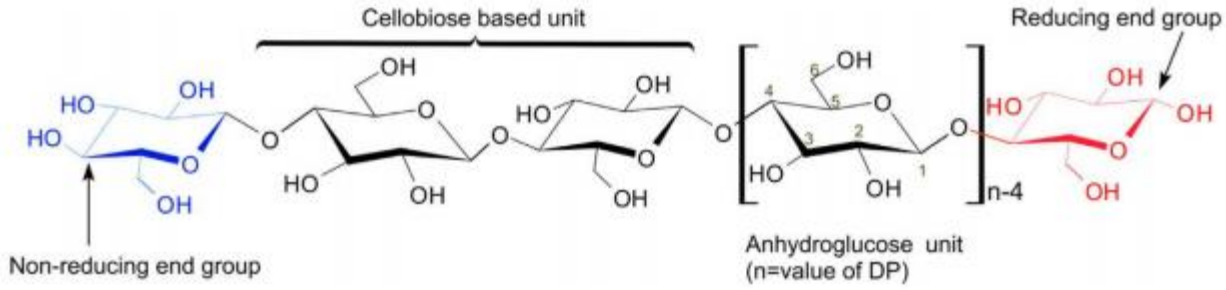

Figure 4: Molecular structure of cellulose showing the numbering of carbon atoms, the reducing end with a hemiacetal, and the non-reducing end with a free hydroxyl at C4 (Trache et al., 2016a)**.**

1.6.2 Applications of MCC

1.6.2.1. Pharmaceutical applications

MCC is generally considered a diluent having the best binding properties and is recognized as one of the preferred direct compression binders (Thorens et al., 2014b). MCC can also be employed as a bulking agent, disintegrant, lubricant, and glidant (Nwajiobi *et al*., 2019). It can be used in direct compression (Doelker, 1993b) for most drugs and saves material, capital, equipment, and labor. Its use in drug research is growing, with applications including immediate release (tablets and liquids), sustained release (multi particulates and matrix tablets), topical preparations, oral liquids, organoleptic improvements (chewable and mouth dissolving tablets), anti-reflux, and nutraceuticals. In addition to being a stability enhancer and a secondary suspending agent (Ali *et al*., 2009).

The applications of the powdered cellulose and the MCC in compounding pharmacies include the oral solid dosage form (capsules) as a bulking agent to enhance the mass in formulations containing small amounts of the active ingredient (Othman *et al*., 2020).

1.6.2.2 Other applications of MCC

MCC is a versatile and widely used material in the food and industrial industries. MCCs have been used as a bulking agent in dairy products, baked foods, desserts, sausage, frozen food, and other food systems. Their presence improves the consistency, mouthfeel, and other organoleptic properties of these products (Nsor-Atindana *et al*., 2017). Additionally, MCC finds diverse applications in industrial products, including adhesives, paints, and coatings (Ali *et al*., 2009).

1.6.3 MCC preparation method

Up until the 1980s, Avicel grades were the only MCC goods on the market, but since then, various manufacturers have introduced a variety of new products (Doelker, 1993b). MCC is typically made by spray drying the neutralized aqueous slurry produced by cellulose hydrolysis. Most commercial grades are formed by manipulating the degree of agglomeration (particle size distribution) and moisture content by altering and adjusting the spray drying conditions (loss on drying). Other drying methods may be utilized, which may necessitate additional post-drying screening steps to control particle size distribution (Kian *et al*., 2017a).

MCC is made from hydrolytic wood pulp from needle-leaf trees or return pulp from cotton-seed fiber with mineral acid first. After removing the amorphous region and impurities, the intermediates are neutralized and washed to purify the MCC (Suzuki & Nakagami, 1999).

MCC is described as cellulose that has been partially hydrolyzed and depolymerized but still contains disorganized amorphous patches. The structure and properties of MCC differ depending on the type of cellulose used and the hydrolysis conditions employed, such as temperature, time, and acid concentration (Kian *et al*., 2017a). MCC is typically characterized by a high degree of crystallinity, however, there are variations within grades; values typically range from 55 to 80% as determined by X-ray diffraction (XRD) (Kian *et al*., 2017a).

Drying is a crucial step in the production of commercial-grade MCC. Spray drying is the most common commercial method, but other methods such as freeze drying, fluidized bed drying, microwave drying, and oven drying can also be used. After drying, the MCC is typically ground to the desired particle size (Trache *et al*., 2016 ; Haldar & Purkait, 2020).

1.7. Paracetamol

Paracetamol (PCM has been used as an analgesic for over-the-counter medication and is recognized as a highly successful treatment for the reduction of pain and fever in both adults and children.PCM, commonly referred to as acetaminophen (N-acetyl-p-aminophenol, 4-acetaminophen), is a common component of many prescription analgesics and cold and flu remedies (Bosch et al., 2006). Moderate water solubility: Increases with

temperature due to the interplay between polar hydroxyl and nonpolar benzene ring.High melting point: 169-172°C, indicating strong intermolecular forces (likely hydrogen bonding)..It is typically formulated as tablets containing 300-500 mg of the drug. PCM is a challenging drug to formulate because it has poor compression properties, low flowability, and a tendency to cap (Martinello *et al*., 2006)).As a result, 400 mg PCM tablets were developed as model drugs, the dilution potential of BS-MCC, BP-MCC, and Avicel PH-101 were assessed.

1.8 Statement of the Problem

The use of cellulose in numerous industrial applications is steadily rising around the world. Because wood (conventional sources) is the primary source of cellulose, increased use, even in countries with limited wood resources, contributes to deforestation. With the rising need for cellulose and its derivatives, conventional resources are finding it increasingly challenging to meet the growing demand (Li *et al*., 2019).

Currently, cellulose which is derived from wood and cotton has its use in industrial applications. However, wood and cotton are expensive and limited. This is because of the shortage of wood resources and the long growth cycle which is considered a limited natural resource from the environmental perspective. Forest supplies are depleting globally, while demand for cellulose and cellulose derivatives is increasing. This is driving scientists to explore alternative fiber sources, particularly those that are non-wood, such as banana biomass waste (Ibrahim *et al*., 2013).

Banana biomass waste is a promising source of cellulose, even though it is often left in the field or taken to open dumps, where it decomposes and releases greenhouse gases. The fruit part of banana plant is only 12 wt % of a plant, and the remaining parts become agricultural wastes (Zuluaga *et al.,* 2007). Banana biomass waste can be used to produce MCC, a valuable pharmaceutical excipient (Kumar *et al.,* 2020). MCC is expensive to buy commercially, and importing raw materials can have a negative impact on the economy. Also, mismanaging agro-industrial waste can lead to environmental problems (Pappu *et al.,* 2015).Therefore, there is a need to develop new sources of MCC from sustainable materials, such as banana fiber waste (Diarsa & Gupte, 2021).

Ethiopia is abundant in banana fiber waste, particularly in the southern and southwestern regions (Mitiku *et al*., 2020). However, there is a lack of research on cellulose and MCC production from banana residue in Ethiopia. This study aims to prepare and characterize cellulose and MCC from BL, BS, and BP, and to assess their potential as direct compressible pharmaceutical excipients.

1.9 Significance of the study

The MCC market size was over USD 630 million in 2015 and is projected to surpass USD 1 billion by 2024, growing at a CAGR (compound annual growth rate) of more than 7% from 2016 to 2024 (Sundarraj & Ranganathan, 2018). This growth is driven by the increasing demand for MCC in healthcare and personal care applications (Haldar & Purkait, 2020). MCC is a versatile excipient used in a wide range of pharmaceutical dosage forms, including tablets, capsules, and suspensions. It is also used in personal care products such as cosmetics, toothpaste, and shampoo (Jahan *et al*., 2014).

Abundant renewable agricultural residues are a valuable source of renewable LCB, with increasing interest in their applications worldwide (Ibrahim *et al*., 2013). MCC has attracted significant attention from both academia and industry in recent decades due to its remarkable properties (Trache *et al.*, 2014). The need for more affordable MCC has motivated researchers to explore other lignocellulosic materials derived from agricultural wastes (Kambli *et al*., 2017a). In recent years, there has been a growing focus on utilizing underutilized lignocellulosic resources, and researchers have investigated various methods to expand the sources of MCC (Li *et al*., 2019).

Wood is currently the primary source of chemical and mechanical pulps, accounting for over 90% of the global pulp and paper market. The investigation of non-wood cellulosic sources such as agricultural wastes and banana fiber has attracted the scientific community's attention (Beroual *et al*., 2021). Currently, because of increasing prices of MCC, additional materials must be investigated as potential sources (Ejikeme, 2008).

Ethiopia imports pharmaceutical excipients, such as MCC, from abroad despite its limited pharmaceutical manufacturing capacity. This requires a significant amount of foreign currency, which can strain the country's economic growth. Local production of MCC would bring economic benefits, such as fulfilling the import substitution strategy,

exporting raw materials, and converting waste products into value-added products. The lack of a study report on BS, BP, and BL cellulose and MCC in Ethiopia necessitates the preparation and characterization of these materials for various pharmaceutical applications.

1.10 Research Questions

1. What is the cellulose and MCC yield potential of BS, BP, and BL?

2. What are the physico-chemical characteristics of BS, BP BL cellulose, and MCC?

3. What are the direct compressible potentials of BS, BP, and BL MCC when compressed with or without active pharmaceutical ingredients?

2. Objectives

2.1 General Objective

- To prepare and characterize native cellulose and MCC from BP, BS, and BL and evaluate MCC as a directly compressible pharmaceutical excipient

2.2 Specific Objectives

- To extract and characterize cellulose from BS, BP, and BL;
- To prepare and characterize MCC from BS, BP, and BL cellulose; and
- To evaluate the potential of MCC as a directly compressible pharmaceutical excipient.

3 MATERIALS AND METHODS

3.1 Materials

BP, BS, and BL were collected from Dilla Zuria Woreda, Gedeo Zone, South Ethiopia a local banana plantation. The voucher specimen (AW001/2023) of the plant, identified and authenticated by Melaku Wendaferash, is deposited at the National Herbarium of Addis Ababa Universit MCC (Avicel® PH-101) and paracetamol powder (China Associate Co Ltd,China) were kindly donated from Ethiopian Pharmaceuticals Manufacturing Factory Sh. Co. in Addis Ababa, Ethiopia. Acetic acid (99.5%) (Sigma-Aldrich, Germany), Formic acid (85%) (Central Drug House (P) Ltd. New Delhi, India), Cupric sulfate pentahydrate (98.5%), Potassium iodide, Zinc chloride (97%), Xylene (98%, extra pure), Silica gel (manufactured by Loba Chemie, India), Hydrogen peroxide (50%) Awash Melkas, Sodium hydroxide (98%) (Alphax chemical industry, India), Hydrochloric acid (37%) (BDH chemicals Ltd, Poole, England),Ammonium hydroxide solution (28%) (Carlo Erba reagents, France), Iodine (Hayashi pure chemical industries ltd) Sodium chloride (99.8%) (Oxford Laboratory, Mumbai, India), and Magnesium stearate (Bulvinos Chemicals Ltd, England), were used as received.

3.2 Methods

3.2.1 Extraction of cellulose from BS, BP, and BL

Cellulose fiber was extracted using the method described by Gabriel *et al*. (2020). The samples were cut to 2-3 cm in size and oven-dried. Then,oven-dried raw material was weighed and placed in a 3 L Erlenmeyer flask. The plant byproducts were pretreated with 5% NaOH at a solid/liquid ratio of 1/10 (w/v) on a water bath at 90 ℃ for 1.5 h. After repeated washing and filtration, the pulps were treated with a mixture of 20% formic acid/20% acetic acid/7.5% hydrogen peroxide (2:1:2) solution on a water bath at 90 ℃ for 1.5 h at a waste to liquor ratio of 1:10 with continuous washing with hot water. Finally, bleaching was performed using 7.5% hydrogen peroxide in alkaline media 5% of sodium hydroxide) at a 1:10 fiber ratio, first at room temperature, followed by heating on a water bath at 70 ℃ for 30 min each. The samples were washed continually with hot distilled water and finally dried in an oven (KOTTERMANN 2711, Germany) for 1 day at 60 ℃.

3.2.2 MCC Preparation

MCC was prepared following Battista's method (1950). Initial experiments involved investigating the effects of hydrochloric acid (HCl) concentration (2 and 2.5 N) and hydrolysis time (15, 20,30, and 45 minutes) on MCC properties. Optimal conditions were established, and MCC preparation proceeded accordingly. A 2.5 N HCl solution was prepared and heated to 105 °C. Cellulose was added to the boiling acid at a fiber-to-liquor ratio of 1:20 and the mixture was stirred with a magnetic bar for 30 minutes. After hydrolysis, the residue was filtered and washed with distilled water repeatedly. The slurry was then treated with a 5% ammonium hydroxide solution to neutralize the acid. The resulting MCC sample was washed again with distilled water until it was acid-free and then dried in an oven (KOTTERMANN 2711, Germany) at 100 ℃ until it had a constant weight.

3.2.3 Estimation of constituents of the plant materials

3.2.3.1. Determination of percent yield

The percent yield of cellulose and MCC were calculated using the following formula (Lin *et al*., 2010) .

$$\% \text{ Yield Cellulose} = \frac{\text{Weight of dry cellulose}}{\text{Weight of the original fiber sample}} X100\ \% \quad \text{.....Eq.1}$$

$$\% \text{ Yield MCC} = \frac{\text{Weight of prepared MCC (g)}}{\text{Original weight of dry cellulose (g)}} X100\ \% \quad \text{.....Eq.2}$$

3.2.3.2. Determination of the amount of hemicellulose in biomasses

To measure the amount of hemicellulose, 10 ml of a 0.5 mol/l solution of sodium hydroxide was added to 1 g of dry extract-free biomass (B) and the temperature was maintained at 80° C for 3.5 hours. The samples were then washed with deionized water until the pH of the solution reached 7 and then dried to constant weight (C). The difference in sample weight before and after this treatment was the hemicellulose content (Lin *et al*., 2010).

Amount of hemicellulose (g) = B - C.....Eq.3

3.2.3.3. Determination of the amount of lignin in biomasses

To determine the amount of lignin, 30 ml of 98% strength by weight sulfuric acid was added to each dry sample of free extractable. The samples were kept at ambient temperature for 24 hours and then boiled at 100 °C for 1 hour. The mixture was filtered and the residue was washed with distilled water until no sulfate ions were detected in the filtrate. The sample was dried in an oven at 110 °C until constant weight was obtained (D). The weight of the residue was recorded as the lignin content (Lin *et al*., 2010).

Amount of Lignin (g) =D…….....Eq.4

3.2.3.4. Determination of the number of extractives in biomasses

To 1 g of each fiber (banana leaf, banana pseudostem, and banana peduncle) (A), 60 mL of acetone was added. The sample was boiled at 90 °C on a hot plate for 2 h. The sample was then dried in an oven at 110 °C until constant weight was obtained (B). The number of extractives was calculated with Eq. 5 (Lin *et al*., 2010).

Amount of Extractives (g) = (A) - (B) ……...Eq.5

3.2.3.5. Estimation of aqueous extracts

Powder samples were treated with distilled water at 100° C for 2 hours, filtered, and dried at 105° C until constant weight was reached. The amount of aqueous extract was calculated as:

Aqueous extracts % = $\frac{W1}{W0} X100$…… Eq.6

where W_1 is the weight loss and W_0 is the initial weight of the sample (before treatment) (Yeasmin & Mondal, 2015).

3.2.4 Characterization of cellulose and microcrystalline cellulose

3.2.4.1 Organoleptic characteristics

The color, taste, odor, and physical appearance of cellulose and MCC samples were observed.

3.2.4.2 Chemical identification test

An iodinated zinc chloride solution was prepared by dissolving 20 g of zinc chloride and 6.5 g of potassium iodide in 10.5 mL of water. 0.5 g of iodine was added and shaken for 15 to 20 min, until well dissolved. 10 mg of cellulose or MCC samples were dispersed in

2 mL of the iodinated zinc chloride solution on a Petri dish. The color change from violet to blue was checked (Setu *et al.*, 2014).

3.2.4.3 Determination of water-soluble substances

5 grams of MCC powder were added to 80 ml of water. The mixture was stirred with a glass rod for 10 min and then filtered with filter paper. The filtrate was placed in a tarred evaporating dish (ED), evaporated in a water bath, and dried for about 1 h at 105 °C. The evaporating dish was cooled to room temperature in desiccators. The weight of the ED was recorded once it was cooled. Finally, the dry beaker was weighed, and the weight of the residue was recorded as the difference between the empty and residue beaker weights. The studies were conducted in triplicate, and the mean percentage values of water-soluble material were calculated (2018).

3.2.4.5 Determination Ash value

A crucible was cleaned and dried in the oven for 30 min at 100 °C. The crucible was cooled for 30 min in a desiccator containing silica gel. 3 g of BL-MCC, BS-MCC, BP-MCC, and Avicel PH 101 were placed onto the crucible (pre-weighed) and heated at a low temperature until the smoking ceased. The samples were charred for 2 h in muffle furnace (Nabertherm, Germany) at 550 °C, cooled for 45-60 min in a desiccator, and weighed. The ash value was calculated as the weight difference between the charred residue and the empty crucible after 2 h divided by the weight of the sample (USP-NF, 2022).

3.2.4.6 pH Determination and Conductivity Test

The pH test for cellulose and the pH and conductivity test for microcrystalline cellulose were performed according to the test procedures and specifications of USP-NF (2022). The tests were performed in triplicate using a calibrated pH-conductivity meter (HANNA, Romania, Europe). The USP specification for conductivity of MCC is not more than 75 µS/cm.

3.2.4.7 Microbial limit test

Ten grams of MCC were weighed into a sterile 250 mL Erlenmeyer flask. One hundred milliliters of sterile Ringer's solution containing 0.1% Tween 80 were added to the flask, and it was shaken vigorously for 15 minutes using a vortex mixer (IKA Vortex 4 Basic, Germany) to disperse the MCC. A 1.0 g portion of the dispersed MCC was then transferred aseptically to a sterile petri dish, and the inoculum was spread evenly over the surface using a sterile spatula. The Petri dish was incubated at 30-35°C for 48-72 hours (Sarstedt C,ELLstar , Germany). After incubation, the number of visible colonies on the plate was counted using a colony counter (Synbiosis ProtoCOL 3 , UK). The number of colonies was expressed as colony forming units (CFU) per gram of MCC. The MCC was deemed to meet the Microbial limit test (MLT) if the number of CFU per gram of MCC was less than or equal to the established microbial limit for MCC, which is 100 CFU/g (USP-NF, 2022).

3.2.4.8 Determination of Degree of Polymerization

Cu $(OH)_2$ was freshly precipitated and dissolved in aqueous ammonia to make the Cuam solution. To start, 28 g of $CuSO_4$.$5H_20$ were dissolved in 600 mL of distilled water and filtered into a beaker. Cu $(OH)_2$ can be precipitated by adding 14 mL of 25% aqueous ammonia. After the precipitate settles, a clear solution was decanted and the settling and decanting cycle was continued with distilled water until the decant liquid was sulfate-free**.** At ambient temperature, the moist sulfate-free Cu $(OH)_2$ was dissolved in 1000 mL of 25% ammonia solution. The viscosity method was used to determine the DP of B-C and B-MCC samples using an Ostwald capillary viscometer (BDH,England). 45 mg of samples was dissolved in 30 ml of Cuam solution to calculate DP. After a thorough shaking, the mixture was poured into a water bath at 25 ℃ for 5 min. After the sample had completely dissolved in the solvent, a suitable volume of the solution was transferred to an Ostwald capillary viscometer for viscosity measurement (Kaminska, 1997).

$$DP=\frac{200(\eta spec)}{C(1+0.29)\eta spec} \quad \text{Eq.7}$$

Where η_{spec}=specific viscosity; c is concentration in g/l, 0.29 is viscometer constant

$\eta spec= (\eta/\eta_0-1)$; $\eta spec$ is specific viscosity; η/η_0 is relative viscosity

$$\eta_{spec}=\frac{t}{t0}-1 \quad \text{Eq.8}$$

The efflux time, t, is the time (in seconds) required for the sample to travel from the upper graduated mark to the lower graduated mark, and t_0 is the time required for a pure solvent to travel from the upper graduated mark to the lower graduated mark.

3.2.4.9. Fourier Transform Infrared Spectroscopy (FTIR)

Perkin Elmer Fourier Transform Infrared Spectrophotometer (L1600400 Spectrum TWO DTGS, SN: 108152, LIantrisant, UK) was used to study the functional groups and chemical structure of BL-C, BS-C, BP-C, BL-MCC, BS-MCC, BP-MCC and Avicel PH-101 in the frequency range of 4000 – 400 cm^{-1}.

3.2.4.10 Scanning electron microscopy (SEM)

The structural morphology and particle size of the sample MCC and cellulose were evaluated using SEM (JSM-6500F, JEOL, Tokyo, Japan). The test was performed at a voltage of 20 kV. The gold layer was prepared on the surface of the sample to generate the conductivity of the surface and it was observed. All images were taken at 200x, 500x, and 1000x magnification.

3.2.4.11 X-Ray Diffraction (XRD)

The crystallinity of as-isolated cellulose, MCC sample, and Avicel PH 101 was analyzed using an XRD-7000 X-ray Diffractometer (SHIMADZU Corporation, Japan) with monochromatic Cu-Kα radiation at 40 kV and 30 mA. The scan speed was 3.0000°/min and the sampling pitch was 0.0200°. The acquired data was plotted in Origin Pro 2022 on a 2θ scale from 10 to 40 degrees (Gabriel *et al.*, 2020).

$$\text{CrI (\%)} = \frac{I200-Iam}{I200} \quad \text{Eq.9}$$

where CrI is the crystallinity index, I_{200} is the maximum intensity (in arbitrary units) of the diffraction from the 200 plane, and Iam is the intensity of the background scatter.

Crystal size was determined by Scherrer method (Eq.10)

$$L=\frac{\kappa\lambda}{\beta\cos\theta} \quad \text{Eq.10}$$

where L is the size of crystallite (nm), κ is the Scherrer constant (0.94), β is the full-width half maximum (FWHM) of the lattice plane reflection in radian and θ is the Bragg angle, and λ is the X-ray wavelength (1.54060 nm) (Trache *et al*., 2014).

3.2.4.12 Thermal analysis

Thermogravimetric analysis (TGA) was performed using a DTG-60H (SHIMADZU Corporation, Japan) to study the degradation characteristics of cellulose, MCC sample, and Avicel PH 101. The samples were heated from room temperature to 700 °C at a heating rate of 10 °C/min under a nitrogen gas flow rate of 60 mL/min. The weight loss (%) at the cellulose decomposition temperature, as well as the residual char (percentage) at 700 °C, were determined (Gabriel *et al*., 2020).

3.2.4.13 Density and related properties

Hausner ratio and Carr's index, bulk, and tapped density of MCC powders were determined according to the method described in USP-30/NF-25 (2022).

3.2.4.13.1 Bulk Density

The Bulk density of each MCC sample was determined using 30 g of powder sample placed in a measuring cylinder and the volume occupied was measured. The bulk density of a powder was calculated as a ratio of the mass of the untapped powder sample and its volume including the contribution of the inter particulate void volume expressed in grams per milliliter (g/mL).

Bulk Density=$\frac{m}{Vb}$……Eq.11

Where m- the mass of the untapped powder sample, vb- apparent volume

3.2.4.13.2. Tapped density

The measuring cylinder was placed in the tapped densitometer (ERWEKA , Germany) and the sample was tapped 10, 500, and 1250 times in order (plus 1250 times for subsequent taps, if necessary). Tapping was ceased when the volume variation was no more than 2 mL. Tapped density was calculated based on the ratio of weight to tapped volume. The average of three readings was used to calculate the tapped density (g/mL).

Tapped density=$\frac{m}{Vt}$ ……Eq.12

Where, m- weight of powder, Vt- tapped volume

3.2.4.13.3 Carr's Index and Hausner Ratio

The bulk density and tapped density data were used to generate Carr's Compressibility Index and the Hausner ratio.

$$\text{Carr's Index}=\frac{(Tapped\ density-Bulk\ density)}{Tapped\ density}X100 \quad \text{Eq.13}$$

$$\text{Hausner ratio (HR)}=\frac{\text{Tapped density}}{\text{Bulk density}} \quad \text{Eq.14}$$

3.2.4.13.4 True Density

The true density MCC powder sample was determined using the liquid displacement method using xylene as the immersion fluid, as described by Ohwoavworhua & Adelakun (2007) . A cleaned glass bottle was filled with xylene and then weighed after wiping away any spilled xylene. A similar bottle was emptied and carefully cleaned, and 2 g of MCC powder sample was added. To release air bubbles, the bottle was half-filled with xylene and swirled with a glass rod. Finally, the bottle was filled to the brim with xylene, and the weight of the bottle was recorded as (b). The following equation was used to calculate MCC's true density.

$$Dt=\frac{W}{\{a+w\}-b}XSg \quad \text{Eq.15}$$

Where the weight of the powder is w, the specific gravity of xylene is Sg(g/ml) 0.85, the weight of the container + xylene is a, and the weight of the bottle + xylene + powder is b.

3.2.4.13.5 Porosity

Using the method proposed by Kambli *et al*., (2017b) the porosity of MCC Powders was calculated using the bulk and tapped density data.

$$E=1-\frac{Db}{Dtrue} \quad \text{Eq.16}$$

Where D_{true} is the true density of MCC, D_b is the bulk density.

3.2.4.14 Determination of moisture content

To determine the moisture content of MCC, a 3 g sample was accurately weighed in a dry Petri dish and dried for 3 hours at 105 °C. The sample was then cooled in a desiccator and reweighed. The weight loss was recorded, and the process of drying, cooling, and reweighing was repeated until the weight remained constant. The moisture content was then calculated using the following equation (Abdel-Halim, 2014).

Moisture content % $=\frac{(W1-W2)100}{W1}$……Eq.17

Where W1- is the initial weight of the sample before drying & W2-weight after drying in g, respectively.

3.2.4.15 Particle size analysis

Particle size analysis was performed using Malvern Mastersizer 2000 laser diffraction particle- size analyzer. A small amount of the MCC sample was dispersed in distilled water (soaking into the sample port of the instrument) until an obscuration of 15 - 20% was obtained. Determinations were done in triplicates. The mean volume particle size distribution, specific surface area, percentile distribution, and mean particle size of samples were determined with the software (El-Sakhawy & Hassan, 2007).

3.2.4.16 Determination of Moisture Sorption Pattern

Five different relative humidity levels were prepared in Pyrex desiccators using distilled water (100% RH), 40%, 31.58%, and 24.66% of NaOH solutions (20%, 40%, and 60% RH, respectively) and saturated solution of NaCl (75.6% RH). MCC samples were pre-dried in an oven for 4 h at 120 °C. Three pre-weighed dry plastic plates, each containing two grams of pre-dried MCC sample, were placed in the five different RH chambers. Samples were equilibrated for four weeks. After four weeks the moisture uptake of each sample was determined and calculated as the weight difference of before and after equilibration in a given RH. Water sorption capacities of the MCC samples were expressed as percent moisture uptake (Stubberud *et al.*, 1996).

3.2.4.17 Hydration capacity

Four 15-ml plastic centrifuge tubes were each loaded with 1 gram of MCC. Then, 10 ml of distilled water was added to each tube. The tubes were vigorously shaken and allowed to stand for 20 minutes, with shaking every 5 minutes. Next, the tubes were centrifuged for 15 minutes at 2000 rpm in a centrifuge (Beckman Coulter Allegra 64R,Germany). The supernatant was decanted, and the tubes were drained for 10 minutes at a 45-degree angle. The tubes were then weighed, and the hydration capacity was determined using Equation 18.

Hydration capacity = $\frac{W2}{W1}$…… Eq.18

Where:W2 is the weight of hydrated MCC (g),W1 is the initial weight of MCC (g) (Ejikeme, 2008).

3.3 Preparation and Evaluation of Tablets

3.3.3 Dilution Potential Study

To evaluate the dilution potential of BS-MCC, BP-MCC, and Avicel PH 101, binary mixtures were prepared comprising 400 mg of paracetamol and varying concentrations of MCC (35%, 45%, 55%, and 65%). The poorly compressible model drug was used to assess the excipient's dilution potential (Benabbas *et al*., 2021). These mixtures were designated BS-MCC, BP-MCC, and Avicel PH101 and were blended using a Turbula® mixer (Willy A. Bachofen AG, Maschinefabrik, Basel, Switzerland) for 10 minutes. Subsequently, paracetamol tablets were manufactured using a tablet compression machine (3D3, Germany). The compression force was adjusted to achieve a crushing strength between 40 and 100 N for the standard Avicel PH-101 formulation. The mixture was subsequently compacted into 400-milligram tablets using a rotary tablet press equipped with 11 mm diameter punches, applying a constant compression force.

3.3.1 Tablet Compression

Tablets made with three different types of MCC: plain BS-MCC, BP-MCC, and Avicel PH-101, were compressed in a rotary tablet compression machine (D3D, Germany) to study their mechanical properties. The desired compression force was determined indirectly using the crushing strength of tablets compressed with plain Avicel PH-101 tablet with hardness of 115 N.

3.3.2 Lubricant Sensitivity Ratio

The lubricant sensitivity ratio (LSR), which is defined as the reduction in crushing strength when MCC powders are mixed with a lubricant, will be used as a quantitative measure to express the sensitivity of MCC powders when mixed with a lubricant. The LSR is the ratio of the decrease in tablet breaking force values due to lubricant mixing to the breaking force values of unlubricated tablets. The following equation was used to calculate the lubricant sensitivity ratio (Almaya & Aburub, 2008)

$$LSR=\frac{To-TL}{To}$$ ……. Eq.19

Where, T_O and T_L are the breaking force values of tablets prepared without and with a lubricant, respectively.

3.3.4 Drug-Excipient Interaction Study

Drug-excipient interaction was studied by using FTIR spectroscopy and Differential scanning calorimetry (DSC) by taking the FTIR spectra of paracetamol powder alone and its physical mixture with the prepared MCC powder and Avicel PH-101 (at a mixture of 1:1 ratio) following the procedure outlined in section 2.5.6 (Chadha & Bhandari, 2014).

DSC was performed on pure paracetamol (PCM) API powder, PCM – BS-MCC (1:1) mixture, and PCM–BP-MCC (1:1) mixture. Five milligrams of the sample was weighed into an aluminum pan. Each sample was heated from 40 °C to 445 °C (by using PerkinElmer DSC 4000, USA) under nitrogen at a flow rate of 10°C/min.

3.3.5 Weight and thickness

Twenty randomly selected tablets from each batch were weighed individually on an analytical balance (Mettler Toledo, PR 203, Switzerland). The average weight and standard deviation were calculated. Tablet thickness and diameter were measured using a sliding caliper scale (Nippon Sokutei, Japan).

3.3.6 Crushing strength

The diametrical crushing strength of the tablets was determined using an electronic hardness tester (Caleva, THT2, England). After 24 hours of production, ten tablets were taken from each batch and their crushing strengths were measured.

3.3.7 Tensile strength

The radial tensile strength was calculated using the data obtained from crushing strength, diameter, and thickness of tablets according to the following equation.

$$TS=\frac{2F}{\pi DT} \quad \text{Eq.20}$$

Where TS is the tensile strength, F is the crushing strength, D is the diameter of the tablet, and T is the tablet thickness.

3.3.8 Friability test

Ten randomly selected tablets from each batch were weighed collectively. The tablets were then placed in a twin drum electronic friabilator (ERWEKA, TAR 20, Germany) and subjected to combined abrasion and shock for 4 min at 25 rpm. The tablets were then de-dusted and re-weighed, and the percentage of weight loss was calculated as friability.

3.3.9 Disintegration Time

The disintegration test was performed according to USP 30/NF 25 specifications (2022). Six randomly selected tablets from each batch were placed in a disintegration tester (ERWEKA, DT504, Germany) filled with distilled water at 37 ± 2 °C. The tablets were considered completely disintegrated when all of the particles passed through the mesh.

3.3.10 Construction of Calibration Curve

A stock solution of 200 µg/ml paracetamol in pH 5.8 phosphate buffer was prepared. Nine different concentrations (3.5, 5, 6.5, 8, 9.5, 11, 12.5, 14, and 15.5 µg/ml) were prepared from this stock solution. The UV absorbance of these solutions was measured using UV/VIS (ERWEKA, DT600, Germany) at 243 nm in triplicate. As a blank, phosphate buffer (pH = 5.8) was utilized. The absorbance of the solutions was plotted against their concentration, and a linear regression equation and correlation coefficient were calculated (USP-NF, 2022).

3.3.11 *In Vitro* Drug Release Study

Dissolution using specification, utilizing a Type II paddle method (ERWEKA, DT600, Germany) stirred at 50 rpm and 900 ml phosphate buffer (pH 5.8) as the dissolution medium at 37±0.5 ° C. Six tablets were randomly chosen from each batch and used simultaneously for the study. At 5, 10, 15, 20, 30, 45, and 60 min, five ml aliquots of the dissolution medium were withdrawn and filtered using filter paper. To maintain a sink condition, an equal amount of fresh medium was transferred into the dissolution vessel at the same temperature. The absorbance was measured with a UV/Visible spectrophotometer at 243 nm after one milliliter of the filter sample was diluted to 25 mL with fresh dissolving medium. As a blank, phosphate buffer (pH = 5.8) was used. After all of the necessary dilution corrections were made, the drug content and cumulative drug release were calculated from the absorbance data (USP-NF, 2022).

3.4. Data Analysis Procedures

A one-way analysis of variance (ANOVA) was performed using Origin 2022(version 10.0) (OriginLab Corporation, MA, USA) and Excel 2019 statistical software to compare the physicochemical properties of MCC powders and their tablet properties. Tukey's multiple comparison test was used to identify the groups that were significantly different from each other. Powder and tablet properties were analyzed at a 95% confidence level ($\alpha = 0.05$). P-values less than 0.05 were considered statistically significant. The results are reported as the mean and standard deviation (SD) of a sufficient number of measurements (specified in each task).

4. RESULTS AND DISCUSSION

4.1 Physicochemical properties of cellulose and microcrystalline cellulose

4.1.1 Extraction condition of Cellulose and MCC

This study extracted, characterized, and evaluated banana fiber (BL, BS, and BP) cellulose as new compressible excipients, following the method of Gabriel *et al*., (2020). Cellulose was extracted from banana fiber using an alkaline treatment, formic acid, acetic acid, hydrogen peroxide treatment, and final bleaching procedure. Extracting cellulose fibers from banana fibers requires the removal of other components such as lignin, hemicellulose, and pectin (Elanthikkal *et al*., 2010). In the preliminary study, different concentrations of NaOH (5%, 10%, and 17.5%) were taken in the first stage of alkaline treatment. In the second stage, we sequentially decreased the FA/AA/H_2O_2 percentage ratio from 85%/100%/10% to 40%/40%/10% and then to 20%/20%/7.5%. The final bleaching process was performed at the end of the treatment process. According to the preliminary studies, there was no noticeable change in the cellulose content or whiteness under the above treatment conditions. The extracted cellulose from the banana leaf, banana pseudostem, and banana peduncle was white and fibrous in appearance, as shown in Figure 5.

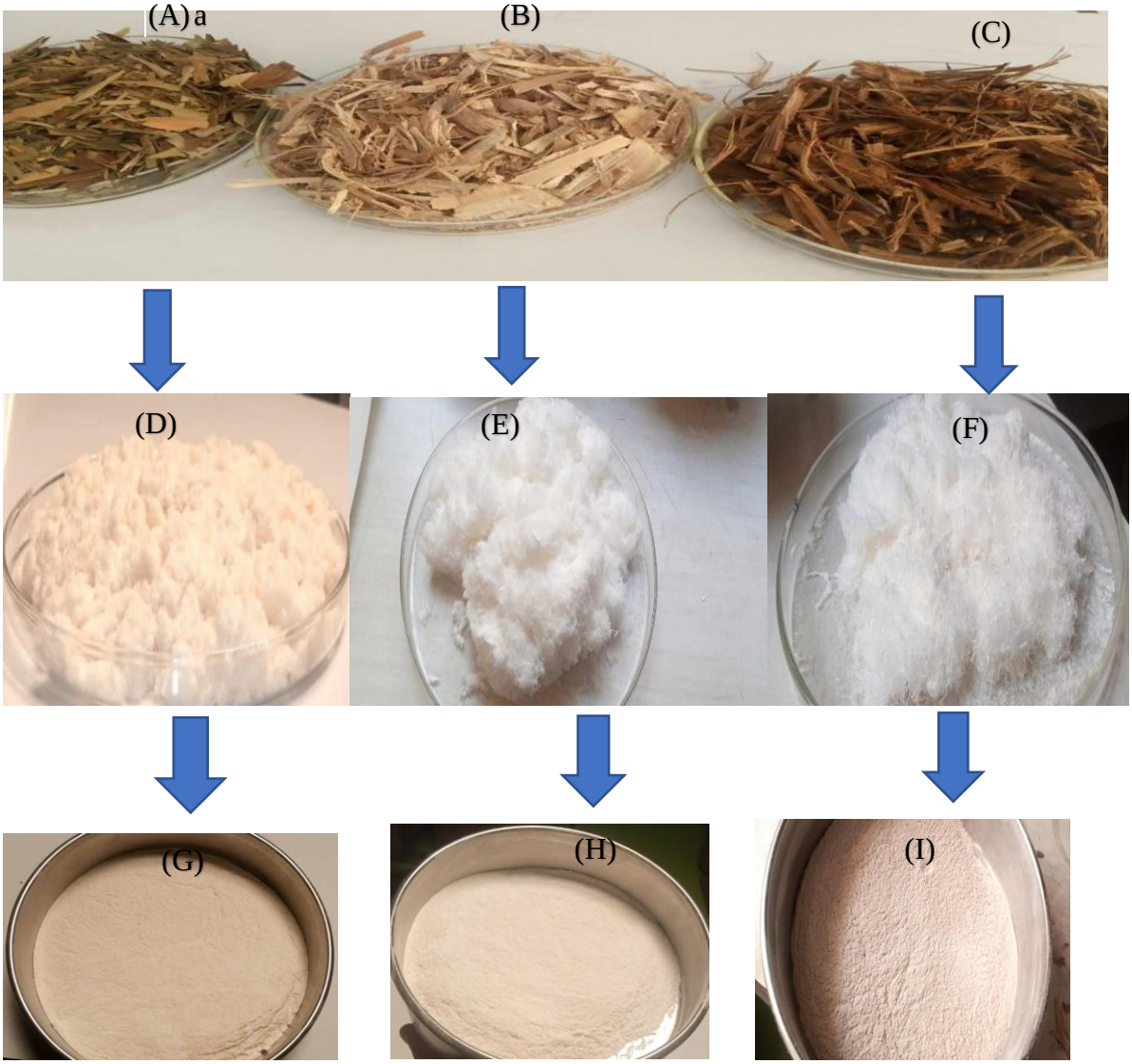

Figure 5:a.Banana leaf, b.Banana Pseudostem, c.Banana punducle, d banana leafcellulose , , e.Banana Pseudostem cellulose , Banana punducle cellulose , g. Banana leaf microcrystalline cellulose , h.Banana Pseudostem microcrystalline cellulose and i.Banana punducle microcrystalline cellulose (pictures taken by Amanuel W/silasse).

Hydrogen peroxide improved the brightness of the sample by generating active hydroperoxide anions (HOO-) in alkaline conditions, which then reacted with the quinone structure and conjugated side chains of lignin to eliminate its chromophoric groups (Wang

et al., 2022). Some lignocellulosics can be efficiently removed of their lignin and hemicelluloses using acetic acid and formic acid (Jahan *et al.*, 2011).

Various extraction procedures have yielded white, fluffy, and fibrous celluloses from plant byproducts. The percent yield and purity of cellulose and MCC extracted from plant biomass are mainly affected by the extraction method, the type of starting biomass, and critical extraction process variables, such as the extraction solvent type, extraction time, and extraction temperature (Adel, El-Wahab, *et al.*, 2011). Pulping banana waste with sodium hydroxide is effective at removing lignin (Nada *et al*., 2010).

4.1.2 Chemical composition of Banana Leaf, Banana pseudostem, and Banana peduncle

The yields of cellulose and microcrystalline cellulose (MCC) from banana leaves (BL), pseudostem (BS), and peduncle (BP) are shown in Table 1. The highest cellulose yield was obtained from BP (45±0.8%), followed by BS (37.33 ±1.4%) and BL (23.1± 1.41%). The yields of MCC from BP, BS, and BL were 87.3±1.4%, 85±0.7%, and 77.5±0.4%, respectively. The yield of BS-C was comparable with the yield of cellulose from Teff straw at 35.2% (Getachew *et al*., 2023).

The yields of cellulose from banana leaf (BL-C) and banana peduncle (BP-C) were consistent with those reported by Fernandes *et al.*, (2013) and Mukwaya *et al.* (2017) which were 26.7% and 44.44%, respectively. The yield of cellulose from the banana pseudostem (BS-C) was 39.12% (Li *et al*., 2010) which is comparable to that of BP-C but higher than those of BL-C and BS-C reported in previous studies. The cellulose content of the banana fibers was lower than that reported for alfa fibers 45% (El Achaby *et al.*, 2018) and Enset fibers 60% (Gabriel *et al.*, 2020).

In comparison to the other biomasses, MCC made from soybean hulls - 83.9% (Merci *et al.*, 2015), breadfruit seed hulls - 86.8 % (Nwajiobi *et al.*, 2019), kenaf bast - 80.9% (Aprilia *et al*., 2016), and Sacred Bali Bamboo - 83.3% (Abdul Khalil *et al*., 2018) had comparable yields with BP-MCC and BS-MCC. The yield of BP-MCC in this study was also higher than the yield from bean and rice hulls (77.58%) and (73.84%), respectively (Adel, *et a*l., 2011) but comparable with the yield of BL-MCC.

The MCC yields from BP-MCC and BS-MCC were comparable to those of MCC from other biomasses, such as soybean hulls (Merci *et al.*, 2015) breadfruit seed hulls (86.8%) (Nwajiobi *et al.*, 2019), kenaf bast (80.9%) (Aprilia *et al.*, 2016), and Sacred Bali bamboo (83.3%) (Abdul Khalil *et al*., 2018). The BP-MCC yield in this study was also higher than the yields from bean hull (77.58%) and rice hulls (73.84%) (Adel, *et a*l., 2011), but comparable to the yield of BL-MCC as shown in Table 1.

Despite the high yields of MCC obtained from this study from BS-MCC, and BP-MCC even higher yields have been reported for MCC from other biomasses, such as cornhusk fibers (98.2%) (Kambli *et al*., 2017a), Sacred Bali bamboo (93.3%) (Khalil *et al*., 2018), Muli bamboo (92.5%) (Pachuau *et al.*, 2014), jute (88.3%) (Jahan *et al*., 2011), and rice straw (90.2%) (Fan *et al.*, 2017). Researchers have suggested that the variations in MCC yields are likely due to the sources of the raw materials and how they were processed or pretreated (Kale *et al.*, 2018).

The chemical composition of BL, BS, and BP are summarized in Table 1. They are composed of hemicellulose lignin and an amount of extractive.

Table 1: Composition of Banana Leaf, Banana pseudostem, and Banana peduncle.

Composition of banana parts	Banana plant parts (Mean ± SD) (n=3)		
	BP	BS	BL
Cellulose %	45±0.8	37.33±1.4	23±1.41
MCC %	87.3±0.6	85±0.7	77.5±0.4
Hemicellulose %	19.66±0.8	22±0.47	25±1.24
Lignin %	18±0.4	20.1±0.6	28..5±0.4
Amount of Extractive	22±0.8	20 ±0.4	16.5±0.4

BP**:** Banana peduncle, BS: Banana pseudostem, BL**:** Banana Leaf

4.1.3 Organoleptic characteristics and chemical identification test

The prepared cellulose and MCC samples all met the USP/NF requirements for organoleptic qualities (USP-NF, 2022). Prepared cellulose and microcrystalline cellulose were all white, flavorless, and odorless. The physical characteristics of cellulose and MCC are fibrous cellulose and fine powders, respectively.

4.1.4 pH, water-soluble substance, and conductivity

All of the developed MCC samples have acceptable pH values, water-soluble substance contents, and conductivities, as shown in Table 2. The conductivity of a solution of MCC in water should not exceed 75 µS/cm to ensure that the product is free of ionic impurities, such as salts and metals, which could affect its performance as a pharmaceutical excipient (USP-NF, 2022).

Table 2: Ash value, pH, moisture content, water-soluble substances, and hydration capacity of microcristaline cellulose (MCC).

Test parameter	Types of MCC and test results				
	BL-MCC	BS-MCC	BP-MCC	Avicel PH 101	Standard as per USP
Moisture content (%)	5.27±0.16	5.36±0.21	5.53±0.20	5.2±0.08	<7
pH	5.9±0.21	6.2±0.26	6.1±0.27	6.6±0.3	5-7
Ash (%)	0.07±0.1	0.05±0.01	0.04±0.01	0.07±0.01	< 0.1
Water soluble substance %	0.24±0.008	0.20±0.01	0.21±0.01	0.18±0.008	≤0.25%
Conductivity	72.3±1.69	67±2.16	63.6±2.62	40.6±1.69	≤ 75 µS/cm
Organoleptic characteristics	white, flavorless, and odorless	white, flavorless, and odorless	white, flavorless, and odorless	white, flavorless, and odorless	white, flavorless, and odorless
DP	270	265	255	240	<350
Microbial tests	absent	absent	absent	absent	absent

BL-MCC**:** Banana Leaf microcrystalline cellulose BS-MCC: Banana Pseudostem microcrystalline cellulose BP-MCC Banana punducle microcrystalline cellulose DP: degree of polymerization (DP)

4.1.5 Microbial Test

All samples of microcrystalline cellulose (MCC) and Avicel PH 101 tested negative for microbial growth, as shown in Table 2.Tests for specific microorganisms: These tests are performed to detect the presence of specific microorganisms, such as *St aphylococcus aureus*, *Pseudomonas aeruginosa*, *Escherichia coli*, and *Salmonella species* (USP-NF, 2022). Microbiological testing of MCC is an important part of quality control for pharmaceutical products. By ensuring that MCC is free of microbial contamination, manufacturers can help to ensure the safety and efficacy of their products.

4.1.6 Moisture content

The moisture content of BL-MCC, BS-MCC, BP-MCC, and Avicel PH-101 was determined by drying the samples at 105 °C for 3 h. The drying loss percentages were 5.27%, 5.36%, 5.53%, and 4.8%, respectively as shown in Table 2.

The drying loss percentages show that the moisture content of all samples was around 5% wt/wt, which is within the acceptable range of 5-7% wt/wt (USP-NF, 2022). The drying loss values observed in this study are comparable to those reported in other studies, such as 4.5% for Sacred Bali Bamboo-MCC (Abdul Khalil *et al.*, 2018), 5.3% for BS-MCC (Shanmugam *et al*. 2015) and 5.75% for *Ensete glaucum* MCC (Pachuau *et al*., 2019). It is important to note that MCC used to produce tablets in medicine should not have more than 5% moisture. This is because large concentrations of water molecules can act as plasticizers, changing the mechanical properties of the MCC and reducing the strength of the tablets that are formed (Khalil *et al*., 2018). Additionally, a higher fiber moisture content can decrease the mechanical properties of polymer composites (Jumaidin *et al*., 2017).

The moisture content of MCC has a significant impact on its tabletability, compaction properties, and tensile strength, (Pachuau *et al*., 2019). Extra moisture in MCC can also promote microbial growth and degradation (Khalil *et al*., 2018).The compressibility of MCC depends on its moisture content, which means that MCC powders with different moisture contents may not produce the same compact porosity when compressed at the same compression pressure (Abu-Thabit *et al*., 2020b)

Moisture may increase cohesion by forming liquid or even solid bridges between particles, which may reduce frictional forces and electrostatic charges between particles as moisture content increases. In the case of MCC, significant changes in flowability were seen as powder cohesiveness, as measured by the compressibility index , increased with rising moisture contents (Crouter & Briens, 2014).

4.1.7 Ash value

The total ash content of BS-MCC, BP-MCC, BL-MCC, and Avicel PH 101 was 0.06%, 0.04%, 0.08%, and 0.07%, respectively, as shown in Table 2. This indicates that all MCC samples are nearly free of inorganic compounds and comply with the U.S.P. requirements

that the ash content not exceed 0.1%. Similar to this study, MCC powder made from banana fiber had an ash value of 0.07%, which is very close to the ash content (0.06%) of a commercial sample (Shanmugam *et al,* 2010). The very low inorganic components typically found in cellulosic materials and the proper MCC preparation may be the reasons for the low amount of ash (Ejikeme, 2008).

4.1.8 Hydration capacity

Hydration capacity is the ability of a material to retain water even after being exposed to external forces such as heat, centrifugation, or pressure. It is directly correlated with the degree and range of polymer porosity. The amount of water that a substance can absorb is determined by its hydration capacity (Nwajiobi *et al*., 2019). The hydration capacity of BL-MCC, BS-MCC, BP-MCC, and Avicel PH-101 was 1.09, 1.07, 1.11, and 1.05, respectively. This shows that the MCC made from banana peduncle fibers had a higher capacity to absorb water than Avicel PH-101. Similarly, a study found that MCC made from cornhusk has a water absorption capacity four times its weight (Kambli *et al*., 2017a).

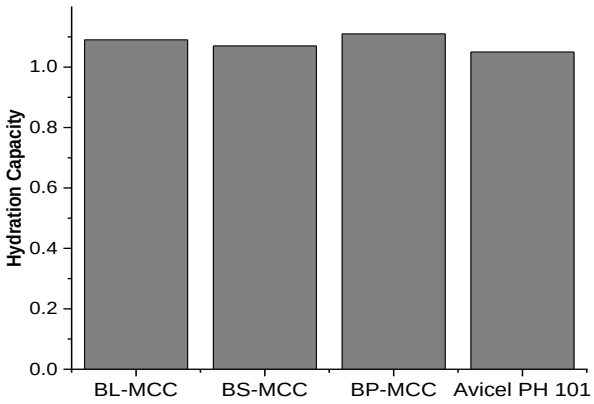

Figure 6:Hydration capacity of Banana Leaf microcrystalline cellulose, Banana Pseudostem microcrystalline cellulose, Banana punducle microcrystalline cellulose and Avicel PH 101.

4.1.9 Degree of polymerization

The degree of polymerization (DP) values of BL-C, BP-C, and BS-C were found to be 566, 598, and 570, respectively, while those of BL-MCC, BS-MCC, BP-MCC, and Avicel

PH 101 were 270, 265, 255, and 240, respectively. These results align with those reported in previous studies, such as Shanmugam *et al*.,(2015), who determined a DP of 267 for banana fiber-MCC, and Pachuau *et al*.,(2014), who reported a DP of 248.5 for Muli bamboo-MCC. Another study by Huang *et al*.,(2012) found that sugarcane bagasse cellulose and MCC had DPs of 560 and 189, respectively.

However, the DP of MCC does not necessarily correlate with its tabletability. For example, powdered cellulose has a higher DP than MCC but is less tabletable. Trache *et al*. (2014) also found that the degree of polymerization of MCC does not have to be linked to its tabletability. Other studies have reported DPs of 178 and 108 for banana waste-MCC and rice straw-MCC, respectively (Ibrahim *et al*., 2013).Softwoods generally exhibit lower cellulose DP compared to hardwoods, with published DP values ranging from 500 to 2500 (Shlieout *et al*., 2002; Isogai et al., 2008; Hubbell & Ragauskas, 2010).

The lower degree of DP of BL, BS, and BP MCC is attributed to the harsh chemical treatments employed to extract cellulose from banana waste. These treatments can induce the degradation of cellulose chains, consequently leading to a reduced DP. During hydrolysis, the DP of cellulose exhibits an exponential decline, as depicted in Table 3. This process is substantially influenced by reaction conditions, including temperature, acid concentration, and reaction duration (Thabit *et al*., 2020).

Studies have demonstrated that MCC types with a higher DP exhibit enhanced water absorption capabilities compared to those with a lower DP (Shlieout *et al*., 2002). Owing to its critical role in determining cellulose properties, DP serves as an identity test in pharmacopoeia standards. MCC , a widely used pharmaceutical excipient, is defined as having a DP below 350 glucose units (Liao *et al*., 2012).

The molecular weights of BL-MCC, BS-MCC, BP-MCC, and Avicel PH 101 were 43740 g/mol, 42930 g/mol, 41320 g/mol, and 38880 g/mol, respectively, as seen in Table 3. A severe loss in molecular weight due to acid hydrolysis, especially to the level-off degree of polymerization (LODP), may be undesirable, as it can lead to a reduction in the mechanical strength of regenerated cellulosic materials (Acharya *et al*., 2021). Moreover, the DP of MCC directly correlates with its molecular weight (Liao *et al*., 2012).

Table 3. DP and Molecular weight of banana leaf cellulose. Banana Pseudostem cellulose, Banana punducle cellulose. Banana leaf microcrystalline cellulose. Banana Pseudostem microcrystalline cellulose and. Banana punducle microcrystalline cellulose and Avicel PH 101.

Sample		DP	Molecular weight (g/mol)
BL	Cellulose	566	91692
	MCC	270	43740
BS	Cellulose	570	92340
	MCC	265	42930
BP	Cellulose	598	96876
	MCC	255	41310
Avicel		240	38880

BL-C:Banana leafcellulose,BS-C:Banana Pseudostem cellulose ,BP-C: Banana punducle cellulose BL-MCC:Banana leaf microcrystalline cellulose,BS-MCC: Pseudostem microcrystalline cellulose and BP-MCC: Banana punducle microcrystalline DP: degree of polymerization

4.2 Fourier Transform Infrared (FTIR) Spectra Analysis

A powerful method for studying the physicochemical and structural characteristics of polymers is FTIR spectroscopy (Khalil *et al*., 2018). Determining the presence or absence of functional groups in compounds is the simplest method to determine chemical structural changes. To analyze the functional groups contained in the structure, FTIR spectra for each sample were taken**.** All samples showed two different absorbance regions, which are located at high wavenumbers (between 2800 and 3500 cm^{-1}) and low wavenumbers (between 500 and 1700 cm^{-1}) (Wanrosli *et al.*, 2011; Haafiz *et al*., 2013).

Figures 6 and 7 show the FTIR spectra of cellulose and MCC from BL, BP and BS in comparison with Avicel PH101. The broad absorption band at 3316 cm^{-1}, 3312 cm^{-1}, 3319 cm^{-1}, and 3313 cm^{-1} in all MCC samples is caused by the intramolecular hydrogen-bonded O-H stretching vibration (Trache *et al*., 2016b). The band at 2888 cm^{-1}, 2883 cm^{-1}, 2882 cm^{-1}, and 2889 cm^{-1} is caused by the presence of $-CH_2$ groups in the MCC samples (Haafiz et al., 2013).

The absorption peaks at 1635 cm^{-1}, 1643 cm^{-1}, 1642 cm^{-1}, and 1629 cm^{-1} in cellulose and 1630 cm^{-1}, 1633 cm^{-1}, 1636 cm^{-1}, and 1630 cm^{-1} in MCC indicate water absorption. This

band is related to the bending modes of water molecules due to a strong interaction between cellulose and water (Johar *et al*., 2012)**.** The absence of peaks between 1509 and 1609 cm^{-1} indicates that the lignin has been completely removed (Nwajiobi *et al.*, 2019). If the absorption band that corresponds to the acetyl or uronic ester group of hemicelluloses is absent in the range of 1700–1740 cm^{-1}, hemicelluloses have been removed (Haafiz, *et al*., 2013).

The bands at 1031 cm^{-1}, 1032 cm^{-1}, 1033 cm^{-1}, 1035 cm^{-1}, 1027 cm^{-1}, 1029 cm^{-1}, 1030 cm^{-1}, and 1034 cm^{-1} in cellulose and MCC samples, respectively, indicate C-O stretching vibration at C-3 and C-C stretching (Kambli *et al*., 2017b). The absorption band at 898 cm^{-1} is attributed to the O-H group out-of-plane deformational vibration, defining the glycosidic linked C-O-C stretching at -(1, 4)-glycosidic links (Abdel-Halim, 2014).

Peaks in the range of 450 to 900 cm^{-1} indicate the presence of aromatic ring stretching in C-C bonds (Kumar *et al*., 2020). The absence of the absorption peak at 1740 cm^{-1} in the spectrum of the prepared MCC indicates that the hemicellulose has been removed (Kalita *et al*., 2013). The produced MCC samples have comparable crystalline characteristics to Avicel PH101 and exhibit a similar magnitude of peak shifting towards a higher wave number and a higher level of broadband in this region as the prepared MCC.

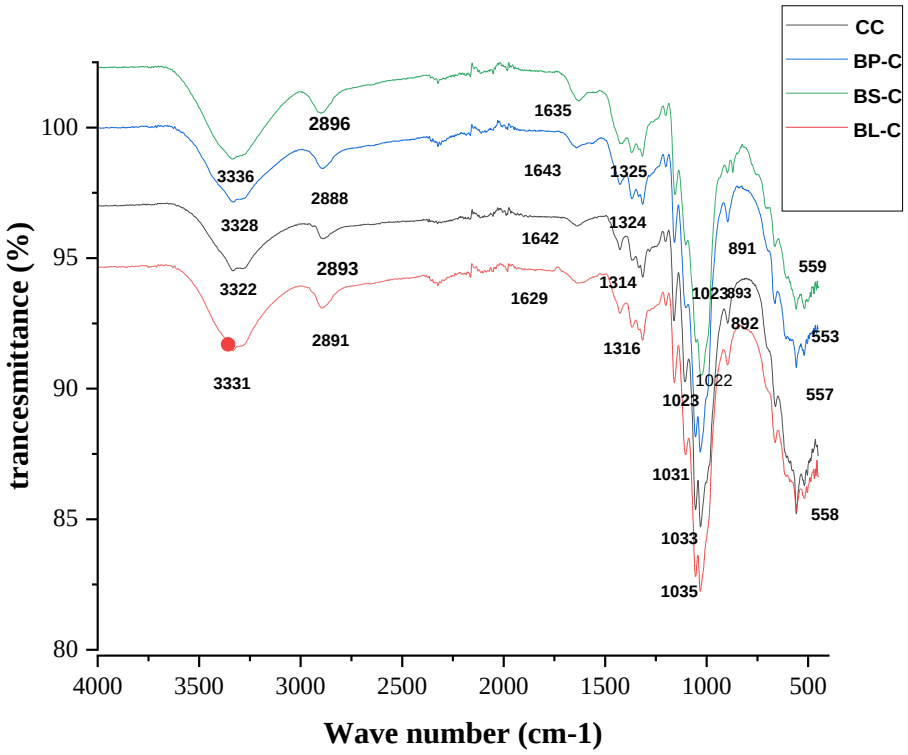

Figure 7: FTIR spectra of Banana Leaf cellulose (BL-C), Banana pseudostem cellulose (BS-C), Banana peduncle cellulose (BP-C), and commercial cellulose (CC).

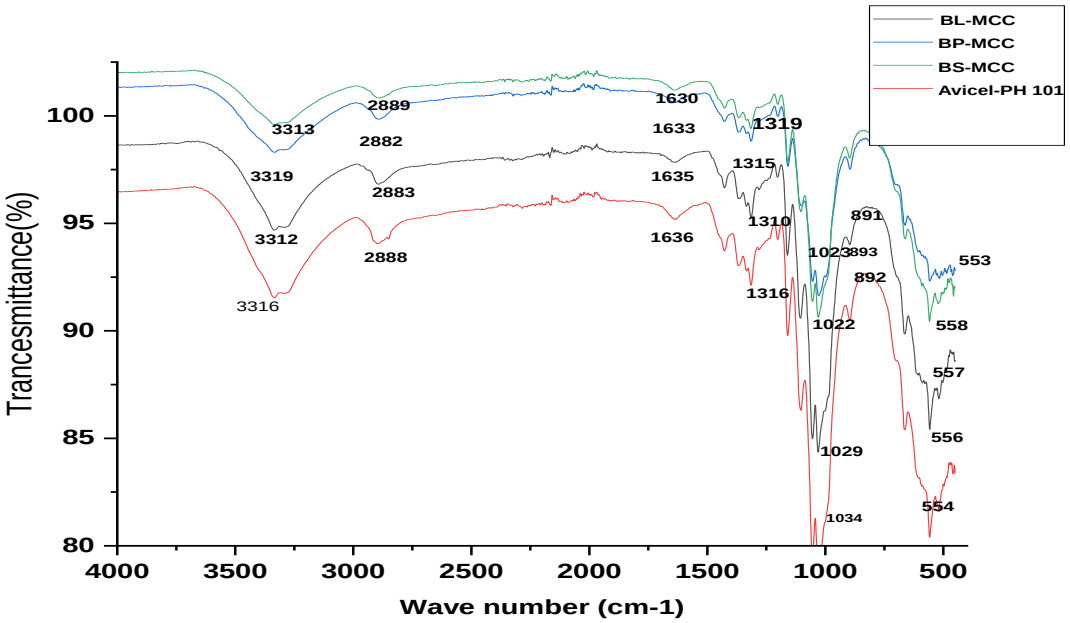

Figure 8: FTIR spectra of Banana Leaf microcrystalline cellulose (BL-MCC), Banana pseudostem microcrystalline cellulose (BS-MCC), Banana peduncle microcrystalline cellulose (BP-MCC), and Avicel PH 101.

4.3 X-ray diffraction (XRD) Analysis

XRD analysis is a non-destructive technique used to identify the crystal structure, phase composition, and other physical properties of materials (Sainorudin *et al.*, 2018). It is used to study the crystalline structure of fibers, which have both crystalline and amorphous regions (Kale *et al.*, 2018). The Crystallinity index (CrI) was calculated by dividing the difference between the height of the highest diffraction peak and the height of the minimum intensity between the major peaks by the peak intensity (French *et al*, 2013).

Figure 9 shows the X-ray diffraction patterns of cellulose and MCC samples prepared from BL, BS, and BP, as well as a commercial Avicel PH-101 sample. All samples have similar patterns, with the main peaks at 15.6, 16.9, 22.8, and 34.6 degrees 2-theta. Also, it indicate that all samples have an I_β type of cellulose structure (French *et al.*, 2013). This is the most common type of cellulose found in nature, and it was not altered by the chemical treatments used to make the MCC samples (Fouad *et al.*, 2020).

The absence of a doublet in the intensity of the mean peak indicates that all samples have the characteristic crystal structure for cellulose I, as illustrated in Figure 9 (Adel *et al.*, 2011). The minimum intensity in the vicinity of the suggested sites for the intensity of the

amorphous fraction (18° 2θ for cellulose I_β and 16° 2 θ for cellulose II) was then used to determine the CI for these patterns (Okhamafe & Rogers, 2012).

The influence of the hydrolysis process on the crystallinity or orderliness of the resultant cellulose fiber species has been studied. As seen in Figure 9, the cellulose that passed the hydrolysis process was more crystalline than the cellulose fibers as evidenced by the sharper primary intensity peak at $2\theta = 22.72^{o}$ with increased intensity. According to the X-ray results, the hydrolysis of glycosidic links in the accessible parts of cellulose fibers was accompanied by a significant increase in the percentage of crystalline polymer, which may be easily explained by the disappearance of a soluble disordered fraction (Adel *et al*., 2010). Hydronium ions can enter the more accessible amorphous areas of cellulose during the hydrolysis process, allowing the hydrolytic cleavage of glycosidic linkages that finally release individual crystallites (Ahmad *et al*., 2016).

The produced MCC powder and the isolated cellulose sample had XRD patterns that were similar to that of Avicel PH-101 (Figure 9). The main peaks were located at the same angles (2-theta), but the peaks of the BL-MCC, BS-MCC, BP-MCC, and Avicel PH-101 were sharper than those of the BL-C, BS-C, and BP-C. This indicates that the chemical treatments used to produce the MCC samples improved the crystallinity of the cellulose The three characteristic peaks at 16.3, 22.3, and 34.7 degrees 2-theta correspond to the (110), (200), and (040) crystallographic planes of the cellulose I lattice, respectively (Liu *et al.*, 2018).

Acid hydrolysis can be used to improve the crystallinity of cellulose, which makes it more rigid and improves the mechanical properties of cellulose-based composites. The CrI of MCCs made from BL, BS, and BP were higher than the CrI of the original cellulose samples. This is because acid hydrolysis breaks down the amorphous regions of cellulose, leaving behind the more crystalline regions (Hussin *et al.*, 2016).

The elimination of the amorphous regions following the hydrothermal treatment is indicated by the crystallinity index of MCC being higher than that of cellulose (Shi et al., 2018). The range of crystallinity for MCC was 65-83%, whereas the range for Avicel PH-

101 powder was 37-93% (Terinte *et al*., 2011). As shown in Table 4, the CrI BL-MCC: 77% > CrI BL-C: 70%, BS-MCC: 84% > CrI BS-C: 72%, BP-MCC: 82% > CrI BP-C: 68%. In another study, the CrI of cellulose powder produced from banana fibers was 72.1% (Thoorens *et al*., 2015).

The CI of the MCCs produced from BL, BS, and BP is comparable to that of MCCs produced from other sources, such as rice straw (78%), bamboo fiber (82.6%) (Rasheed *et al.*, 2020), Roselle fibers (78%) (Kian *et al.*, 2017b), African breadfruit seed hulls (76%) (Nwajiobi *et al*., 2019) oil palm biomass (87%) (Haafiz *et al*., 2014), tea waste (81.0%) (Zhao *et al*., 2018), and corn husk fibers (80.9%) (Kambli *et al*., 2017a). The crystallinity of the MCC produced in this study was higher than that of MCC isolated from other sources, such as *Ensete glaucum* (54%) (Pachuau *et al*., 2019), oil palm fronds (62%) (Owolabi *et al*., 2017), alfa fibers (73%) (Trache *et al.*, 2014), cotton sliver (73.91%) (Kale *et al*., 2018), date seeds (70%), oceanica brown algae (74.23%) (Tarchoun *et al*., 2019), and pomelo peel (72%) (Liu *et al*., 2018).

The crystallinity of MCC can be affected by various processing factors, such as reaction temperature, time, mechanical agitation of slurry, and drying conditions (Zhao *et al*., 2018). Other factors, such as the amount of acid present and the source of the cellulosic material may also play a role (Khalil *et al*., 2018).

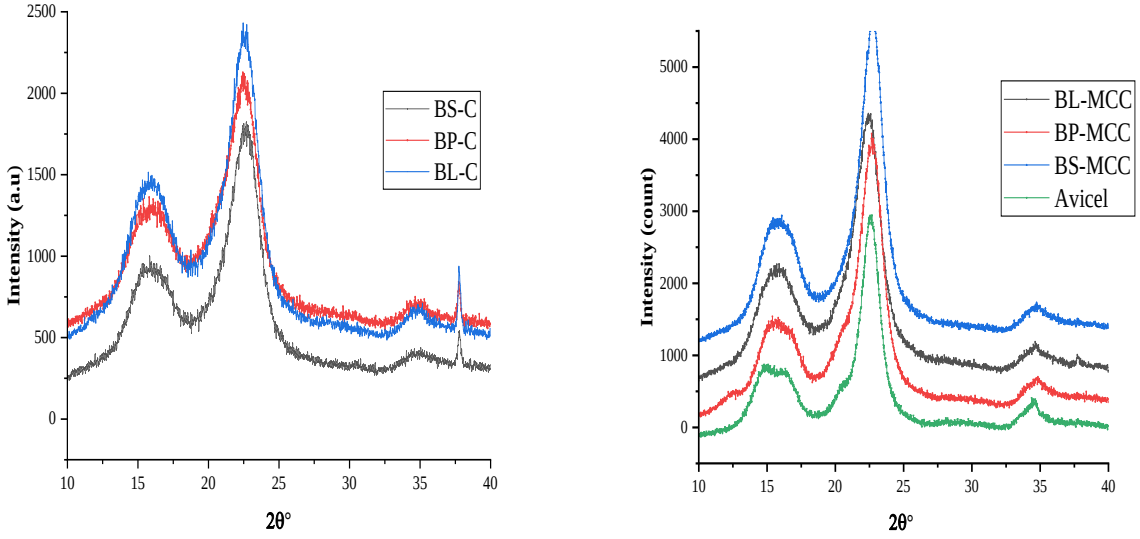

Figure 9: X-ray diffraction pattern of Banana Leaf cellulose (BL-C), Banana pseudostem cellulose (BS-C), Banana peduncle cellulose (BP-C), Banana Leaf microcrystalline cellulose (BL-MCC), Banana pseudostem microcrystalline cellulose (BS-MCC), Banana peduncle microcrystalline cellulose (BP-MCC), and Avicel PH 101.

The apparent crystallite sizes (L) of cellulose and MCC from BL, BS, and BP were calculated using the Scherrer equation. The results are shown in Table 4. The crystallite size of cellulose and MCC from BS was larger than that of cellulose and MCC from banana leaf and banana peduncle. This may be due to the origin of the plant and the associated crystallinity index. Avicel PH-101 had the largest crystallite size of all samples.

Table 4: Crystallinity index and crystallite size of Banana Leaf cellulose, Banana pseudostem cellulose , Banana peduncle cellulose , Banana Leaf microcrystalline cellulose, Banana pseudostem microcrystalline cellulose , Banana peduncle microcrystalline cellulose, and Avicel PH 101.

Crystallinity Parameter	Banana Leaf	Banana pseudostem	Banana Penducle	Avicel PH 101
CrI Cellulose %	68	72	70	-
CrI MCC %	77	84	83	85
L (nm) cellulose	2.82	2.79	2.5	-
L (nm) MCC	3.14	3.69	3.41	4.61

CrI: Crystallinity index, L:crystallite size MCC: microcrystalline cellulose, -:

4.4 Thermal Analysis

The thermal characteristics of cellulose and microcrystalline cellulose (MCC) samples were investigated using thermogravimetric analysis (TGA)/differential thermogravimetric (DTG) studies. The thermal stability of cellulose and MCC materials is important in determining their performance and suitability for use in a variety of industries (Beroual *et al*., 2021). It is essential to determine the thermal stability and characteristics of natural fibers for their potential use in biocomposites (Johar *et al*., 2012). It is a well-established set of techniques for obtaining qualitative and quantitative information about the effect of various heat treatments on materials (Trache *et al.*, 2016)

Figures 10 and 11 show the TGA and DTG curves, respectively of cellulose and MCC samples extracted from different sources, compared to a commercial MCC sample (Avicel PH-101). All of the samples have two main phases of weight loss: phase 1: Drying step (60-140 °C) due to the evaporation of water; and phase 2: Thermal degradation (200-500 °C) due to the decomposition of the cellulose structure. The TGA and DTG curves of the commercial MCC sample (Avicel PH-101) show the highest thermal stability, with an onset temperature of around 300 °C. The TGA and DTG curves of the cellulose and MCC samples extracted from different sources show similar thermal behavior, with onset temperatures of around 250 °C (Trache *et al*., 2014).

The amount of weight loss depends on the initial moisture content of the fiber sample. At higher temperatures, there is a sharper decrease in weight, as the cellulose structure begins to decompose (Johar *et al.*, 2012).

The first stage of weight loss for the BL-C, BS-C, BP-C, BL-MCC, BS-MCC, BP-MCC, and Avicel PH101 samples occurred in the temperature range of 66-111 °C, with corresponding weight losses of 7.92%, 4.48%, 10.83%, 4.04%, 6.82%, 6.47%, and 5.65%, respectively (Figure 10). The second decomposition peak for the BL-C, BS-C, BP-C, BL-MCC, BS-MCC, BP-MCC, and Avicel PH-101 samples respectively appeared at 217 - 377 ^{o}C, 219 - 377 ^{o}C, 220 - 373 ^{o}C, 284 - 380 ^{o}C, 287 - 377 ^{o}C, 279-380 and 285 -378 ^{o}C, respectively. This indicates that all of the samples exhibited one type of thermal decomposition at high temperatures between 250 and 380 °C. This decomposition is caused by some immediate processes, such as depolymerization, dehydration, decarboxylation, and the breakdown of glycosyl units, followed by the formation of a charred residue (Trache *et al.*, 2014).

BL-MCC, BS-MCC, BP-MCC, and Avicel PH-101 all began to degrade during the second degradation peak at temperatures higher than the thermal degradation temperatures of BL-C, BS-C, and BP-C 213 °C, 219 °C, and 220 °C, respectively. The result indicates that cellulose has greater thermal stability when it is more crystalline. This might be caused by the removal of the amorphous component present in the cellulose during the acid hydrolysis process, the absence of hemicellulose and lignin, and other factors (Khalil *et al*., 2018).

Cellulose and MCC samples showed T50% at BL-C (325.22 °C), BS-C (326.88 °C), BP-C (332.72 °C), BL-MCC (333.72 °C), BS-MCC (333.79 ^{o}C), BP- MCC (338.38 °C), and Avicel PH-101 (336.46 °C). It was found that the MCC samples had higher T50% temperature (temperature that cause a 50% weight loss) than the cellulose samples. This might be due to MCC's higher crystallinity and increased thermal stability (Hussin *et al*., 2016b; Tarchoun *et al*., 2019).

At 550 °C, MCC lost weight more quickly than cellulose, likely due to its higher purity. Overall, the TGA study showed that MCC samples prepared from Cellulose samples have better thermal stability (Eichhorn, *et al.*, 2013). These results indicate that the MCC

sample has good thermal stability and might be used to make green biocomposites (Shi *et al*., 2018). Fortunately, no weight loss peaks at 450 °C for TGA curves of all MCC samples were observed, proving that all of the lignin was eliminated (Zhao *et al*., 2018).

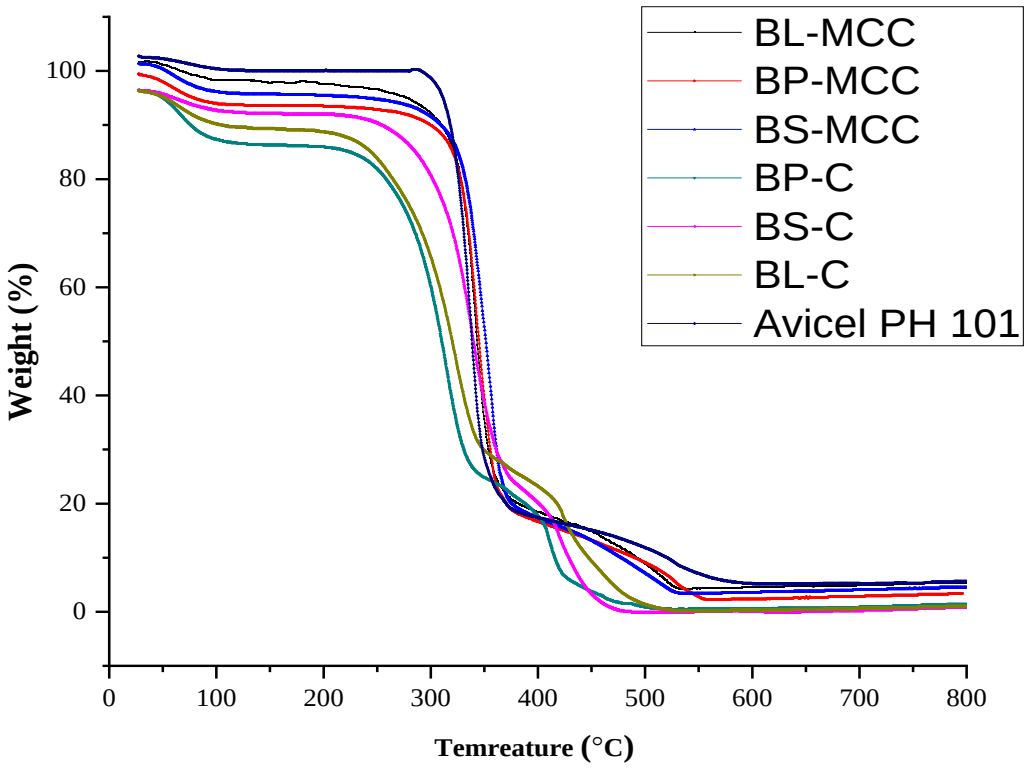

Figure 10: TGA thermograms of Banana Leaf cellulose (BL-C), Banana pseudostem cellulose (BS-C), Banana peduncle cellulose (BP-C), Banana Leaf microcrystalline cellulose (BL-MCC), Banana pseudostem microcrystalline cellulose (BS-MCC), Banana peduncle microcrystalline cellulose (BP-MCC), and Avicel PH 101.

When cellulose and MCC samples are heated to 550 °C in a nitrogen atmosphere, the residue left behind indicates the presence of carbonaceous materials. The main decomposition stage of BL-MCC, BS-MCC, and BP-MCC is in the range of 310-382 °C, while that of BL-C, BS-C, and BP-C is in the range of 240-356 °C (Figure 10). This difference is due to the higher crystallinity and thermal stability of MCC (Hassan, *et al*., 2013). Shi *et al*. (2018) observed similar thermal degradation onset temperature (T_o) and maximum decomposition temperature (T_{max}) for MCC samples as seen in Figure 11. This is because BL-MCC, BS-MCC, and BP-MCC are purer forms of cellulose, with lowest

lignin and hemicellulose contents. Lignin and hemicellulose are impurities that can lower the thermal stability of cellulose (Liu *et al*., 2018).

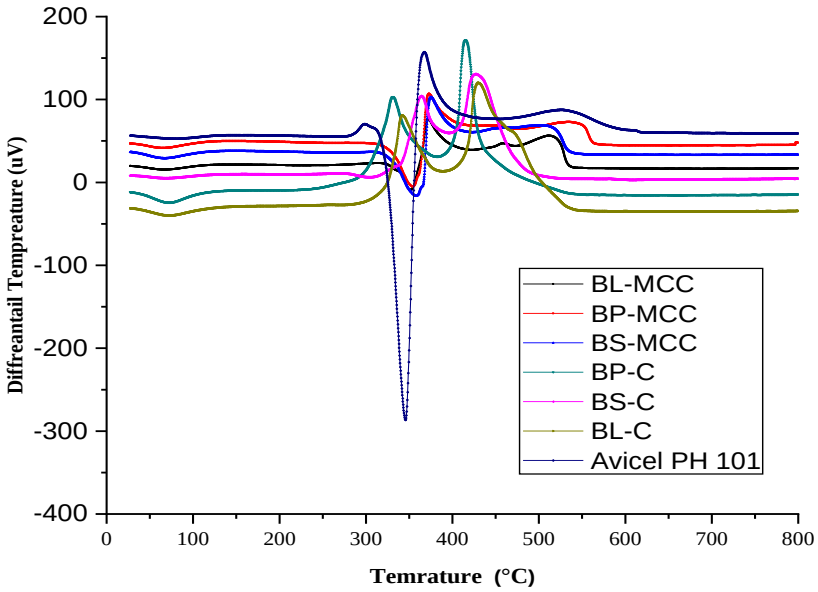

Figure 11: DTA thermograms of Banana Leaf cellulose (BL-C), Banana pseudostem cellulose (BS-C), Banana peduncle cellulose (BP-C), Banana Leaf microcrystalline cellulose (BL-MCC), Banana pseudostem microcrystalline cellulose (BS-MCC), Banana peduncle microcrystalline cellulose (BP-MCC), and Avicel PH 101.

4.5 Morphology of cellulose and MCC

Scanning electron microscopy (SEM) was used to investigate the morphology of cellulose and MCC from, BL, BS, and BP. The SEM images in Figure 12 show that the cellulose fibers from BL-C, BS-C, and BP-C are smooth, long, and uniform. This observation is consistent with the findings of Zhao *et al*. (2018). This is because the various treatments used during cellulose isolation remove non-cellulosic components such as lignin, hemicellulose, and other impurities. These results are supported by the FTIR analysis, which showed that lignin and hemicellulose were removed (Beroual *et al*., 2021).

The SEM image of MCC shows an individualized and fibrous structure (Figure 12). The MCC fibers are rod-shaped and form a network structure with irregular fiber segments (Trache *et al*., 2014). When cellulose is exposed to hydrochloric acid, its fibrillar structure

is disrupted and transformed into small, irregular particles (Shi *et al*., 2018). The MCC samples (BL-MCC, BS-MCC, and BP-MCC) have a changed and non-uniform shape, with micro-sized fibrils with a rougher surface, compared to the cellulose samples (BL-C, BS-C, and BP-C). This is because the hydrochloric acid treatment used to produce MCC enters the amorphous areas of cellulose during hydrolysis and breaks the β-1,4-glucopyranose linkages, which fragments the cellulose fibers into smaller-sized microcrystalline fibrils (Kian *et al.*, 2017a).

Additionally, the surface of the MCC sample looks smoother than that of crude cellulose, which may be due to further damage to the amorphous area of cellulose during partial hydrolysis (Thabit *et al*., 2020). The MCC sample obtained in this study had morphologies that corresponded to those described in the literature by Mohamad Haafiz, *et al*. (2013). Avicel PH101 has consistent particle sizes and is more spherical than the prepared MCC samples. This is likely due to the different sources of the raw materials and different preparation techniques used for MCC.

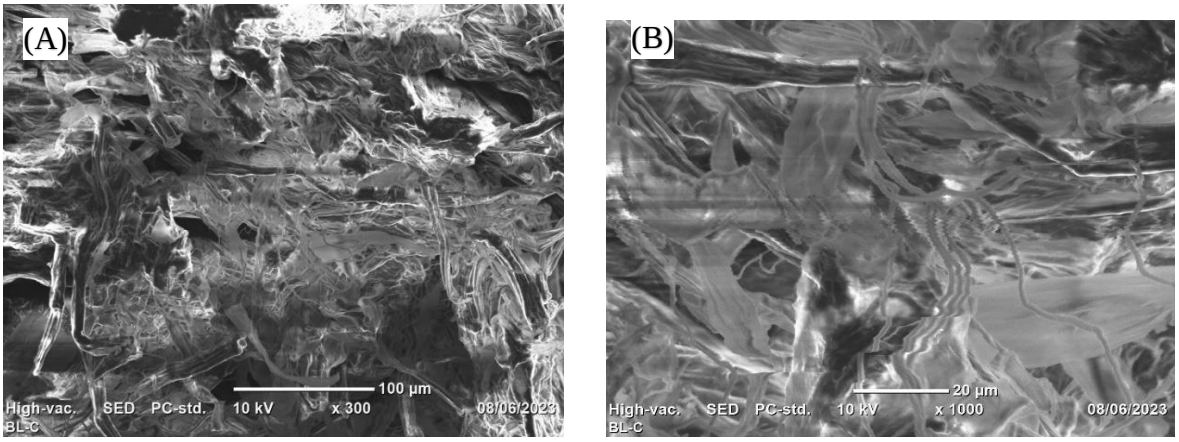

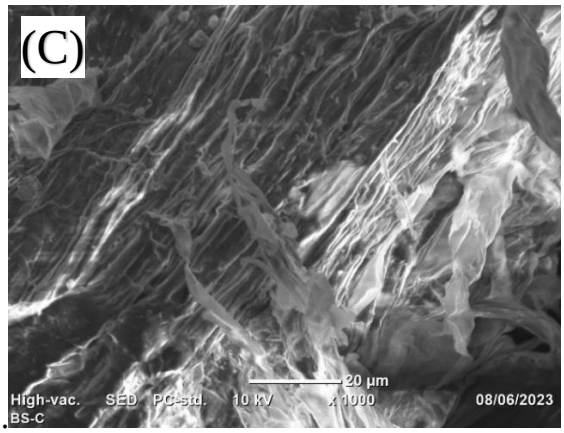
(C)
20 µm
High-vac. SED PC-std. 10 kV x 1000 08/06/2023
BS-C

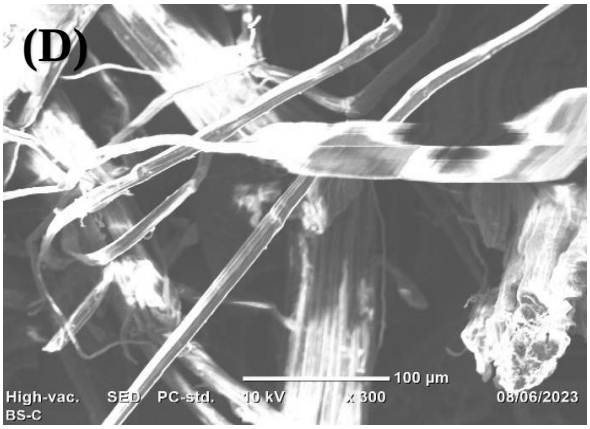
(D)
100 µm
High-vac. SED PC-std. 10 kV x 300 08/06/2023
BS-C

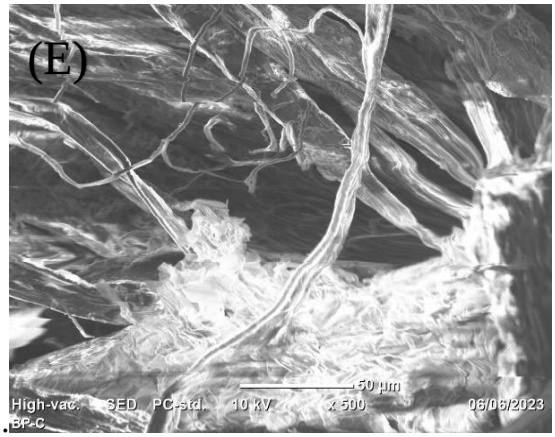
(E)
50 µm
High-vac. SED PC-std. 10 kV x 500 06/06/2023
BP-C

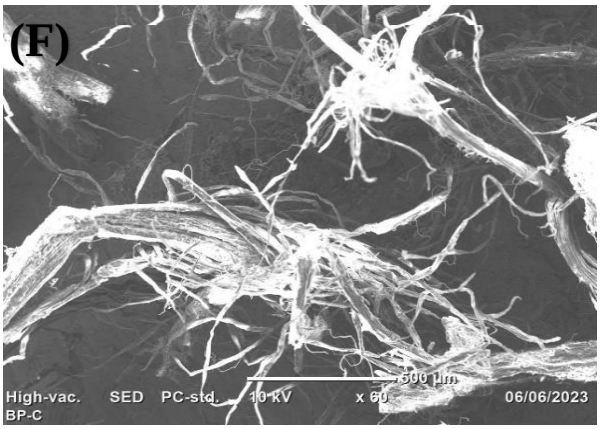
(F)
300 µm
High-vac. SED PC-std. 10 kV x 60 06/06/2023
BP-C

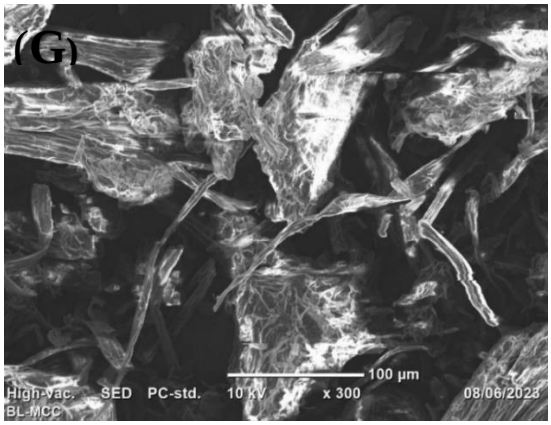
(G)
100 µm
High-vac. SED PC-std. 10 kV x 300 08/06/2023
BL-MCC

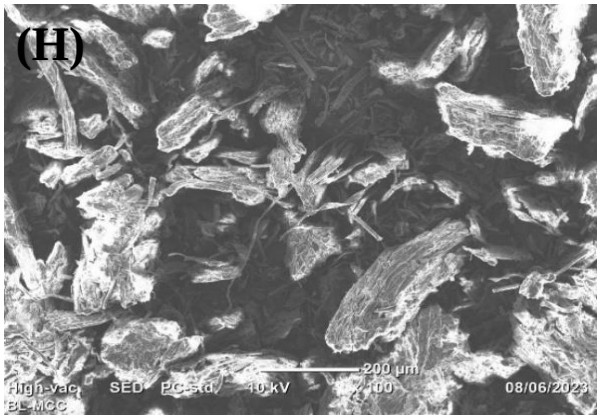
(H)
200 µm
High-vac. SED PC-std. 10 kV x 100 08/06/2023
BL-MCC

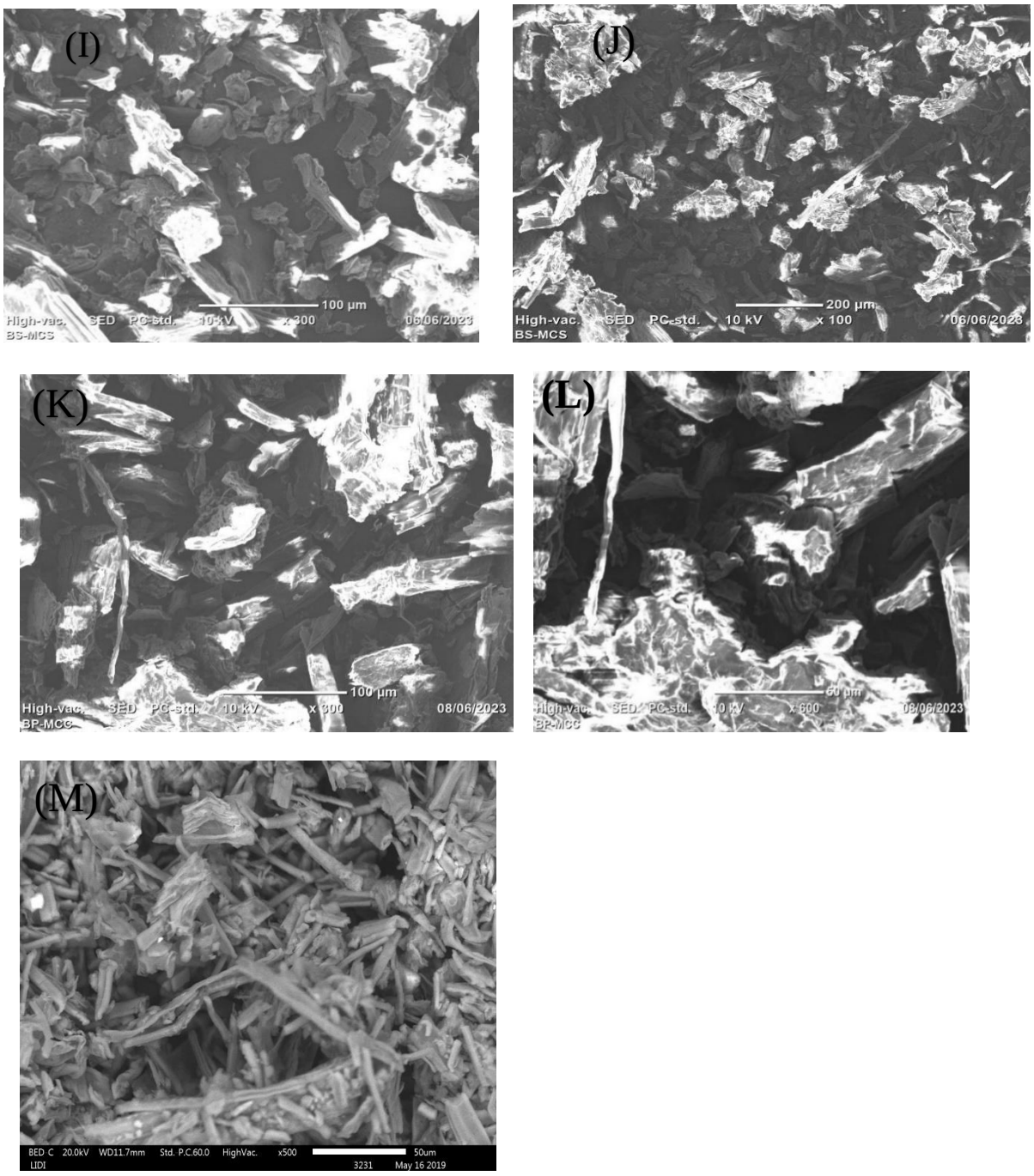

Figure 12: SEM image of cellulose from Banana Leaf cellulose (BL-C) (a,b), Banana pseudostem cellulose (BS-C) (c,d), Banana peduncle cellulose (BP-C) (e,f), Banana Leaf microcrystalline cellulose (BL-MCC) (g,h), Banana pseudostem microcrystalline cellulose (BS-MCC) (i,j), Banana peduncle microcrystalline cellulose (BP-MCC) (k,l), and Avicel PH 101 (M).

4.6 Particle Size and Particle Size Distribution

Figures 13-16 show the particle size distributions of the MCC samples and Avicel PH-101. It can be seen from the figures that a smaller span results in a narrower particle size distribution. This was observed with BP-MCC, which had a slightly narrower particle size distribution than BL-MCC and BS-MCC. However, the particle size distribution of BP-MCC was relatively close to that of Avicel-PH101. This is important because particle size distribution can affect the properties of MCC, such as its flowability, compressibility, and tabletability. A narrower particle size distribution is generally desirable for MCC used in pharmaceutical and food applications (Trache *et al*., 2016)

The particle size and particle size distribution of MCC are two of its most important properties, and they are affected by a complex interplay of factors, including the original material's structure, the hydrolysis process, and the history of mechanical treatment (Wang *et al*., 2010). The particle size of MCC depends on how much the cellulose molecule is broken down. The amount of acid used, the length of the hydrolysis process, and the temperature all affect these criteria. The particle size distributions of the powders, on the other hand, depend on how much they aggregate during the drying of MCC (Aprilia *et al*., 2016). Particle size has very little effect on the tabletability of neat MCC, which is MCC that has not been lubricated or combined with other excipients or active pharmaceutical ingredients (APIs) (Thorens *et al*., 2014a). But, in the case of MCC developed from sugarcane bagasse, the type of acid utilized did not affect the particle size (El-Sakhawy & Hassan, 2007).Tabletability of sieved MCC powders decreased consistently with increasing particle size (or decreasing surface area) when the actual size distribution of each sieved powder was used (Sun & Himmelspach, 2006).

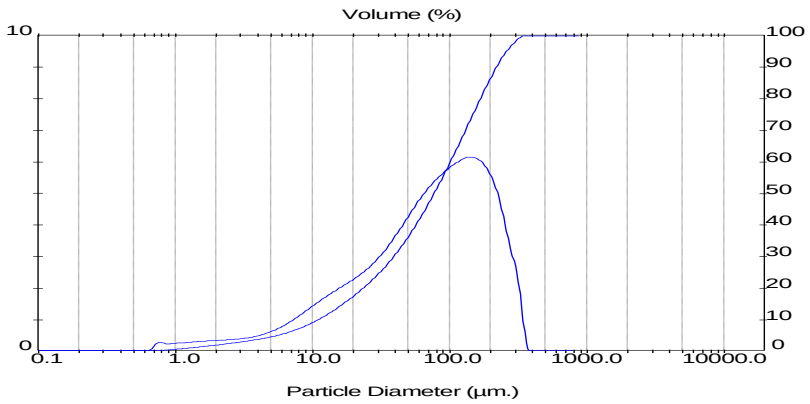

Figure 13: Volumetric Particle size distribution of Banana leaves microcrystalline cellulose

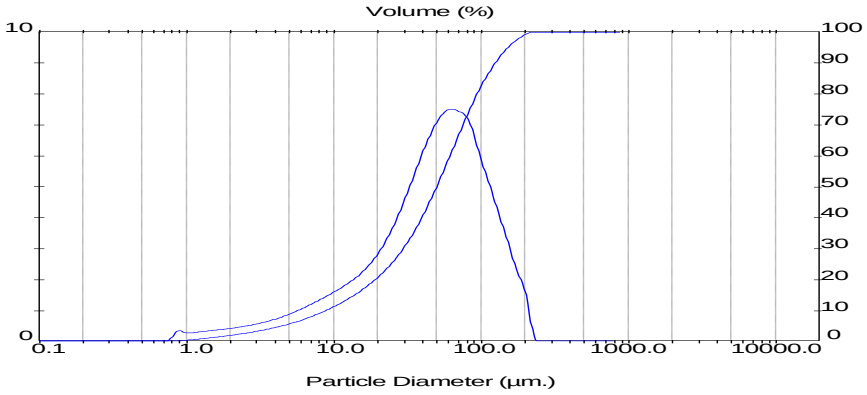

Figure 14: Volumetric Particle size distribution of Banana peduncle microcrystalline cellulose

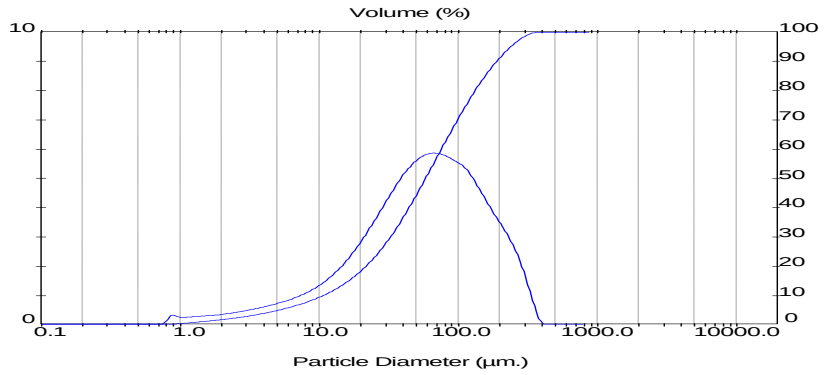

Figure 15: Volumetric Particle size distribution of Banana pseudostem microcrystalline cellulose

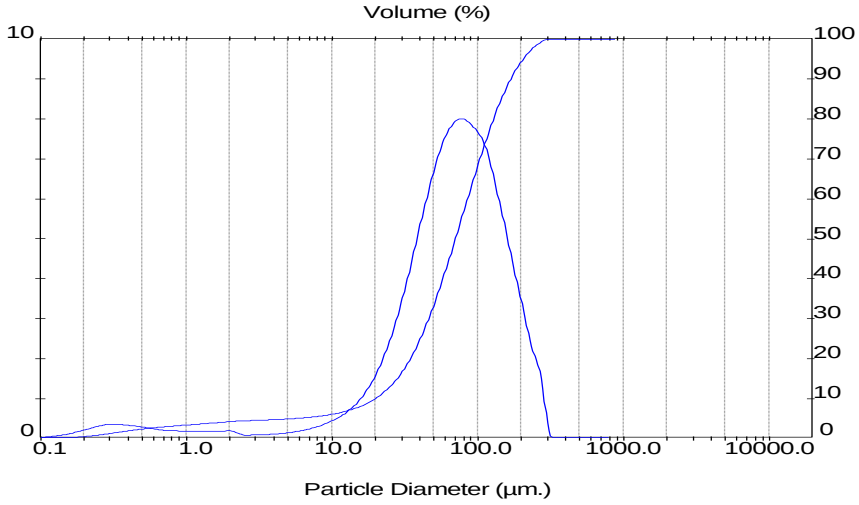

Figure 16: Volumetric Particle size distribution of Avicel PH 101.

Table 5 shows the results of the particle size study of the four different types of MCC: BL-MCC, BS-MCC, BP-MCC, and Avicel PH 101. The mean particle size of BS-MCC was higher than that of BP-MCC but lower than that of Avicel PH 101. The mean particle size of BS-MCC is not significantly different from Avicel PH 101 ($P>0.05$), but BL-MCC and BP-MCC have significantly different mean particle sizes from Avicel PH 101($P<0.05$).

The particle size distribution of MCC is described by three values: D(v, 0.1), D(v, 0.5), and D(v, 0.9). D(v, 0.1) is the diameter below which 10% of the MCC particles fall. D(v, 0.5) is the median diameter or the diameter below which 50% of the MCC particles fall. D(v, 0.9) is the diameter below which 90% of the MCC particles fall. In other words, D(v,

0.1), D(v, 0.5), and D(v, 0.9) provide information about the range of particle sizes in an MCC sample. Additionally, D (v, 0.5) expresses the MCC sample's median diameter. The median particle sizes of these materials are consistent with the range described by Aprilia *et al.*, (2016). The mean particle size and median particle size of BS-MCC are also consistent with the range described by Wang *et al.*, (2010) for kenaf fibers MCC (71.16 µm). Compared to BL-MCC, BP-MCC, and BS-MCC, Avicel PH-101 has a much narrower particle size distribution (lower span value). This means that the particles of Avicel PH-101 are more uniform in size. BL-MCC has a broad particle size distribution, meaning that the particles have a wide range of sizes. This is different from BS-MCC and Avicel PH-101, which have narrower particle size distributions.

Table 5: Particle size and size distribution of Banana leaves microcrystalline cellulose (BL-MCC), Banana pseudostem microcrystalline cellulose (BS-MCC), Banana peduncle microcrystalline cellulose BP-MCC, and Avicel PH-101.

Parameter	Types of MCC			
	BL-MCC	BS-MCC	BP-MCC	Avicel PH 101
Mean size(µm)	93.95 ±3.3	77.92±2.45	60.67± 1.7	84.74±0.7
Dv10(µm)	10.75±0.24	10.32±0.24	9.38±0.5	23.01667±2.2
Dv50(µm)	73.73±2.7	56.04±1.5	51.45±1.6	71.02±0.5
Dv90(µm)	210.32±7.4	180.03±7.2	125.31 ±3.5	167.8133±0.8
SSAm2/g	0.22±0.001	0.22±0.004	0.24±0.006	0.25±0.22
Span	3.02±0.	2.7±0.001	2.25±0.047	2.04±0.063

SSAm2/g:Specific surface area

4.7 Density and related properties

The density and related properties of MCC are important factors to consider when using it in pharmaceutical formulations. These properties can affect the flowability, compressibility, and release properties of MCC (Trache et al., 2016b)

4.7. 1 Bulk density and Tapped density

As shown in Table 6, BL-MCC, BS-MCC, BP-MCC, and Avicel PH-101 have bulk densities of 0.35, 0.26, 0.27, and 0.37 g/cm^3, respectively and tapped densities of 0.51, 0.35, 0.33, and 0.47 g/cm^3, respectively. The BL-MCCs bulk density and Avicel PH-101 bulk density is comparable. The bulk density of BL-MCC is comparable to that of MCC made from the seed husk of African breadfruit (0.33 g/ml) and Rice Husk (0.36g/ml) (Zuliahani *et al*., 2016), but higher than kenaf fibers MCC bulk density (0.24 g/ml) (Wang *et al.*, 2010) which is comparable bulk density of BS-MCC. Their different crystallinities and particle shapes were presumably responsible for the differences in bulk density. BS-MCC and BP-MCC with their low bulk density will have a greater dilution potential and may work better to make up for the API's poor tableting properties (Wang *et al*., 2010).

Bulk density is a measure of how much a material can flow, while tapped density is a measure of how well a powder can be packed in a small space after repeated tapping. In

general, materials with higher bulk and tapped densities have better flowability and can be rearranged more easily under compression (Pachuau *et al*., 2019). During the manufacture of tablets, a higher bulk density of MCC would lead to a reduced loading volume. Additionally, low bulk-density MCC has a greater diluting potential, which can be useful for compensating for the poor tableting characteristics of active pharmaceutical ingredients (APIs) (Thorens *et al.*, 2014b).

Table 6: Micrometrics properties of Banana leaves microcrystalline cellulose (BL-MCC), Banana pseudostem microcrystalline cellulose (BS-MCC), Banana peduncle microcrystalline cellulose BP-MCC, and Avicel PH-101.

Properties	Types of MCC			
	BL-MCC	BS-MCC	BP-MCC	Avicel PH 101
True density (g/ml)	1.38±0.009	1.44±0.02	1.46±004	1.45±008
Bulk density (g/ml)	0.34±0.004	0.26±0.004	0.27±0.008	0.37±0.008
Tapped density (g/m)	0.53±0.004	0.35±0.001	0.34±0.008	0.47±0.004
Hausner's quotient	1.51±0.001	1.34±0.005	1.22±0.003	1.23±0.009
Compressibility index (%)	35±0.01	25.7±0.03	20.5±0.03	21.8±0.02
Porosity (%)	74.5±0.004	82 ±0.003	81±0.006	74.7±0.007

All value represent mean ±SD (n=3)

High bulk density is often associated with small particle size and low moisture content. For example, Zuliahani *et al*. (2016) found that MCC prepared by 1M HCl and 2M HCl have bulk densities of 0.34 g/cm^3 and 0.36 g/cm^3, respectively, while MCC prepared by 1M HNO_3 and 2M HNO_3 have bulk densities of 0.29 g/cm^3 and 0.32 g/cm^3, respectively. Liao *et al*. (2012) found that tablet strength (TS) decreases with increasing bulk density and tapped density.

4.7.2 True density

The true densities of the different MCC samples are shown in Table 6. BL-MCC, BS-MCC, and BP-MCC have slightly lower true densities than commercial Avicel PH-101. BS-MCC is likely to have better compressibility because it has a higher true density than BL-MCC and BP-MCC. This is because there is a direct correlation between the degree of crystallinity of cellulose and its true density (Ejikeme, 2008). When measured in a non-polar liquid, the true density of MCC powder made from banana tree parts was found to be comparable to that of Avicel PH-101. The true densities of BS-MCC, BP-MCC, and Avicel PH-101 powders were not statistically significantly different ($P > 0.05$).

A study by Ogochukwu *et al*. (2014) found that MCC made from Indian bamboo (*Bambusa vulgaris*) had a true density of 1.642 g/ml, while MCC made from *Ensete glaucum* had a true density of 1.478 g/ml (Pachuau *et al*., 2019). True density analysis findings indicate that all samples would have relatively similar levels of crystallinity (Pachuau *et al*., 2014).

4.7.3 Hausner ratio and the Carr's index

Carr's compressibility index and Hausner index are two indirect measures of powder flowability. They are calculated using the tapped and bulk densities of a powder. Values for both indices decrease with better particle flow. The Hausner index measures the cohesiveness between particles, while Carr's compressibility index estimates how much a powder can be compressed (Ejikeme, 2008).

The flow properties of a substance are critical for determining whether it can be used as a direct compression excipient (Kambli *et al.*, 2017b). Table 6 provides the Hausner ratio and Carr's index values for BL-MCC, BS-MCC, BP-MCC, and Avicel PH-101. BP-MCC and Avicel PH-101 exhibit fair to good flow properties, respectively .The Hausner ratio and Carr's index values for BP-MCC and Avicel PH-101 are comparable, indicating similar flowability characteristics (Pachuau *et al*., 2019).

The flow characteristics of powdered substances can be evaluated using the Hausner ratio and Carr's index. A Hausner ratio below 1.20 indicates good flowability, while a value of 1.5 or higher suggests poor flowability (Akseli *et al*., 2019). Similarly, the Carr's index is used to assess flowability, with lower values indicating better flowability. A Carr's index

of 5-10 indicates excellent flowability, 12-16 indicates good flowability, 18-21 indicates fair flowability, and 23-28 indicates poor flowability (USP 41-NF36, 2022).

Based on the flowability indices, BL-MCC powders exhibit poor flow characteristics. Consequently, incorporating a glidant becomes necessary when utilizing BL-MCC in the development of solid dosage forms (Ohwoavworhua and Adelakun, 2010). Discharging materials with a compressibility of 40% to 50% can pose significant challenges (Bhimte & Tayade, 2007). Similarly, a study conducted by Ohwoavworhua and Adelakun (2010) determined that the Hausner ratio and Carr's compressibility index for MCC derived from Sorghum caudatum were 1.71 and 43.75, respectively, indicating that this type of MCC possesses high cohesiveness and poor flowability.

4.7.4 Porosity

Porosity is the amount of void space in a material. The volume of this space is called the void volume. The space between particles is known as the void. The porosities of BL-MCC, BS-MCC, BP-MCC, and Avicel PH-101 are 74%, 82%, 81%, and 74.7%, respectively (Table 6). BS-MCC has a high tapped density and a high total porosity (81%). The porosity of a material is related to its density (Nwajiobi *et al*., 2019). Intraparticle porosity in MCC is remarkably high, with 90–95% of the surface area being internal. Therefore, the nominal particle size has no direct impact on surface area (Doelker, 1993b). Due to the capillary action of the pores, which allows water to enter the hydrophilic tablet matrix, and resulting breaking of the hydrogen bonds, this high porosity BS-MCC and BP-MCC promotes swelling and disintegration of MCC tablets (Thorens *et al*., 2014a).

4.7.5 The moisture sorption capacity

Figure 17 shows the moisture sorption capacity of BL-MCC, BS-MCC, BP-MCC, and Avicel PH-101 at different relative humidity levels (20%, 40%, 75.5%, 80%, and 100%) over one-month period. The moisture sorption capacity of a substance is a measure of how much moisture it can absorb. It is important in pharmaceutical applications because it can affect the stability of tablets prepared with MCC when they are stored in a humid environment (Khalil *et al*., 2018). Only the amorphous parts of MCC can absorb water, not the crystalline parts. Therefore, the total amount of water absorbed is not related to the

surface area of MCC, but to the amount of amorphous material it contains (Thoorens *et al*., 2014a).

The moisture sorption capacity of a material is a measure of its sensitivity to moisture. Because MCC is sensitive to ambient humidity, it should be stored in a tightly sealed container (Nwajiobi *et al*., 2019). Therefore, BP-MCC, BL-MCC and BS-MCC require better control of moisture than Avicel PH-101.

Different raw materials may also contribute to the variations in moisture absorption rates. Both the origin of the materials and their crystallinity can likely affect the rate at which MCC absorbs moisture (Khalil *et al.*, 2018). This is because MCC with higher crystallinity has lower moisture content, and the moisture sorption of cellulose is proportional to its crystallinity (Wang *et al*., 2010). At all relative humidity levels, BL-MCC, which has the lowest crystallinity, showed the highest moisture sorption. Avicel PH-101, on the other hand, has a high level of crystallinity and lowest moisture sorption, which may contribute to its relative stability (Mihranyan *et al*., 2004).

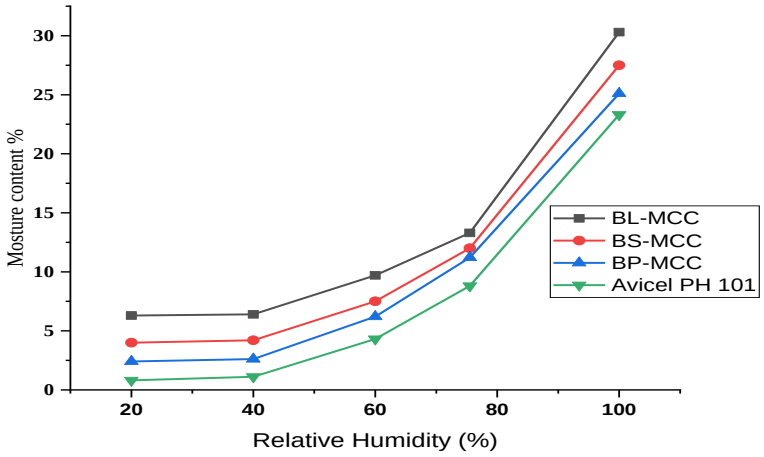

Figure 17: Moistures sorption patterns of Banana leaves microcrystalline cellulose (BL-MCC) Banana Pseudostem microcrystalline cellulose ,(BS-MCC)), Banana Peduncle microcrystalline, (BP-MCC) and Avicel PH-101 at different RH conditions at room temperature.

4.8 Evaluation of tablet property

4.8.1 Dilution potential

Three types of MCC were extracted from BL, BS, and BP. The physicochemical characterization test results of each MCC type were compared with each other and with Avicel PH-101, revealing that all test results were comparable. BS-MCC and BP-MCC were selected for further studies due to their high yield, the large quantities required for dilution potential and compressibility studies, the need for multiple batches and tablet preparations, and the assurance of comparable results based on the initial physicochemical characterization.

The dilution potential of MCC is a measure of its ability to maintain the compressibility and mechanical properties of tablets when increasing amounts of a poorly compatible API are added (Rojas *et al*., 2013; Goyanes & Martínez-Pacheco, 2015). Based on the tensile strength values observed in this study, it can be concluded that BS-MCC and Avicel PH-101 exhibit comparable dilution capacities for the model drug. A decrease in tensile strength or an increase in friability as the API concentration increases indicates a lower dilution potential for the MCC (Martinello *et al*., 2006)). A study by Kuentz and Leuenberger (2000) found a dilution capacity of 79.9%, while an earlier study by Habib *et al*.(1996) reported a lower dilution capacity of 65%.The dilution potential of BS-MCC, BP-MCC, and Avicel PH-101 was evaluated by using paracetamol as a model drug. For the purpose of comparison, all tablets were compressed at a fixed compression force.

4.8.2 Mechanical properties of plain microcrystalline cellulose tablets

To evaluate the mechanical properties of different MCC samples, tablets were compressed using the same compression force as standard Avicel PH 101. The crushing strength, friability, tensile strength, and disintegration time of the tablets were then measured. The results are presented in Table 7.

MCC is the best dry binder for direct compression formulations because it is compatible with a wide range of APIs and has good mechanical properties. In the pharmaceutical industry, powders are compressed to form tablets in punch and die systems (Doelker, 1993a). These systems are often used to evaluate the mechanical properties of powders.

MCC has been shown to have good compressibility and tensile strength, making it ideal for use in direct compression formulations (Mashadi & Newton, 1987).

Ta fdble 7:Hardness, tensile strength, friability, and disintegration time of all compressed plain tablets of Banana pseudostem microcrystalline cellulose (BS-MCC), Banana peduncle microcrystalline cellulose (BP-MCC), and Avicel PH-101.

Parameter	Types of MCC		
	BS-MCC	BP-MCC	Avicel PH 101
Hardness (N)	98±9.6	93± 11.7	115±9.37
Friability (%)	0.68	0.73	0.57
Tensile strength (Kg/cm2)	11.53± 04	10.5± 07	13.41± 1.8
Disintegration time (min)	3.6±0.47	4.3±1.24	5.33±2.05

Mean ± SD (n=10)

4.8.2.1 Crushing strength and Tensile strength

Tablet crushing strength is a measure of a tablet's ability to withstand pressure. It can be used as a preliminary evaluation of potential direct compression excipients. At the same compression force, the crushing strength values of the ordinary BS-MCC, BP-MCC, and Avicel PH 101 tablets were comparable (Ohwoavworhua & Adelakun, 2010). Tensile strength is another measure of a compact's strength (El-Sakhawy & Hassan, 2007).

Table 7 shows that the hardness of tablets prepared with Avicel PH-101 was higher than those prepared with BS-MCC or BP-MCC. This difference in hardness may be due to differences in the degree of crystallinity and specific surface area of the MCC samples (Bastos *et al.*, 2008). Oral tablets should have a minimum hardness of 40 N, according to USP requirements. The hardness of tablets prepared with all three MCC samples exceeded this requirement. However, Avicel PH-101 tablets had the highest hardness, suggesting that they may be more resistant to breakage and chipping.

The strength of a compact can be described in terms of its tensile strength. Tensile strength is a measure of a material's ability to resist being pulled apart. Avicel PH-101 tablets are

expected to have higher tensile strength than BS-MCC or BP-MCC tablets, based on their higher hardness. The tensile strength of tablets made from different MCC samples was lower than that of Avicel PH 101 tablets, likely due to their higher density (Hassan & El-Sakhawy, 2007). Avicel PH-101 has a much higher tensile strength than other MCC samples, which may be related to its higher crystallinity (Jahan *et al.*, 2011).

4.8.2.2 Friability

Friability is a measure of a tablet's ability to withstand damage during handling, packaging, and transportation. It is linked to the strength of the tablet. Friability values less than 1% are generally considered acceptable for pharmaceutical tablets which meets with the USP's requirements for friability test. The friability of tablets made from different MCC samples was evaluated. The tablets from Avicel PH101, BS-MCC, and BP-MCC showed weight losses of 0.57%, 0.68%, and 0.73%, respectively. These results show that Avicel PH101 tablets had the lowest friability, followed by BP-MCC and BS-MCC tablets. The lower friability of Avicel PH101 tablets may be due to their higher hardness and tensile strength (Bastos *et al*., 2008).

4.8.2.3 Disintegration time

Table 7 shows the disintegration times of plain tablets made from different MCC samples. All of the tablets disintegrated within 15 min, as required by the British Pharmacopoeia for uncoated tablets. Tablets made from the derived MCC samples (BS-MCC and BP-MCC) disintegrated faster than those made from Avicel PH-101 because of their high porosity, which promotes swelling and disintegration (Eraga *et al.*, 2020). This is likely because the BS-MCC and BP-MCC tablets had lower hardness. Harder tablets take longer to disintegrate because water has more difficulty penetrating the tablet matrix (Rana *et al*., 2022). Due to this, increases in hardness result in longer disintegration times and slower dissolution rates (Haruna *et al*., 2020).

4.8.3 Lubricant sensitivity ratio

Lubrication is a necessary step in tableting. It helps to reduce friction between particles and prevent the material from sticking to the punch and die surfaces. This makes it easier to eject the tablets after compression (Wang *et al.*, 2010). Lubricants work by coating the particle surfaces or forming a film layer at interparticulate surfaces. This interferes with

inter particulate bonding and reduces the tensile strength. Lubricant sensitivity ratio (LSR) testing is done to determine how much the tableting material is affected by lubricants. Materials that are plastic deforming are more susceptible to lubricants than brittle materials, depending on the mechanical properties (Paul & Sun, 2017; Arshad *et al*., 2021).

Lubricants are added to tablet formulations in small amounts (0.25-0.5% w/w) to prevent sticking, picking, and capping problems. They work by forming a stable coating around particles or surfaces. The type and amount of lubricant used, as well as the way it is incorporated into the formulation and applied, can all affect the tablet compression process (Arshad *et al*., 2021).

Magnesium stearate (MgSt) is a well-known and widely used lubricant in tablet compression. It is a hydrophobic lubricant, meaning that it repels water. This is important for tablet compression because it helps to prevent the material from sticking to the punch and die surfaces (Rojas *et al*., 2013). MgSt also helps to improve the flowability of the tablet material. MgSt offers several benefits for tablet compression (Thoorens *et al*., 2014).

Lubricants can make it easier to compress powders into tablets, but they can also make the tablets softer and slower to disintegrate. Therefore, it is important to use the right amount of lubricant to achieve the desired tablet properties (Takeuchi *et al*., 2005).

Figure 18 shows the lubricant sensitivity ratio (LSR) of MCC and magnesium stearate concentration for tablets crushed from unlubricated MCC and MCC lubricated with different concentrations (0.5% to 1.5%) of magnesium stearate. The LSR of MCC made from the sample and Avicel PH-101 increased significantly as the concentration of magnesium stearate in the binary mixture increased from 0.5% to 1.5%.

As shown in Figure 18, Avicel PH-101 has the highest LSR, followed by BP-MCC and BS-MCC. This is because Avicel PH-101 has the least porous structure, highest bulk density, and best flow property, which facilitate the creation of a continuous lubricating film. In addition to having better flow characteristics, Avicel PH-101 is the most sensitive to lubrication with magnesium stearate (Getachew et al., 2023b). The LSR powder of MCC is significantly influenced by the degree to which the lubricant surface film

develops, which depends on both the flow property and surface area of the powder (Thoorens *et al*., 2014a).

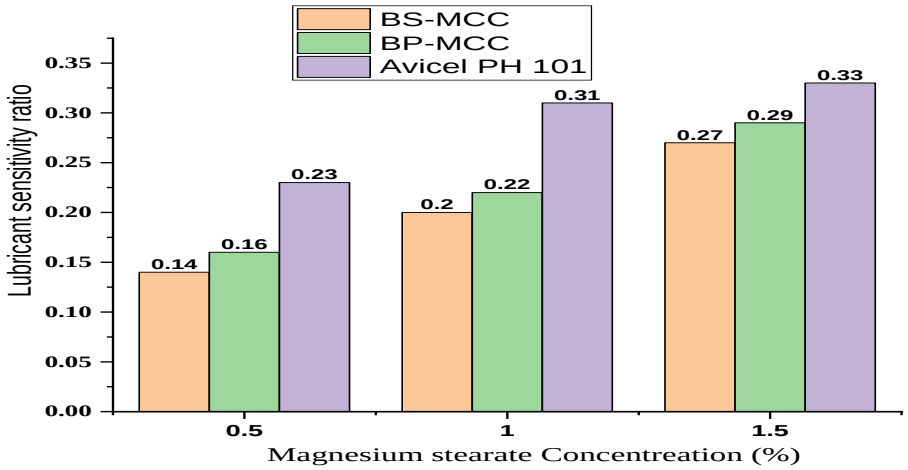

Figure 18: Effect of Lubricant concentrations on lubricant sensitivity ratio at Banana pseudostem microcrystalline cellulose (BS-MCC), Banana peduncle microcrystalline cellulose (BP-MCC), and Avicel PH-10.

4.8.4 Compatibility study of Drug and Microcrystalline cellulose sample

Figure 19 shows the FTIR spectrum of pure Paracetamol (PCM) powder. Figure 20 shows the FTIR spectra of physical mixtures of PCM and three different MCC samples (BS-MCC, BP-MCC, and Avicel PH 101) in a 1:1 ratio. PCM contains different functional groups, including -NH, O-H, C=O, and an aromatic ring containing C=C. The C=O band was selected for quantification because it has minimal interference from the excipients in the pharmaceutical formulation (Mallah *et al*., 2015). PCM has a characteristic FTIR spectrum with peaks at specific wavenumbers. These peaks can be used to identify paracetamol and to quantify its amount in a sample

PCM exhibits distinctive peaks in its FTIR spectrum at the following wavenumbers, 808 cm^{-1} (amide group deformation), 968 cm^{-1} and 1259 cm^{-1} (C-N stretching vibrations), 1655 cm^{-1} (C=O stretching and C-NH deformation), 3034 cm^{-1} (N-H stretching), 3161 cm^{-1} and 3325 cm^{-1} (O-H stretching (Burgina *et al*., 2004; Leyk & Wesolowski, 2019).

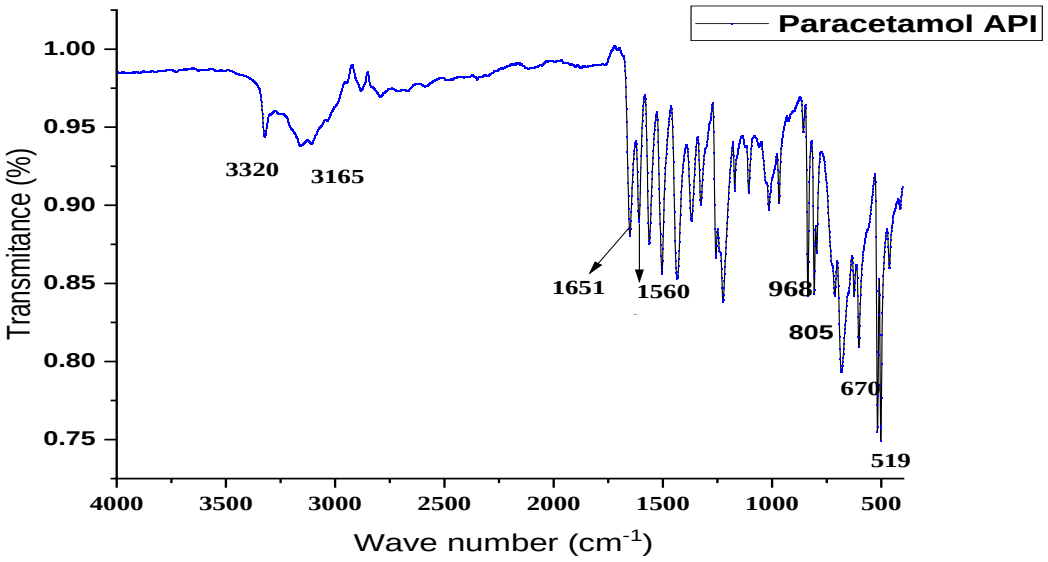

Figure 19: FTIR spectrum of pure paracetamol

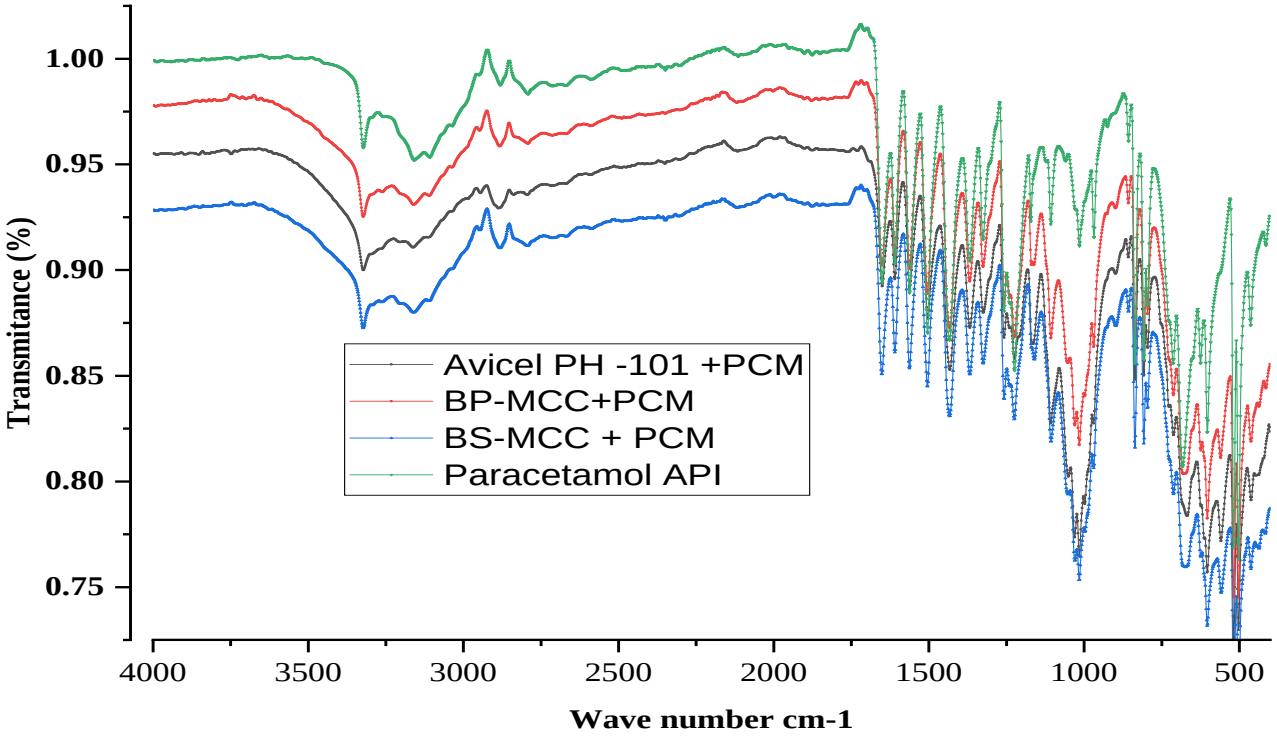

Figure 20: FTIR spectra of Avicel PH-101 + Paracetamol,Banana pseudostem microcrystalline cellulose + Paracetamol.(BS-MCC+PCM), and Banana peduncle microcrystalline cellulose+ Paracetamol(BP-MCC+PCM)

The vibrational peaks of PCM were seen in the FT-IR spectra (Figure 19) at 3325 and 3162–3035 cm^{-1}, which were attributed to O–H and CH_3 stretching, respectively. The stretching of C=O (amide I) and C=C, caused the vibrational peaks at 1653 and 1609 cm^{-1}, respectively. Additionally, bending of the N-H amide II, asymmetrical bending of the C-H bending, and C-C stretching were each attributed to vibrational peaks at 1555, 1506, and 1437 cm^{-1}, respectively (Burgina *et al*., 2004; Habiba *et al*., 2021).The absorption bands of BS-MCC and PCM, BP-MCC and PCM, or Avicel PH 101 and PCM were the same as those of pure paracetamol, as shown in Figure 20.

This study employed DSC as a rapid and effective tool to evaluate the compatibility of drug substances with excipients, a technique widely utilized in the field (Balestrieri *et al*.,

1996). PCM exhibited a sharp melting point at 170 °C, as depicted in Figure 21. Subsequently, PCM was combined with both BS-MCC and BP-MCC at a 1:1 ratio.

DSC analysis of these mixtures revealed a sharp endothermic peak at approximately 168-172 °C, corresponding to the melting point of PCM. The sharpness and definition of this peak indicate the drug's purity and crystalline form, consistent with the results obtained for pure PCM. Additionally, a semi-broad endothermic peak may be present around 310 °C, although its presence and intensity depend on the specific experimental conditions employed (Giordano *et al*., 2002; Kaerger *et al*., 2004). Notably, a high degree of similarity was observed between the thermograms of pure PCM and its mixtures with BS-MCC and BP-MCC. This suggests that there is no interaction between the components, indicating compatibility between PCM and MCC, in line with previous studies (Elsayed *et al*., 2018).

The results of FTIR and DSC studies indicate that there are no chemical interactions between paracetamol and any of the MCC excipients. This is important for pharmaceutical formulations, as it ensures that the drug will remain stable and effective.

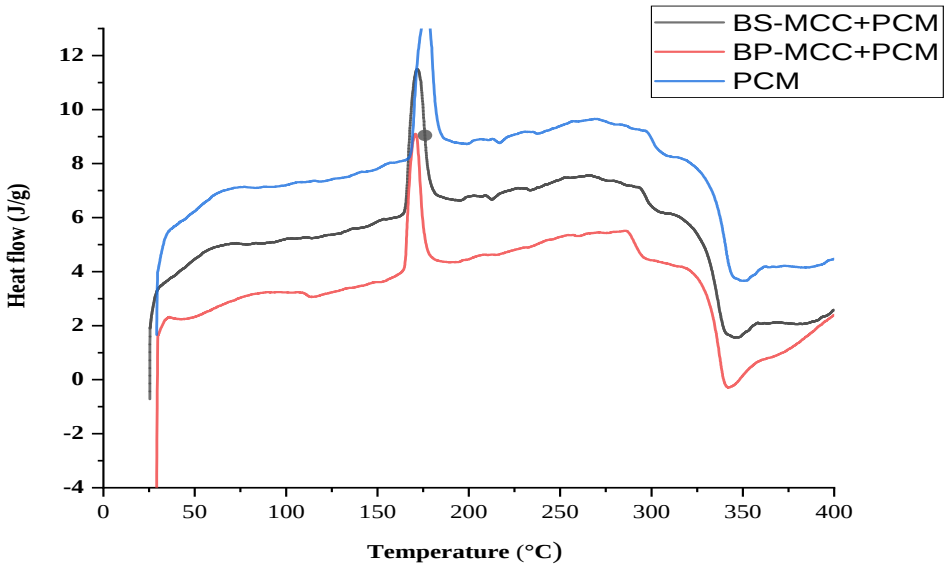

Figure 21: DSC thermograms of pure paracetamol and paracetamol with microcrystalline celluloses derived from banana pseudostem and peduncle.

4.8.5 Tablets Compressed from *microcrystalline celluloses* Powders Loaded with Paracetamol

4.8.5.1 Weight Variation, Thickness, and Diameter

PCM-MCC tablets were evaluated for weight uniformity, thickness, and diameter using a binary mixture of paracetamol API and MCC made from BS, BP, and Avicel PH-101 in different amounts (Table 8). The thickness and diameter values of the tablets were comparable across all formulations, based on the dies and punches used in this study. The USP allows a maximum of 5% weight variation for tablets weighing 250 mg or more, and the weight fluctuation of the tablets in this study was within this acceptable range (USP 41-NF36, 2023).

There was a slight difference in tablet thickness between the different batches of BS-MCC, BP-MCC, and Avicel PH101, as shown in Table 8. The two main factors that determine the weight of the tablets are the size of the die and the amount of powder filled in the die, which is affected by the flowability of the powder (Al-Dulaimi *et al.*, 2021).

The slight variation in tablet weight between the different batches of MCC may be related to differences in powder density and compaction behavior. Tablet thickness did not differ significantly between the different MCC powders or formulations ($p > 0.05$). To ensure

tablet weight uniformity and the production of tablets with consistent and reproducible properties, the powder must flow smoothly and uniformly into the tablet machine dies (Crouter & Briens, 2014).

Table 8:Weight variation thickness, and diameter at different Paracetamol concentration.

Parameter	Drug: Excipient ratio	Types of MCC		
		BS-MCC	BP-MCC	Avicel PH 101
Weight (mg)	35%	391.45±5.24	392.3 ±5.1	394.05±5.41
	45%	382.9±4.78	380.9±4.85	386.35±4.25
	55%	379±4.80	376.45±4.02	382 ±5.30
	65%	374.4 ±4.41	374.7 ± 3.08	380.2±4.50
Thickness (mm)	35%	4.21±0.06	4.22±0.06	4.22±05
	45%	4.23±0.06	4.23± 0.03	4.23±01
	55%	4.24±0.04	4.24 ±0.07	4.25±04
	65%	4.26±0.07	4.25±0.05	4.26±03
Diameter (mm)	35%	11.84±01	11.84±02	11.84±04
	45%	11.84±02	11.84±01	11.84±02
	55%	11.85±01	11.85±03	11.85±03
	65%	11.85±03	11.86±01	11.86±02

Microcrystalline cellulose= MCC, BS-MCC= Banana pseudostem microcrystalline cellulose, Banana peduncle microcrystalline cellulose (BP-MCC), and Avicel PH-101.Mean ± SD (=20)

4.8.5.2 Crushing strength, friability, and tensile strength

Tablet hardness is tested to determine a tablet's ability to withstand the mechanical shocks of production, packaging, and transportation. It has recently been discovered that tablet hardness is also related to drug dissolution (release) rate. The hardness of all PCM-loaded MCC and Avicel PH-101 tablets used in the study fell within the acceptable range of 40

to 80 N, as specified by USP guidelines for uncoated tablets (Table 9) (Hamrah *et al.*, 2020).

MCC and paracetamol tablets (with 35-55% w/w PCM) have hardness or breaking forces greater than 40 N, making them strong enough to withstand mechanical stresses during storage, handling, and transportation (Table 9). Increasing the amount of MCC and Avicel increased crushing strength and decreased friability. The hardness and friability test was performed to determine whether produced tablets can withstand the physical forces of transportation (Setu *et al.*, 2014). The crushing strength of tablets made with different MCC and Avicel PH101 diluents decreased significantly ($p<0.05$) as the paracetamol concentration increased.

Friability testing is performed to determine whether tablets can withstand damage during transportation. The tablets pass the test if the weight loss is less than 1%, as required by the USP-NF (2023). Most tablet batches passed the friability test (Table 9), but only BP-MCC and BS-MCC with 65% PCM failed. This is likely due to the low crushing strength values and poor PCM compressibility of these formulations (Eraga *et al.*, 2020).

Table 9: Crushing strength, tensile strength, and friability of Paracetamol loaded tablets.

Sample	Tablet properties	Paracetamol concentration			
		35%	45%	55%	65%
Avicel PH 101	CS (N)	90.66±7.10	78.37± 2.95	67.44±3.37	48 ± 3.03
	TS (Kg/cm^2)	11.62±03	10.07±09	8.4±0.15	6.11±11
	Friability (%)	0.10	0.23	0.57	0.77
BS-MCC	CS (N)	88±5.66	71±6.64	65±5.19	38±5.11
	TS (Kg/cm^2)	11.46±0.2	9.9±0.8	8.6±0.24	5.06±0.73
	Friability	0.29	0.43	0.76	1.25
BP-MCC	CS (N)	79±4.03	68±6.33	61±6.21	36±2.49
	TS (Kg/cm^2)	10.06±0.16	9.05±0.11	8.06±022	4.79±0.17
	Friability	0.52	0.64	0.78	1.15

Mean ± SD (=10), CS: Crushing Strength, TS: Tensile strength

The tensile strength (TS) of a tablet is an essential characteristic since the tablet needs to be mechanically strong enough to withstand additional handling, such as film coating, packaging, transportation, and patient use. As MCC concentrations increased the tensile strength of paracetamol tablets containing binary combinations increased, whereas friability decreased (Pitt & Heasley, 2013). According to Table 9, paracetamol 35, 45, 55, and 65% tablet formulations developed with Avicel PH-101 consistently displayed much higher crushing strengths and TS than those prepared with BS-MCC, and BP-MCC. This could be a result of Avicel PH-101's increased crystallinity, which results in stronger packing when the compression force is applied (Juban *et al.*, 2015).

As MCC concentrations increase, the TS of paracetamol tablets containing binary combinations increases, while friability decreases (Pitt & Heasley, 2013). According to Table 9, paracetamol tablets containing Avicel PH-101 consistently exhibited much higher crushing strengths and TS than those prepared with BS-MCC and BP-MCC. This may be due to the increased crystallinity of Avicel PH-101, which results in stronger packing when compression force is applied (Juban *et al.*, 2015). The TS of BS-MCC, BP-MCC,

and Avicel PH-101 tablets were not statistically significantly different at any drug loading level except 65%.

Increasing the concentration of MCC and Avicel PH 101 appears to increase the tensile and mechanical strength of the tablets, as evidenced by the increase in tablet hardness and decrease in friability across all batches (Table 9). This finding suggests that the MCC sample, which was obtained at different concentrations, had significant compressibility.

4.8.5.3 Determination of disintegration time of the tablets

MCC is an important drug delivery material because it can be used to make tablets that are both hard and fast-disintegrating. This is because MCC particles expand when they come into contact with water, which decreases the bonding forces holding them together. Pharmaceutical tablets must dissolve quickly and completely for effective drug delivery so that the released active ingredient is available for absorption (Pachuau et al., 2019). Before the dissolution process can begin, the tablet must be broken down into small pieces. For some oral tablets, disintegration is the rate-limiting step for absorption and bioavailability (Al-Dulaimi *et al*., 2021).

Figure 22 displays the BS-MCC, BP-MCC, and Avicel PH-101 disintegration times. As the concentration of paracetamol increased, the disintegration times of tablets made with BS-MCC, BP-MCC, and Avicel PH-101 decreased. The decrease in disintegration times (DT) could be attributed to tablet sensitivity with increased paracetamol concentration. Hardness often affects the disintegration time. The DT of the paracetamol-loaded BS-MCC, BP-MCC and Avicel PH-101 tablets in this prepared formulation was shorter than 15 min, which is the USP/NF specification for uncoated tablets (USP-NF, 2022). It is widely understood that a tablet's porosity directly influences how quickly water and other body fluids enter and pass through the tablet matrix (Yassin *et al*., 2015). From prepared tablets with 35% w/w of the test, PCM had the slowest rate of disintegration, whereas those with 65% w/w of PCM had the fastest rate. The DT of paracetamol tablets made with BS-MCC, BP-MCC, and Avicel PH-101 decreased as the concentration of paracetamol increased (Figure 22). As the amount of MCC and Avicel increased, tablet disintegration times decreased. However, the proportion of MCC in the direct compression excipients increased along with the disintegration time (Iyer *et al*., 2014). All tablets made

from BS-MCC, BP-MCC, and Avicel PH-101 disintegrated more slowly as the concentration of MCC increased (Eraga *et al.*, 2020).

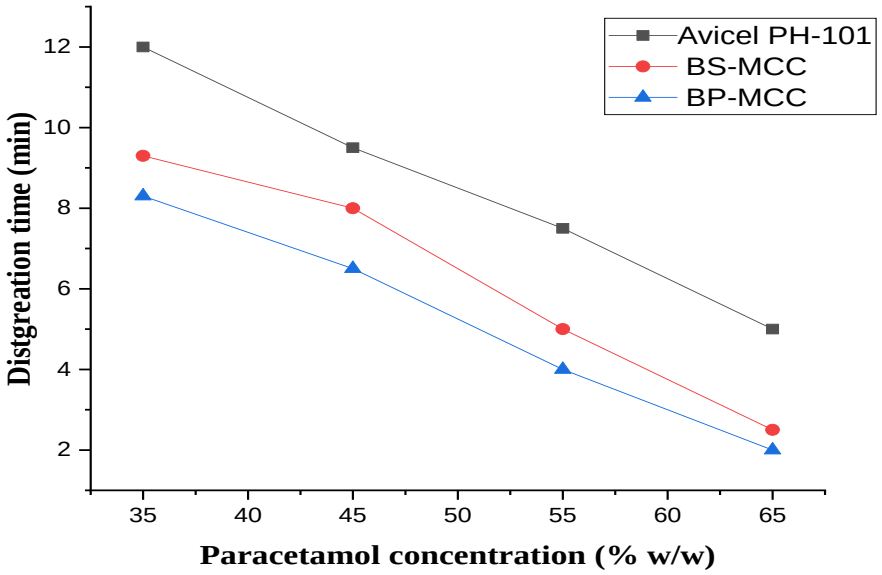

Figure 22: Effect of Paracetamol concentration on the disintegration time of tablets containing. Banana pseudostem microcrystalline cellulose (BS-MCC), Banana peduncle microcrystalline cellulose (BP-MCC), and Avicel PH-101.

4.8.5.4 UV calibration curve of paracetamol

A linear regression equation and correlation coefficient were generated by plotting the absorbance versus concentration of the paracetamol solutions (Figure 23). This standard curve was used to measure the amount of paracetamol released in the dissolution medium after a predetermined amount of time. The correlation coefficient of the straight line was greater than 0.999, indicating a very strong correlation between the concentration and absorbance values. This means that the standard curve is reliable and can be used to accurately measure the amount of paracetamol released in the dissolution medium.

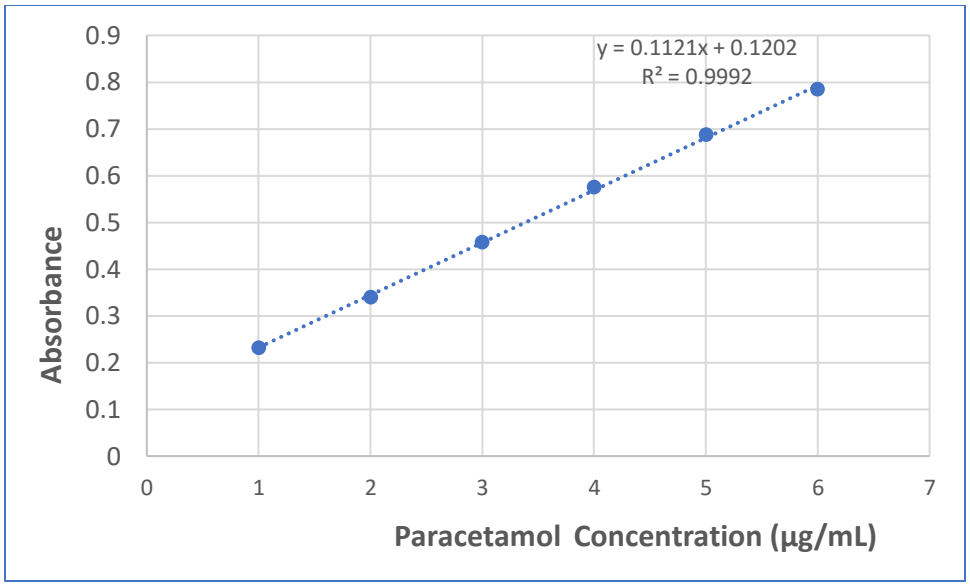

Figure 23: Standard calibration curve of paracetamol in phosphate buffer (pH = 5.8) at 243 nm with 95% confidence bands for the mean, (R^2 =0.999).

4.8.5.5 *In vitro* drug release study

Figure 24 shows the *in vitro* dissolution profiles of paracetamol tablets containing 35%, 45%, 55%, and 65% of BS-MCC, BP-MCC, and Avicel PH-101. All formulations containing BS-MCC, BP-MCC, and Avicel PH-101 met the USP/NF specifications, with >75-80% of the tablet content released within 30 minutes. This suggests that the directly compressed paracetamol tablet dosage forms released the drug well. Overall, this data suggests that the MCC made from BS and BP is comparable to the commercial Avicel PH-101.

Figure 24 shows that increasing the amount of MCC and Avicel PH-101 in the tablets reduced disintegration time and increased drug dissolution time. The rate of dissolution of a drug influences its rate and extent of absorption, which affects the therapeutic outcome. The factors that affect dissolution include the type and amount of binder, tablet hardness, drug surface area, diffusion distance, drug solubility, manufacturing process (wet granulation, dry granulation, or direct compression), and diluents. *In vitro* dissolution testing is often used to model and predict the *in vivo* performance of oral drug products in the GI tract (Lex *et al*., 2022).

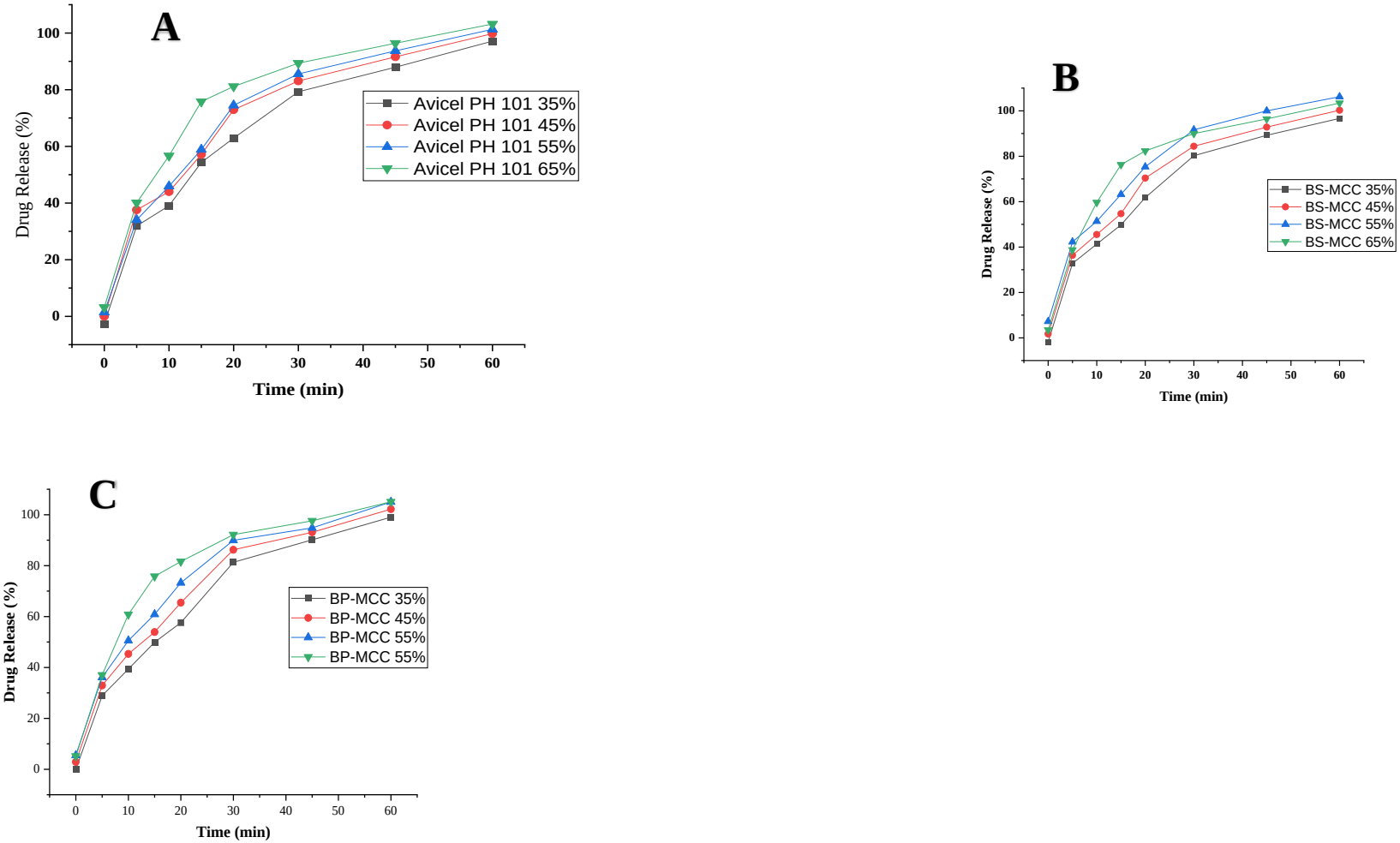

Figure 24: Dissolution profiles of paracetamol tablets containing 35%, 45%, 55%, and 65% of A) Avicel PH-101, B) Banana pseudostem microcrystalline cellulose (BS-MCC) and C) Banana peduncle microcrystalline cellulose (BP-MCC).

5. CONCLUSIONS

Banana fibers, a readily available and sustainable agricultural waste, offer a promising alternative source of cellulose. In this study, cellulose was successfully extracted from banana fibers (BL, BS, and BP) using a chlorine-free process. FT-IR, XRD, and SEM analyses confirmed that BL-MCC, BS-MCC, and BP-MCC have similar chemical composition, crystallinity, morphology, and particle size to commercial-grade MCC (Avicel PH-101). Due to high cellulose and MCC yields and the substantial quantities required for further studies, only BS-MCC and BP-MCC were selected for in-depth investigation. This study also showed that MCC isolated from banana fibers (BS, and BP) has direct compression ability and meets compendial standards for crushing strength, friability, disintegration time, and dissolution profile (except for 65% PCM, which failed). The prepared MCC also met all USP specifications for chemical identity and DP. This suggests that MCC extracted from BS and BP can be used as a locally sourced, cost-effective, and sustainable alternative to commercial-grade MCC.

SUGGESTION FOR FURTHER STUDY

This study provided insights into some physicochemical properties and the direct compressibility of BL-MCC, BS-MCC, and BP-MCC. Therefore, based on the promising results of this study, the following are suggested for further investigation

- Co-processing MCC with other excipients to improve flowability
- Producing different grades of MCC
- Blending various grades of MCC to design robust formulations
- Long- and short-term stability studies of tablets produced from BS-MCC and BP-MCC
- Assess the performance of microcrystalline cellulose (MCC) as a diluent in wet-granulated tablets and a filler for capsules and spheres

REFERENCES

Abdel-Halim, E. S. (2014). Chemical modification of cellulose extracted from sugarcane bagasse: Preparation of hydroxyethyl cellulose. *Arabian Journal of Chemistry*.***7***:362–371.

Abdelmouleh, M., Boufi, S., Belgacem, M. N., Duarte, A. P., Ben Salah, A., & Gandini, A. (2004). Modification of cellulosic fibres with functionalised silanes: Development of surface properties. *International Journal of Adhesion and Adhesives*.***24***: 43–54.

Abdul Khalil, H. P. S., Lai, T. K., Tye, Y. Y., Paridah, M. T., Fazita, M. R. N., Azniwati, A. A., Dungani, R., & Rizal, S. (2018). Preparation and Characterization of Microcrystalline Cellulose from Sacred Bali Bamboo as Reinforcing Filler in Seaweed-based Composite Film. *Fibers and Polymers*.***19***:423–434.

Abdullah, N., Sulaiman, F., & Taib, R. M. (2013). Characterization of banana (Musa spp.) plantation wastes as a potential renewable energy source. *AIP Conference Proceedings*, **8**:325–330.

Abu-Thabit, N. Y., Judeh, A. A., Hakeem, A. S., Ul-Hamid, A., Umar, Y., & Ahmad, A. (2020). Isolation and characterization of microcrystalline cellulose from date seeds (Phoenix dactylifera L.). *International Journal of Biological Macromolecules*.**155**:730–739.

Acharya, S., Hu, Y., & Abidi, N. (2021). Cellulose dissolution in ionic liquid under mild conditions: Effect of hydrolysis and temperature. *Fibers*.***9*:**1–14.

Adel, A. M., Abd El-Wahab, Z. H., Ibrahim, A. A., & Al-Shemy, M. T. (2011). Characterization of microcrystalline cellulose prepared from lignocellulosic materials. Part II: Physicochemical properties. *Carbohydrate Polymers*.***83***:676–687.

Adel, A. M., El-wahab, Z. H. A., Ibrahim, A. A., & Al-shemy, M. T. (2011). *Characterization of microcrystalline cellulose prepared from lignocellulosic materials . Part II : Physicochemical properties*. .***83***:676–687.

Adel, A. M., El-Wahab, Z. H. A., Ibrahim, A. A., & Al-Shemy, M. T. (2010). Characterization of microcrystalline cellulose prepared from lignocellulosic

materials. Part I. Acid catalyzed hydrolysis. *Bioresource Technology*.**101**:4446–4455.

Ahmad, Z., Roziaizan, N. N., Rahman, R., Mohamad, A. F., & Wan Ismail, W. I. N. (2016). Isolation and characterization of Microcrystalline Cellulose (MCC) from Rice Husk (RH). *MATEC Web of Conferences*:**47**:8-11

Al-Dulaimi, A., Al-kotaji, M., & Abachi, F. (2021). Paracetamol/ naproxen co-crystals; a simple way for improvement of flowability, tableting and dissolution properties. *Iraqi Journal of Pharmacy*.**18**:1–19.

Alemdar, A., & Sain, M. (2008). Isolation and characterization of nanofibers from agricultural residues - Wheat straw and soy hulls. *Bioresource Technology* .**99**:1664–1671.

Almaya, A., & Aburub, A. (2008). Effect of particle size on compaction of materials with different deformation mechanisms with and without lubricants. *AAPS PharmSciTech*.**9**: 414–418.

Amin, F. R., Khalid, H., Zhang, H., Rahman, S., Zhang, R., Liu, G., & Chen, C. (2017). Pretreatment methods of lignocellulosic biomass for anaerobic digestion. *AMB Express*. **7**:3–6.

Arca, H. C., Mosquera-Giraldo, L. I., Bi, V., Xu, D., Taylor, L. S., & Edgar, K. J. (2018). Pharmaceutical Applications of Cellulose Ethers and Cellulose Ether Esters. *Biomacromolecules* .**19**:2351–2376.

Assaf, S. M., Subhi Khanfar, M., Bassam Farhan, A., Said Rashid, I., & Badwan, A. A. (2019). Preparation and characterization of co-processed starch/MCC/chitin hydrophilic polymers onto magnesium silicate. *Pharmaceutical Development and Technology*.***24***:761–774.

Azraaie, N., Zainul Abidin, N. A. M., Ibrahim, N. A., Mamat Razali, N. A., Aziz, F. A., & Radiman, S. (2014). X-ray diffraction (XRD) analysis of cellulose from banana (Musa acuminata) pseudo-stem waste. *Advanced Materials Research*.**895**:174–177.

.895.174Badawy, S. I. F., Gray, D. B., & Hussain, M. A. (2006). A study on the effect of wet granulation on microcrystalline cellulose particle structure and performance.

Pharmaceutical Research.**23**:634–640.

Balestrieri, F., Magrì, A. D., Magrì, A. L., Marini, D., & Sacchini, A. (1996). Application of differential scanning calorimetry to the study of drug-excipient compatibility. *Thermochimica Acta*.***285***:337–345.

Baruah, J., Nath, B. K., Sharma, R., Kumar, S., Deka, R. C., Baruah, D. C., & Kalita, E. (2018). Recent trends in the pretreatment of lignocellulosic biomass for value-added products. *Frontiers in Energy Research*.**6**:1–19.

Bastos, M. D. O., Friedrich, R. B., & Beck, R. C. R. (2008). Effects of filler-binders and lubricants on physicochemical properties of tablets obtained by direct compression: A 22 factorial design. *Latin American Journal of Pharmacy*.**27**:578–583.

Batista Meneses, D., Montes de Oca-Vásquez, G., Vega-Baudrit, J. R., Rojas-Álvarez, M., Corrales-Castillo, J., & Murillo-Araya, L. C. (2022). Pretreatment methods of lignocellulosic wastes into value-added products: recent advances and possibilities. *Biomass Conversion and Biorefinery*.**12**:547–564.

Battista, O. A. (1950). Hydrolysis and Crystallization of Cellulose. *Industrial & Engineering Chemistry*:**42**:502–507.

Benabbas, R., Sanchez-Ballester, N. M., Aubert, A., Sharkawi, T., Bataille, B., & Soulairol, I. (2021). Performance evaluation of a novel biosourced co-processed excipient in direct compression and drug release. *Polymers*.***13***:3–7.

Beroual, M., Boumaza, L., Mehelli, O., Trache, D., Tarchoun, A. F., & Khimeche, K. (2021). Physicochemical Properties and Thermal Stability of Microcrystalline Cellulose Isolated from Esparto Grass Using Different Delignification Approaches. *Journal of Polymers and the Environment*.***29***:130–142.

Bhandari, K., Roy Maulik, S., & Bhattacharyya, A. R. (2020). Synthesis and Characterization of Microcrystalline Cellulose from Rice Husk. *Journal of The Institution of Engineers (India): Series E*.**101**:99–108.

Bhimte, N. A., & Tayade, P. T. (2007). Evaluation of microcrystalline cellulose prepared from sisal fibers as a tablet excipient: A technical note. *AAPS PharmSciTech*. ***8***:1–7.

Bosch, M. E., Sánchez, A. J. R., Rojas, F. S., & Ojeda, C. B. (2006). Determination of paracetamol: Historical evolution. *Journal of Pharmaceutical and Biomedical Analysis*, *42*(3), 291–321. https://doi.org/10.1016/j.jpba.2006.04.007

Brinchi, L., Cotana, F., Fortunati, E., & Kenny, J. M. (2013). Production of nanocrystalline cellulose from lignocellulosic biomass: Technology and applications. *Carbohydrate Polymers*. ***94***:154–169.

Burgina, E. B., Baltakhinov, V. P., Boldyreva, E. V., & Shakhtschneider, T. P. (2004). IR spectra of paracetamol and phenacetin. 1. Theoretical and experimental studies. *Journal of Structural Chemistry* .***45***:64–73.

Chadha, R., & Bhandari, S. (2014). Drug-excipient compatibility screening-Role of thermoanalytical and spectroscopic techniques. *Journal of Pharmaceutical and Biomedical Analysis*.***87***:82–97.

Cheah, W. Y., Sankaran, R., Show, P. L., Ibrahim, T. N. B. T., Chew, K. W., Culaba, A., & Chang, J. S. (2020). Pretreatment methods for lignocellulosic biofuels production: Current advances, challenges and future prospects. *Biofuel Research Journal*.***7***:1115–1127.

Crouter, A., & Briens, L. (2014). The effect of moisture on the flowability of pharmaceutical excipients. *AAPS PharmSciTech*. ***15***:65–74.

Dagnew, A., Assefa, W., Kebede, G., & Ayele, L. (2021). Evaluation of Banana (Musa spp .) Cultivars for Growth , Yield and Fruit Quality Bananas (Musa spp .) are important fruits in the tropics and subtropics . Ethiopia is. *Ethiopian Journal Agricuture*. ***31***:1–25.

Das, A., Mondal, C., & Roy, S. (2015). Pretreatment methods of ligno-cellulosic biomass: A review. *Journal of Engineering Science and Technology Review*.***8***:141–165.

Das, K., Ray, D., Bandyopadhyay, N. R., & Sengupta, S. (2010). Study of the Properties of Microcrystalline Cellulose Particles from Different Renewable Resources by XRD, FTIR, Nanoindentation, TGA and SEM. *Journal of Polymers and the Environment*.**18**:355–363.

De Menezes, F. F., da Silva Fernandes, R. H., de Moraes Rocha, G. J., & Maciel Filho, R. (2016). Physicochemical characterization of residue from the enzymatic hydrolysis of sugarcane bagasse in a cellulosic ethanol process at pilot scale. *Industrial Crops and Products*. ***94***:463–470.

Diarsa, M., & Gupte, A. (2021). Preparation, characterization and its potential applications in Isoniazid drug delivery of porous microcrystalline cellulose from banana pseudostem fibers. *3 Biotech*,.***11***:1–13.

Dinand, E., Chanzy, H., & Vignon, M. R. (1996). Parenchymal cell cellulose from sugar beet pulp: Preparation and properties. *Cellulose* .***3***:183–188.

Doelker, E. (1993). Comparative compaction properties of various microcrystalline cellulose types and generic products. *Drug Development and Industrial Pharmacy*.***19***:2399–2471.

Ejikeme, P. M. (2008). Investigation of the physicochemical properties of microcrystalline cellulose from agricultural wastes I: Orange mesocarp. *Cellulose*. ***15***:141–147.

El-Sakhawy, M., & Hassan, M. L. (2007). Physical and mechanical properties of microcrystalline cellulose prepared from agricultural residues. *Carbohydrate Polymers*, ***67***:1–10.

El Achaby, M., Kassab, Z., Barakat, A., & Aboulkas, A. (2018). Alfa fibers as viable sustainable source for cellulose nanocrystals extraction: Application for improving the tensile properties of biopolymer nanocomposite films. *Industrial Crops and Products*. ***112***:499–510.

Elanthikkal, S., Gopalakrishnapanicker, U., Varghese, S., & Guthrie, J. T. (2010). Cellulose microfibres produced from banana plant wastes: Isolation and characterization. *Carbohydrate Polymers* .***80***:852–859.

Elsayed, A., Al-Remawi, M., Maghrabi, I., Hamaidi, M., & Jaber, N. (2018). Evaluation of calcium magnesium silicate-date palm cellulose as a potential tablet excipient. *Journal of Excipients and Food Chemicals*. ***9***:106–115.

Eraga, S. O., Elue, D. N., & Iwuagwu, M. A. (2020). Evaluation of the Direct

Compression Properties of Microcrystalline Cellulose Obtained from Cassava Fermentation Waste in Paracetamol Tablet Formulations. *Nigerian Journal of Pharmaceutical Research*. ***16***:31–37.

Fan, G. Z., Wang, Y. X., Song, G. Sen, Yan, J. T., & Li, J. F. (2017). Preparation of microcrystalline cellulose from rice straw under microwave irradiation. *Journal of Applied Polymer Science*. ***134***:1–8.

Fernandes, E. R. K., Marangoni, C., Souza, O., & Sellin, N. (2013). Thermochemical characterization of banana leaves as a potential energy source. *Energy Conversion and Management* . ***75***:603–608.

Flores-Velázquez, V., Córdova-Pérez, G. E., Silahua-Pavón, A. A., Torres-Torres, J. G., Sierra, U., Fernández, S., Godavarthi, S., Ortiz-Chi, F., & Espinosa-González, C. G. (2020). Cellulose obtained from banana plant waste for catalytic production of 5-HMF: Effect of grinding on the cellulose properties. *Fuel*. ***265***:50-57.

Fouad, H., Kian, L. K., Jawaid, M., Alotaibi, M. D., Alothman, O. Y., & Hashem, M. (2020). Characterization of microcrystalline cellulose isolated from conocarpus fiber. *Polymers*. ***12***:1–11.

French, A. D., & Santiago Cintrón, M. (2013). Cellulose polymorphy, crystallite size, and the Segal Crystallinity Index. *Cellulose*. ***20***:583–588.

Gabhane, J., Prince William, S. P. M., Gadhe, A., Rath, R., Vaidya, A. N., & Wate, S. (2014). Pretreatment of banana agricultural waste for bio-ethanol production: Individual and interactive effects of acid and alkali pretreatments with autoclaving, microwave heating and ultrasonication. *Waste Management*. ***34***:498–503.

Gabriel, E., García, J., Mora, K. R., Bernal, C., Química, E. D. I., Rica, U. D. C., Caribe, S., Rica, C., Forestales, U. D. R., Investigaciones, I. De, Rica, U. D. C., & Rica, C. (2020). Cellulose Nanofiber Production from Banana Rachis. *Indian Journal of Pharmaceutical Sciences*. ***10***:24683–24689.

Gabriel, T., Belete, A., Hause, G., Neubert, R. H. H., & Gebre-Mariam, T. (2021). Isolation and Characterization of Cellulose Nanocrystals from Different Lignocellulosic Residues: A Comparative Study. *Journal of Polymers and the*

Environment. ***29***:2964–2977.

Gabriel, T., Belete, A., Syrowatka, F., Neubert, R. H. H., & Gebre-Mariam, T. (2020). Extraction and characterization of celluloses from various plant byproducts. *International Journal of Biological Macromolecules*, ***158***:1248–1258.

Garrote, G., Domínguez, H., & Parajó, J. C. (1999). Hydrothermal processing of lignocellulosic materials. *Holz Als Roh - Und Werkstoff*, ***57***:191–202.

Getachew, M., Gabriel, T., Belete, A., & Gebre-Mariam, T. (2023a). Extraction and Characterization of Cellulose and Microcrystalline Cellulose from Teff Straw and Evaluation of the Microcrystalline Cellulose as Tablet Excipient. *Journal of Natural Fibers*, ***20***:5–16.

Giordano, F., Rossi, A., Bettini, R., Savioli, A., Gazzaniga, A., & Novák, C. (2002). Thermal behavior of paracetamol-polymeric excipients mixtures. *Journal of Thermal Analysis and Calorimetry*, ***68***:575–590.

Gong, J., Li, J., Xu, J., Xiang, Z., & Mo, L. (2017). Research on cellulose nanocrystals produced from cellulose sources with various polymorphs. *RSC Advances*, ***7***: 33486–33493.

Goyanes, A., & Martínez-Pacheco, R. (2015). New co-processed MCC-based excipient for fast release of low solubility drugs from pellets prepared by extrusion-spheronization. *Drug Development and Industrial Pharmacy*, ***41***:362–368.

Guo, J. H., Skinner, G. W., Harcum, W. W., & Barnum, P. E. (1998). Pharmaceutical applications of naturally occurring water-soluble polymers. *Pharmaceutical Science and Technology Today*, ***1***:254–261.

Haafiz, M. K. M., Hassan, A., Zakaria, Z., & Inuwa, I. M. (2014). Isolation and characterization of cellulose nanowhiskers from oil palm biomass microcrystalline cellulose. *Carbohydrate Polymers*, ***103***:119–125.

Habib, Y., Augsburger, L., Reier, G., Wheatley, T., & Shangraw, R. (1996). Dilution potential: A new perspective. *Pharmaceutical Development and Technology*, ***1***: 205–212.

Habiba, U., Alam, A., Rahman, S., Shamim, S., & Piya, A. (2021). IR spectra of paracetamol. *Bangladesh Journal of Scientific and Industrial Research*, ***56***:255–262.

Haldar, D., & Purkait, M. K. (2020). Micro and nanocrystalline cellulose derivatives of lignocellulosic biomass: A review on synthesis, applications and advancements. *Carbohydrate Polymers*, ***250***:11-15

Hamrah, K. T. K. A., Al-Shaibani, A. J. N., Al-Edresi, S. S., & Al-Gburi, K. M. H. (2020). A comparative study of quality control testing on candesartan cilexetil conventional tablets in Iraq. *International Journal of Applied Pharmaceutics*, ***12***:103–108.

Haruna, F., Apeji, Y. E., Oparaeche, C., Oyi, A. R., & Gamlen, M. (2020). Compaction and tableting properties of composite particles of microcrystalline cellulose and crospovidone engineered for direct compression. *Future Journal of Pharmaceutical Sciences*, ***6***:35-36.

Hassan, M. L., & El-Sakhawy, M. (2007). Physical and Mechanical Properties of Microcrystalline Cellulose Prepared from Local Agricultural Residues. *Carbohydrate Polymers*, ***67***:1–10.

Hendriks, A. T. W. M., & Zeeman, G. (2009). Pretreatments to enhance the digestibility of lignocellulosic biomass. *Bioresource Technology*, ***100***:10–18.

Hubbell, C. A., & Ragauskas, A. J. (2010). Effect of acid-chlorite delignification on cellulose degree of polymerization. *Bioresource Technology*, ***101***:7410–7415.

Hussin, M. H., Pohan, N. A., Garba, Z. N., Kassim, M. J., Rahim, A. A., Brosse, N., Yemloul, M., Fazita, M. R. N., & Haafiz, M. K. M. (2016a). Physicochemical of microcrystalline cellulose from oil palm fronds as potential methylene blue adsorbents. *International Journal of Biological Macromolecules*, ***92***:11–19.

Ibrahim, M. M., El-Zawawy, W. K., Jüttke, Y., Koschella, A., & Heinze, T. (2013). Cellulose and microcrystalline cellulose from rice straw and banana plant waste: Preparation and characterization. *Cellulose*, ***20***:2403–2416.

Ismail, F., Othman, N. E. A., Wahab, N. A., Hamid, F. A., & Aziz, A. A. (2021).

Preparation of Microcrystalline Cellulose from Oil Palm Empty Fruit Bunch Fibre Using Steam-Assisted Acid Hydrolysis. *Journal of Advanced Research in Fluid Mechanics and Thermal Sciences*, ***81***:88–98.

Isogai, T., Yanagisawa, M., & Isogai, A. (2008). Degrees of polymerization (DP) and DP distribution of dilute acid-hydrolyzed products of alkali-treated native and regenerated celluloses. *Cellulose*, ***15***:815–823.

Iyer, R. M., Hegde, S., DiNunzio, J., Singhal, D., & Malick, W. (2014). The impact of roller compaction and tablet compression on physicomechanical properties of pharmaceutical excipients. *Pharmaceutical Development and Technology*, ***19***:583–592.

Jahan, M. S., Rumee, J. N., Rahman, M. M., & Quaiyyum, A. (2014). Formic acid/acetic acid/water pulping of agricultural wastes. *Cellulose Chemistry and Technology*, ***48***:111–118.

Jahan, M. S., Saeed, A., He, Z., & Ni, Y. (2011). Jute as raw material for the preparation of microcrystalline cellulose. *Cellulose*, ***18***:451–459.

Jayaprabha, J. S., Brahmakumar, M., & Manilal, V. B. (2011). Banana pseudostem characterization and its fiber property evaluation on physical and bioextraction. *Journal of Natural Fibers*, ***8***:149–160.

Johar, N., Ahmad, I., & Dufresne, A. (2012). Extraction, preparation and characterization of cellulose fibres and nanocrystals from rice husk. *Industrial Crops and Products*, ***37***:93–99.

Juban, A., Nouguier-Lehon, C., Briancon, S., Hoc, T., & Puel, F. (2015). Predictive model for tensile strength of pharmaceutical tablets based on local hardness measurements. *International Journal of Pharmaceutics*, ***490***:438–445.

Jumaidin, R., Sapuan, S. M., Jawaid, M., Ishak, M. R., & Sahari, J. (2017). Thermal, mechanical, and physical properties of seaweed/sugar palm fibre reinforced thermoplastic sugar palm Starch/Agar hybrid composites. *International Journal of Biological Macromolecules*, ***97***: 606–615.

Kaerger, J. S., Edge, S., & Price, R. (2004). Influence of particle size and shape on

flowability and compactibility of binary mixtures of paracetamol and microcrystalline cellulose. *European Journal of Pharmaceutical Science*, ***22***:173–179.

Kale, R. D., Bansal, P. S., & Gorade, V. G. (2018). Extraction of Microcrystalline Cellulose from Cotton Sliver and Its Comparison with Commercial Microcrystalline Cellulose. *Journal of Polymers and the Environment*, ***26***:355–364.

Kalita, R. D., Nath, Y., Ochubiojo, M. E., & Buragohain, A. K. (2013). Extraction and characterization of microcrystalline cellulose from fodder grass; Setaria glauca (L) P. Beauv, and its potential as a drug delivery vehicle for isoniazid, a first line antituberculosis drug. *Colloids and Surfaces B: Biointerfaces*, ***108***:85–89.

Kambli, N. D., Mageshwaran, V., Patil, P. G., Saxena, S., & Deshmukh, R. R. (2017a). Synthesis and characterization of microcrystalline cellulose powder from corn husk fibres using bio-chemical route. *Cellulose*, ***24***:5355–5369.

Kambli, N. D., Mageshwaran, V., Patil, P. G., Saxena, S., & Deshmukh, R. R. (2017b). Synthesis and characterization of microcrystalline cellulose powder from corn husk fibres using bio-chemical route. *Cellulose*, ***24***:5355–5369.

Kambli, N. D., Samanta, K. K., Basak, S., Chattopadhyay, S. K., Patil, P. G., & Deshmukh, R. R. (2018). Characterization of the corn husk fibre and improvement in its thermal stability by banana pseudostem sap. *Cellulose*, ***25***:5241–5257.

Kaminska, E. (1997). Determination of degree of polymerization of cellulose in ligneous papers. *Materials Research Society Symposium - Proceedings*, ***462***:45–51.

Karande, V. S., Bharimalla, A. K., Hadge, G. B., Mhaske, S. T., & Vigneshwaran, N. (2011). Nanofibrillation of cotton fibers by disc refiner and its characterization. *Fibers and Polymers*, ***12***:399–404.

Kian, L. K., Jawaid, M., Ariffin, H., & Alothman, O. Y. (2017). Isolation and characterization of microcrystalline cellulose from roselle fibers. *International Journal of Biological Macromolecules*, ***103***:931–940.

Kim, J. S., Lee, Y. Y., & Kim, T. H. (2016). A review on alkaline pretreatment technology for bioconversion of lignocellulosic biomass. *Bioresource Technology*,

199:42–48.

Klemm, D., Heublein, B., Fink, H. P., & Bohn, A. (2005). Cellulose: Fascinating biopolymer and sustainable raw material. *Angewandte Chemie - International Edition*, ***44***:3358–3393.

Kuentz, M., & Leuenberger, H. (2000). A new theoretical approach to tablet strength of a binary mixture consisting of a well and a poorly compactable substance. *European Journal of Pharmaceutics and Biopharmaceutics*, ***49***:151–159.

Kumar, M., Shukla, S. K., Upadhyay, S. N., & Mishra, P. K. (2020). Analysis of thermal degradation of banana (Musa balbisiana) trunk biomass waste using iso-conversional models. *Bioresource Technology*, ***310***:20-32

Kumar, P., Barrett, D. M., Delwiche, M. J., & Stroeve, P. (2009). Methods for pretreatment of lignocellulosic biomass for efficient hydrolysis and biofuel production. *Industrial and Engineering Chemistry Research*, *48*(8), 3713–3729. https://doi.org/10.1021/ie801542g

Lavanya, D., Kulkarni, P. K., Dixit, M., Raavi, P. K., & Krishna, L. N. V. (2015). Sources of cellulose and their applications- A review. *International Journal of Drug Formulation and Research*, ***2***:19–38.

Li, K., Fu, S., Zhan, H., Zhan, Y., & Lucia, L. A. (2010). Analysis of the chemical composition and morphological structure of banana pseudo-stem. *BioResources*, ***5***:576–585.

Li, M., He, B., Li, J., & Zhao, L. (2019). Physico-chemical Characterization and Comparison of Microcrystalline Cellulose from Several Lignocellulosic Sources. *BioResources*, ***14***: 7886–7900.

Li, W., Zhang, Y., Li, J., Zhou, Y., Li, R., & Zhou, W. (2015). Characterization of cellulose from banana pseudo-stem by heterogeneous liquefaction. *Carbohydrate Polymers*, ***132***:513–519.

Liao, Z., Zhang, N., Zhao, G., Zhang, J., Liang, X., Zhong, S., Wang, G., & Chen, X. (2012). Multivariate analysis approach for correlations between material properties and tablet tensile strength of microcrystalline cellulose. *Pharmazie*, ***67***:774–780.

Ligero, P., Villaverde, J. J., de Vega, A., & Bao, M. (2008). Delignification of Eucalyptus globulus saplings in two organosolv systems (formic and acetic acid). Preliminary analysis of dissolved lignins. *Industrial Crops and Products*, ***27***:110–117.

Lin, L., Yan, R., Liu, Y., & Jiang, W. (2010). In-depth investigation of enzymatic hydrolysis of biomass wastes based on three major components: Cellulose, hemicellulose and lignin. *Bioresource Technology*, ***101***:8217–8223.

Liu, F., Li, J., Yu, H., Li, Y., Wang, Y., Gao, H., Peng, H., Hu, Z., Wang, H., Zhang, G., Tu, Y., & Peng, L. (2021). Optimizing two green-like biomass pretreatments for maximum bioethanol production using banana pseudostem by effectively enhancing cellulose depolymerization and accessibility. *Sustainable Energy and Fuels*, ***5***:3467–3478.

Liu, Y., Liu, A., Ibrahim, S. A., Yang, H., & Huang, W. (2018). Isolation and characterization of microcrystalline cellulose from pomelo peel. *International Journal of Biological Macromolecules*, ***111***:717–721.

Löbmann, K., & Svagan, A. J. (2017). Cellulose nanofibers as excipient for the delivery of poorly soluble drugs. *International Journal of Pharmaceutics*, ***533***:285–297.

Ma, Q., Wang, L., Zhai, H., & Ren, H. (2021). Lignin dissolution model in formic acid – acetic acid – water systems based on lignin chemical structure. *International Journal of Biological Macromolecules*, ***182***:51–58.

Mallah, M. A., Sherazi, S. T. H., Bhanger, M. I., Mahesar, S. A., & Bajeer, M. A. (2015). A rapid Fourier-transform infrared (FTIR) spectroscopic method for direct quantification of paracetamol content in solid pharmaceutical formulations. *Spectrochimica Acta - Part A: Molecular and Biomolecular Spectroscopy*, ***141***:64–70.

Manimaran, P., Sanjay, M. R., Senthamaraikannan, P., Jawaid, M., Saravanakumar, S. S., & George, R. (2019). Synthesis and characterization of cellulosic fiber from red banana peduncle as reinforcement for potential applications. *Journal of Natural Fibers*, ***16***:768–780.

Martinello, T., Kaneko, T. M., Val, M., Velasco, R., Elena, M., Taqueda, S., & Consiglieri, V. O. (2006). *Optimization of poorly compactable drug tablets manufactured by direct compression using the mixture experimental design*. ***322***:87–95.

Mashadi, A. B., & Newton, J. M. (1987). The characterization of the mechanical properties of microcrystalline cellulose: a fracture mechanics approach. *Journal of Pharmacy and Pharmacology*, ***39***:961–965.

Meng, F., Wang, G., Du, X., Wang, Z., Xu, S., & Zhang, Y. (2019). Extraction and characterization of cellulose nanofibers and nanocrystals from liquefied banana pseudo-stem residue. *Composites Part B: Engineering*, ***160***:341–347.

Merci, A., Urbano, A., Grossmann, M. V. E., Tischer, C. A., & Mali, S. (2015). Properties of microcrystalline cellulose extracted from soybean hulls by reactive extrusion. *Food Research International*, ***73***:38–43.

Mihranyan, A., Llagostera, A. P., Karmhag, R., Strømme, M., & Ek, R. (2004). Moisture sorption by cellulose powders of varying crystallinity. *International Journal of Pharmaceutics*, ***269***:433–442.

Mitiku, A. A., Andeta, A. F., Borremans, A., Lievens, B., Bossaert, S., Crauwels, S., Aernouts, B., Kechero, Y., & Van Campenhout, L. (2020). Silage making of maize stover and banana pseudostem under South Ethiopian conditions: evolution of pH, dry matter and microbiological profile. *Microbial Biotechnology*, ***13***:1477–1488.

Mohamad Haafiz, M. K., Eichhorn, S. J., Hassan, A., & Jawaid, M. (2013). Isolation and characterization of microcrystalline cellulose from oil palm biomass residue. *Carbohydrate Polymers*, ***93***:628–634.

Mohamad Haafiz, M. K., Hassan, A., Zakaria, Z., Inuwa, I. M., & Islam, M. S. (2013). Physicochemical characterization of cellulose nanowhiskers extracted from oil palm biomass microcrystalline cellulose. *Materials Letters*, ***113***:87–89.

Mosier, N., Wyman, C., Dale, B., Elander, R., Lee, Y. Y., Holtzapple, M., & Ladisch, M. (2005). Features of promising technologies for pretreatment of lignocellulosic biomass. *Bioresource Technology*, ***96***:673–686.

Mukwaya, V., Yu, W., Asad, R. A. M., & Yagoub, H. (2017). An environmentally friendly method for the isolation of cellulose nano fibrils from banana rachis fibers. *Textile Research Journal*, ***87*:**81–90.

Munarin, F., Tanzi, M. C., & Petrini, P. (2013). Corrigendum to Advances in biomedical applications of pectin gels [International Journal of Biological Macromolecules 51 (2012) 681-689]. *International Journal of Biological Macromolecules*, ***55***:307-308

Nada, A. M. A., El-Gendy, A. A., & Mohamed, S. H. (2010). Banana leaves as adsorbents for removal of metal ions from waste water. *Carbohydrate Polymers*, ***82***:1025–1030.

Nascimento, R. E. A., Monte, J., Cadima, M., Alves, V. D., & Neves, L. A. (2021). Rendering banana plant residues into a potentially commercial byproduct by doping cellulose films with phenolic compounds. *Polymers*, *13*(5), 1–15. https://doi.org/10.3390/polym13050843

Neves, R. M., Ornaghi, H. L., Zattera, A. J., & Amico, S. C. (2021). Recent studies on modified cellulose/nanocellulose epoxy composites: A systematic review. *Carbohydrate Polymers*, ***255***:117-120

Nsor-Atindana, J., Chen, M., Goff, H. D., Zhong, F., Sharif, H. R., & Li, Y. (2017). Functionality and nutritional aspects of microcrystalline cellulose in food. *Carbohydrate Polymers*, ***172***:159–174.

Nwajiobi, C. C., Otaigbe, J. O. E., & Oriji, O. (2019). Physicochemical, spectroscopic and tableting properties of microcrystalline cellulose obtained from the African breadfruit seed hulls. *African Journal of Biotechnology*, ***18***:371–382.

Ogochukwu, U., C, N., Chizoba, N. A., & Ifeanyichukwu, O. S. (2014). Physico - Chemical Properties of Microcrystalline Cellulose Derived from Indian Bamboo. *Int. J. Pharm. Sci. Rev. Res. International Journal of Pharmaceutical Sciences Review and Research*, ***29***:5–9.

Ohwoavworhua, F. O., & Adelakun, T. A. (2007). Phosphoric Acid-Mediated Depolymerization and Decrystallization of α-Cellulose Obtained from Corn Cob: Preparation of Low Crystallinity Cellulose and Some Physicochemical Properties.

Tropical Journal of Pharmaceutical Research, ***4***:509–516.

Ohwoavworhua, F. O., & Adelakun, T. A. (2010). Non-wood fibre production of microcrystalline cellulose from Sorghum caudatum: Characterisation and tableting properties. *Indian Journal of Pharmaceutical Sciences*, ***72***:295–301.

Okareh, O. T. (2015). Proximate and mineral composition of plantain (Musa Paradisiaca) wastes flour; a potential nutrients source in the formulation of animal feeds. *African Journal of Food Science and Technology*, ***6***:53–57.

Okhamafe, A. O., & Rogers, R. D. (2012). Physicochemical properties of maize cob cellulose powders reconstituted from ionic liquid solution. *Cellulose*, ***19***:425–433.

Oliveira, L., Cordeiro, N., Evtuguin, D. V., Torres, I. C., & Silvestre, A. J. D. (2007). Chemical composition of different morphological parts from "Dwarf Cavendish" banana plant and their potential as a non-wood renewable source of natural products. *Industrial Crops and Products*, ***26***:163–172.

Orlando J., R. (2016). Cellulose Chemistry and Properties: Fibers, Nanocelluloses and Advanced Materials. In *Springer* , 271:1-10

Othman, N. A., Adam, F., & Mat Yasin, N. H. (2020). Reinforced bioplastic film at different microcrystalline cellulose concentration. *Materials Today: Proceedings*, ***41***:77–82.

Owolabi, A. F., Haafiz, M. K. M., Hossain, M. S., Hussin, M. H., & Fazita, M. R. N. (2017). Influence of alkaline hydrogen peroxide pre-hydrolysis on the isolation of microcrystalline cellulose from oil palm fronds. *International Journal of Biological Macromolecules*, ***95***:1228–1234.

Pachuau, L., Dutta, R. S., Hauzel, L., Devi, T. B., & Deka, D. (2019). Evaluation of novel microcrystalline cellulose from Ensete glaucum (Roxb.) Cheesman biomass as sustainable drug delivery biomaterial. *Carbohydrate Polymers*, ***206***:336–343.

Pachuau, L., Vanlalfakawma, D. C., Tripathi, S. K., & Lalhlenmawia, H. (2014). Muli bamboo (Melocanna baccifera) as a new source of microcrystalline cellulose. *Journal of Applied Pharmaceutical Science*, ***4***:87–94.

Pappu, A., Patil, V., Jain, S., Mahindrakar, A., Haque, R., & Thakur, V. K. (2015). Advances in industrial prospective of cellulosic macromolecules enriched banana biofibre resources: A review. *International Journal of Biological Macromolecules*, ***79***:449–458.

Paul, S., & Sun, C. C. (2017). Lubrication with magnesium stearate increases tablet brittleness. *Powder Technology*, ***309***:126–132.

Pitchayya Pillai, G., Manimaran, P., & Vignesh, V. (2021). Physico-chemical and Mechanical Properties of Alkali-Treated Red Banana Peduncle Fiber. *Journal of Natural Fibers*, ***18***:2102–2111.

Pitt, K. G., & Heasley, M. G. (2013). Determination of the tensile strength of elongated tablets. *Powder Technology*, ***238***:169–175.

Ramos, L. P. (2003). The chemistry involved in the steam treatment of lignocellulosic materials. *Advanced Materials Research*, ***26***:863–871.

Rasheed, M., Jawaid, M., Karim, Z., & Abdullah, L. C. (2020). Morphological, Physiochemical and Thermal Properties of Microcrystalline Cellulose (MCC) Extracted from Bamboo Fiber. *Molecules*, ***25***:12–16.

Ravindran, R., & Jaiswal, A. K. (2016). A comprehensive review on pre-treatment strategy for lignocellulosic food industry waste: Challenges and opportunities. *Bioresource Technology*, ***199***: 92–102.

Reddy, N., & Yang, Y. (2005). Properties and potential applications of natural cellulose fibers from cornhusks. *Green Chemistry*, ***7***:190–195.

Reddy, N., & Yang, Y. (2007). Preparation and characterization of long natural cellulose fibers from wheat straw. *Journal of Agricultural and Food Chemistry*, ***55***:8570–8575.

Rojas, J., Aristizabal, J., & Henao, ; Manuel. (2013). Screening of several excipients for direct compression of tablets: A new perspective based on functional properties. *Journal of Basic and Applied Pharmaceutical Sciences Rev Ciênc Farm Básica Apl*, ***34***:17–23.

Sainorudin, M. H., Mohammad, M., Kadir, N. H. A., Abdullah, N. A., & Yaakob, Z. (2018). Characterization of several microcrystalline cellulose (Mcc)-based agricultural wastes via x-ray diffraction method. *Solid State Phenomena*, ***280***:340–345.

Seddiqi, H., Oliaei, E., Honarkar, H., Jin, J., Geonzon, L. C., Bacabac, R. G., & Klein-Nulend, J. (2021). Cellulose and its derivatives: towards biomedical applications. In *Cellulose* , **28**:1-13

Setu, M. N. I., Mia, M. Y., Lubna, N. J., & Chowdhury, A. A. (2014). Preparation of microcrystalline cellulose from cotton and its evaluation as direct compressible excipient in the formulation of naproxen tablets. *Dhaka University Journal of Pharmaceutical Sciences*, ***13***:187–192.

Shanmugam*, R. D. N. and M. K., & ICAR-Central. (2010). Microcrystalline cellulose powder from banana pseudostem fibres using bio-chemical route. *Indian Journal of Natural Products and Resources*, ***66***:42–50.

Shanmugam, N., Nagarkar, R. D., & Kurhade, M. (2015). Microcrystalline cellulose powder from banana pseudostem fibres using bio-chemical route. *Indian Journal of Natural Products and Resources*, ***6***:42–50.

Shi, S., Zhang, M., Ling, C., Hou, W., & Yan, Z. (2018). Extraction and characterization of microcrystalline cellulose from waste cotton fabrics via hydrothermal method. *Waste Management*, ***82***:139–146.

Shikinaka, K., Otsuka, Y., Nakamura, M., Masai, E., & Katayama, Y. (2018). Utilization of lignocellulosic biomass via novel sustainable process. *Journal of Oleo Science*, ***67***: 1059–1070.

Shimizu, F. L., Monteiro, P. Q., Ghiraldi, P. H. C., Melati, R. B., Pagnocca, F. C., Souza, W. de, Sant'Anna, C., & Brienzo, M. (2018). Acid, alkali and peroxide pretreatments increase the cellulose accessibility and glucose yield of banana pseudostem. *Industrial Crops and Products*, ***115***:62–68.

Shlieout, G., Arnold, K., & Müller, G. (2002). Powder and mechanical properties of microcrystalline cellulose with different degrees of polymerization. *AAPS*

PharmSciTech, ***3***:1–10.

Sri Aprilia, N. A., Davoudpour, Y., Zulqarnain, W., Abdul Khalil, H. P. S., Che Mohamad Hazwan, C. I., Hossain, M. S., Dungani, R., Fizree, H. M., Zaidon, A., & Mohamad Haafiz, M. K. (2016). Physicochemical characterization of microcrystalline cellulose extracted from kenaf bast. *BioResources*, ***11***:3875–3889.

Stubberud, L., Arwidsson, H. G., Larsson, A., & Graffner, C. (1996). Water solid interactions II. Effect of moisture sorption and glass transition temperature on compactibility of microcrystalline cellulose alone or in binary mixtures with polyvinyl pyrrolidone. *International Journal of Pharmaceutics*, ***134***:79–88.

Sun, C., & Himmelspach, M. W. (2006). Reduced tabletability of roller compacted granules as a result of granule size enlargement. *Journal of Pharmaceutical Sciences*, ***95***:200–206.

Sundarraj, A. A., & Ranganathan, T. V. (2018). Comprehensive review on cellulose and microcrystalline cellulose from agro-industrial wastes. *Drug Invention Today*, ***10***:2783–2788.

Suzuki, T., & Nakagami, H. (1999). Effect of crystallinity of microcrystalline cellulose on the compactability and dissolution of tablets. *European Journal of Pharmaceutics and Biopharmaceutics*, ***47***:225–230.

Takeuchi, H., Nagira, S., Aikawa, M., Yamamoto, H., & Kawashima, Y. (2005). Effect of lubrication on the compaction properties of pharmaceutical excipients as measured by die wall pressure. *Journal of Drug Delivery Science and Technology*, ***15***:177–182.

Tarchoun, A. F., Trache, D., Klapötke, T. M., Derradji, M., & Bessa, W. (2019). Ecofriendly isolation and characterization of microcrystalline cellulose from giant reed using various acidic media. *Cellulose*, ***26***:7635–7651.

Thakur, V. K., & Thakur, M. K. (2014). Processing and characterization of natural cellulose fibers/thermoset polymer composites. *Carbohydrate Polymers*, ***109***:102–117.

The United States Pharmacopeial Convention. (2023). USP 1216 Tablet Friability. In

USP30 - NF25 Vol. 32, 289.

Thoorens, G., Krier, F., Leclercq, B., Carlin, B., & Evrard, B. (2014a). Microcrystalline cellulose, a direct compression binder in a quality by design environment - A review. In *International Journal of Pharmaceutics* **473**:64–72.

Thoorens, G., Krier, F., Rozet, E., Carlin, B., & Evrard, B. (2015). Understanding the impact of microcrystalline cellulose physicochemical properties on tabletability. *International Journal of Pharmaceutics*, ***490***:47–54.

Tibolla, H., Pelissari, F. M., Martins, J. T., Vicente, A. A., & Menegalli, F. C. (2018). Cellulose nanofibers produced from banana peel by chemical and mechanical treatments: Characterization and cytotoxicity assessment. *Food Hydrocolloids*, ***75***:192–201.

Trache, D., Donnot, A., Khimeche, K., Benelmir, R., & Brosse, N. (2014). Physico-chemical properties and thermal stability of microcrystalline cellulose isolated from Alfa fibres. *Carbohydrate Polymers*, ***104***:223–230.

Trache, D., Hussin, M. H., Hui Chuin, C. T., Sabar, S., Fazita, M. R. N., Taiwo, O. F. A., Hassan, T. M., & Haafiz, M. K. M. (2016). Microcrystalline cellulose: Isolation, characterization and bio-composites application—A review. *International Journal of Biological Macromolecules*, ***93***:789–804.

Tuan Rohadi, T. N., Ridzuan, M. J. M., Abdul Majid, M. S., Khasri, A., & Sulaiman, M. H. (2020). Isolation and characterisation of cellulose from cortex, pith and whole of the Pennisetum purpureum: Effect of sodium hydroxide concentration. *Journal of Materials Research and Technology*, ***10***:15057–15071.

United State Pharmacopoia 42the ed.National formulary 37 ed. USP 42/NF 37)(2022a). Excipient Monographs : Microcrystalline Cellulose. United States Pharmacopeia, Stage 4 Harmonization,

United State Pharmacopoia 42the ed.National formulary 37 ed (2022b). The United States pharmacopeia Disintegration. In The United States Pharmacopeial Convention

United State Pharmacopoia 41the ed.National formulary 36 ed. (2022). The United

States Pharmacopeial Convention - U.S. Pharmacopeia National Formulary.

Vora, R. S., & Shah, Y. D. (2015). Production of Micro Crystalline Cellulose from Corn Husk and Its Evaluation as pharmaceutical. *Indian Journal of Pharmaceutical Education and Research*, ***2****:*69–74.

Wang, D., Shang, S. bin, Song, Z. qian, & Lee, M. K. (2010). Evaluation of microcrystalline cellulose prepared from kenaf fibers. *Journal of Industrial and Engineering Chemistry*, ***16***:152–156.

Wang, Jennifer, Wen, H., & Desai, D. (2010). Lubrication in tablet formulations. *European Journal of Pharmaceutics and Biopharmaceutics*, ***75***:1–15.

Wang, Jian, Zhang, R., Quan, C., Shao, X., Hu, N., Yao, X., & Dong, C. (2022). Green preparation of porous corncob microcrystalline cellulose, and its properties and applications. *Cellulose*, ***29***:7125–7138.

Wanrosli, W. D., Rohaizu, R., & Ghazali, A. (2011). Synthesis and characterization of cellulose phosphate from oil palm empty fruit bunches microcrystalline cellulose. *Carbohydrate Polymers*, ***84***:262–267.

Westermarck, S., Juppo, A. M., Kervinen, L., & Yliruusi, J. (1999). Microcrystalline cellulose and its microstructure in pharmaceutical processing. *European Journal of Pharmaceutics and Biopharmaceutics*, ***48***:199–206.

Yassin, S., Goodwin, D. J., Anderson, A., Sibik, J., Wilson, D. I., Gladden, L. F., & Zeitler, J. A. (2015). The Disintegration Process in Microcrystalline Cellulose Based Tablets, Part 1: Influence of Temperature, Porosity and Superdisintegrants. *Journal of Pharmaceutical Sciences*, ***104***:3440–3450. h

Yeasmin, M. S., & Mondal, M. I. H. (2015). Synthesis of highly substituted carboxymethyl cellulose depending on cellulose particle size. *International Journal of Biological Macromolecules*, ***80***, 725–731.

YILMAZ, N., Sulak, M., Yilmaz, K., & Khan, G. (2017). Effect of Chemical Treatments on Physico-Chemical Properties of Fibres from Banana Fruit and Bunch Stems. *Indian Journal of Fibre & Textile Research*, ***42***:111–117.

Yu, G., Li, B., Liu, C., Zhang, Y., Wang, H., & Mu, X. (2013). Fractionation of the main components of corn stover by formic acid and enzymatic saccharification of solid residue. *Industrial Crops and Products*, ***50***:750–757.

Zhang, M., Qi, W., Liu, R., Su, R., Wu, S., & He, Z. (2010). Fractionating lignocellulose by formic acid: Characterization of major components. *Biomass and Bioenergy*, ***34***:525–532

Zhao, T., Chen, Z., Lin, X., Ren, Z., Li, B., & Zhang, Y. (2018). Preparation and characterization of microcrystalline cellulose (MCC) from tea waste. *Carbohydrate Polymers*, ***184***: 164–170.

Zuliahani, A., Nurul Nadhirah, R., Rozyanty, A. R., Nawawi, W. I., & Nor Hanani, A. B. (2016). Crystallinity, Tapping and Bulk Density of Microcrystalline Cellulose (MCC) Isolated from Rice Husk (RH). *Applied Mechanics and Materials*, ***835***:272–276.

Zuluaga, R., Putaux, J. L., Cruz, J., Vélez, J., Mondragon, I., & Gañán, P. (2009). Cellulose microfibrils from banana rachis: Effect of alkaline treatments on structural and morphological features. *Carbohydrate Polymers*, ***76***:51–59.

Zuluaga, R., Putaux, J. L., Restrepo, A., Mondragon, I., & Gañán, P. (2007). Cellulose microfibrils from banana farming residues: Isolation and characterization. *Cellulose*, ***14***:585–592.